OPTIMIZATION OF INDUCTIVELY COUPLED PLASMA DRY ETCHING FOR PLANAR WAVEGUIDE FABRICATION

By
LIM WENG HONG
Department of Physics
Faculty of Science
University Of Malaya

Dissertation Presented For The
Degree of Master of Science
UNIVERSITY OF MALAYA
2010

UNIVERSITI MALAYA

ORIGINAL LITERARY WORK DECLARATION

Name of Candidate: **Lim Weng Hong** (I.C/Passport No: 850913-14-5193)

Registration/Matric No: **SGR 080054**

Name of Degree: **Degree of Master of Science**

Title of Project Paper/Research Report/Dissertation/Thesis ("this Work"):

Optimization of Inductively Coupled Plasma Dry Etching for Planar Waveguides Fabrication.

Field of Study:

I do solemnly and sincerely declare that:

(1) I am the sole author/writer of this Work;
(2) This Work is original;
(3) Any use of any work in which copyright exists was done by way of fair dealing and for permitted purposes and any excerpt or extract from, or reference to or reproduction of any copyright work has been disclosed expressly and sufficiently and the title of the Work and its authorship have been acknowledged in this Work;
(4) I do not have any actual knowledge nor do I ought reasonably to know that the making of this work constitutes an infringement of any copyright work;
(5) I hereby assign all and every rights in the copyright to this Work to the University of Malaya ("UM"), who henceforth shall be owner of the copyright in this Work and that any reproduction or use in any form or by any means whatsoever is prohibited without the written consent of UM having been first had and obtained;
(6) I am fully aware that if in the course of making this Work I have infringed any copyright whether intentionally or otherwise, I may be subject to legal action or any other action as may be determined by UM.

Candidate's Signature Date:

Subscribed and solemnly declared before,

Witness's Signature Date:

Name: **Dr. Harith Bin Ahmad**
Designation: **Professor**

ABSTRACT

Optimization of the Inductively Coupled Plasma (ICP) dry etching process parameters has been carried out. Seven main etching characteristics were considered in order to produce good etching quality. These characteristics are glass etching rates, selectivity of chromium to glass etching rate, channel side wall roughness, channel side wall vertical profile, channel cleanliness, critical dimension and resolution. Several ICP parameters that are affecting the etching characteristic were optimized in this work. These optimised ICP parameters obtained from this work are ICP power (880 W), bias power (45 W), operating chamber pressure (10 mtorr), reactant gas composition, reactant gas flow rate (35sccm of C_2F_6 and 9sccm of H_2), and working distance (5 cm from reference point). Following the above, the dry etching process showed significant improvement from the original etching process. The etching rate was increased to 255nm/min (equivalent to 13% improvement) with selectivity of 45 (equivalent to 80% increment). Moreover, there are clear improvements in cleanliness and no polymerization was observed as compared to non-optimised samples. Furthermore, comparison between Scaning Elelctro Microscope (SEM) images of the etched surface before and after the optimization process, showing major improvements in the reduction of plasma induced surface damage also know as pin hold effect.

ABSTRAK

Optimisasi proses perpindahan corak kaca secara kering (Inductively Coupled Plamsa dry etching) telah dilaksanakan. 7 ciri-ciri proses perpindahan corak kaca secara kering telah diambil kira supaya mendapat corak kaca yang bagus. Ciri-ciri ini adalah, kadar perpindahan corak, nisbah kadar perpindahan corak kaca kepada topi kromium, kekasaran permukaan dinding saluran, profil menegak (sudut dinding) saluran, kebesihan saluran, dimensi kritikal dan resolusi. Beberapa pembolehubah ICP yang menpengaruhi ciri-ciri proses perpindahan corak kaca secara kering telah dikaji dengan teliti. Pembolehubah ICP yang memberi perpindahan corak kaca yang terbaik adalah kuasa ICP (880 W), kuasa bias (45 W), tekanan proces (10 mTorr), komposisi gas, kadar pengaliran gas (35 sccm untuk gas C_2F_6 dan 9 sccm untuk gas $H_{2)}$, dan posisi sample (5 cm dari kedudukan rujukan) dalam bilik proses. Dengan menggunakan resepi diatas, proses perpindahan corak kaca secara kering menunjukan peningkatan yang tinggi. Kadar perpindahan corak telah dinaikkan 13% kepada 255 nm/min. Nisbah kadar perpindahan corak kaca kepada topi kromium juga dibaiki kepada 45 bersamaan 80% kenaikan. Di samping itu, terdapat peningkatan mutu yang mendadak dari segi kebesihan dan tiada pemendapan polimer dikesan jika berbanding dengan sample yang dibuat sebelum proses optimisasi. Selain itu, dengan membanding gambaran SEM bagi sampel sebelum dan selepas proses optimisasi, kesan “pinhole” telah banyak dikurangkan.

ACKNOWLEDGEMENT

I would like to express my gratitude to all those who made it possible for me to complete this dissertation. I am deeply indebted to my respected supervisor Prof. Dr. Harith Ahmad and Dr. Faisal Rafiq Mahamd Adikan for giving me the opportunity to work in this project. Not to forget his interesting insight, valuable guidance and encouragement that has helped me in this research at all times.

Also, I am very grateful and would like to thank to Mr Chong Wu Yi for their help, support, constructive criticism and fruitful discussion. The same appreciation goes to Mr. Nizam Tamchek, Mr. Chuah Khoon Seah and Mr. Pua Chang Hong .

Special thanks also to my family for their love and support that has enabled me to complete this project. Last but not least, a grateful acknowledgement should be given to University of Malaya for providing me the opportunity to carry out this dissertation in term of facility in photonic research center and also fully financial support by UM fellowship. This valuable experience will definitely benefits my future life.

CONTENTS

CHAPTER 4: OPTIMIZATION OF THE ETCHING PROCESS USING ICP

CHAPTER 5: MORE ON ICP

LIST OF FIGURES

Chapter 4

Chapter 5

LIST OF TABLES

LIST OF SYMBOLS AND ABBREVIATIONS

Ar	Argon
at%	Atomic Percent
AWG	Arrayed Waveguides Gratings
B	Boron
B_2O_3	Boric Oxide
BCl_3	Boron chloride
C_2F_6	Hexafluoroethane
C_4F_8	Octafluorocyclobutane
C-band	Communication band
CD	Critical Dimension
CF_4	Tetrafluoromethane
CH_4	Methane
CHF_3	Trifluoromethane
Cl_2	Chlorine
CO_2	Carbon Dioxide
Cr	Chromium
$Cr(NO_3)_3$	Chromium (III) Nitrate
DC	Direct current
DI	De-Ionized
DSL	Digital subscriber line
EDX	Energy dispersive X-ray spectroscopy
FHD	Flame Hydrolysis Deposition
FTTH	Fiber-to-the-home
$GeCl_4$	Germanium Chloride
GeO_2	Germanium Dioxide

HBr	Hydrogen bromide
ICP	Inductively coupled plasma
MFC	Mass Flow controller
O_2	Oxygen gas
P_2O_3	Diphosphorous Trioxide
PECVD	Plasma enhanced chemical vapour deposition
PIC	Photonic integrated circuit
PID	Plasma induced damage
PISD	Plasma induced surface damage
PLCs	Planar Lightwave circuits
$POCl_3$	Phosphorous chloride
PR	Photoresist
RF	Radio frequency
RI	Refractive Index
RIE	Reactive ion etching
Sccm	Standard centimetre cubic per minute
SEM	Scanning Electron Microscope
SF_6	Sulfur Hexafluoride
Si	Silicon
$SiCl_4$	Silicon tetrachloride
TIR	Total internal reflection
UV	Ultra-violet

CHAPTER 1

INTRODUCTION

1.1 Birth of the Planar Lightwave Circuit (PLC)

Optoelectronic technology and optical networking are the best solutions to overcome the restriction of bandwidth and bit-error rate in traditional electrical signal technology. For example, the bandwidth for electronics is only about 10GHz, while the bandwidth for single mode fibre is about 50 THz which is 5000 times larger. Due to this reason the concept of fibre-to-the-home (FTTH) becomes a hot topic in current years. Many countries like Japan, North America, and Europe have adopted FTTH technologies into their communication system. In 2006, Japan alone has had more than 6 million FTTH subscribers online, and became the first country to connect more new FTTH customers than digital-subscriber-line (DSL) customers [1]. While in Malaysia, the FTTH project was launched on July 17th , 2007 to provide FTTH broadband access by the second half of 2008 in Klang Valley, and other major urban centres in Peninsula Malaysia as a preliminary step towards the ultimate digital home experience [2].

Similar to electronics network, optical network require components to switch and manipulate optical signals. The majority of the components used in current systems are electronics based which require optical-electrical-optical (OEO) signal conversion. This

type of signal manipulation technique is costly in terms of network speed, power consumption, hardware complexity and signal integrity (noise). Hence, all-optical switching is becoming more and more important. All-optical switching refers to the direct manipulation of optical signals without conversion to electrical signals before switching takes place [3]. However, conventional bulk optics are relatively large in size and suffer from alignment related issues. As a result, the idea of photonics integrated circuits (PICs) was introduced. The advantage of photonics integrated circuit include long term stability, less susceptible to interference by thermal, and environmental influences, multifunctional, and most importantly the reduction of alignment issues [4]. Although to date, only simple functional chips come into realization due to the limitation of current fabrication technologies, optical power and wavelength splitting chips are playing an important role in many optical network systems such as FTTH network as mentioned earlier. One of the most common types of photonics integrated circuit in recent year is Planar Lightwave Circuits (PLC).

PLC has the property of high component density on a single chip. The components here not only refer to optical components, but also electronics components. In other words, electronics functions can be integrated into a PLC and function together with the optical components in a single chip. Examples of these components are waveguides, grating, emitter (laser source), detector (photodiode), and splitter. Due to its great potential, PLC is attractive to other field like medical, military, and aerospace beside telecommunications. As a result, the application of PLC is expected to grow wider in the future [1].

1.2 PLC as optical waveguides

PLC is a type of optical waveguide that is fabricated on a flat substrate such as silica, silicon or any insulator. A waveguides is a structure that is able to guide wave such as electromagnetic wave. There are many types of optical material suitable for PLC waveguide fabrication. These include silica on silicon, silicon on insulator, silicon oxynitrides, indium phosphide, lithium niobate, and polymer to name a few. However, PLC waveguide that uses silica on silicon is attractive because this platform takes advantages of the well established semiconductor processing technology, low fabrication cost, low optical propagation loss in the optical communication band (C-band), and high coupling efficiency with conventional silica based optical fibres [5]. While silicon wafer offer the advantages of high degree of planarity, good adhesion to silica deposition, high melting point of about $1400^{o}C$ that enables it to withstand the glass transitional temperature of silica, good heat conductive property, availability in market, and a relatively low cost due to its mass production [4].

Silica on silicon refers to two or three layers of silica with different optical properties that are deposited on top of the silicon substrate. These silica layers are responsible for the waveguide operation. The basic operation principle of PLC waveguide is similar to optical fibre, in which light is guided in the silica layer that has a higher refractive index (usually know as core) then the surrounding silica layer (usually know as cladding). This phenomenon is known as total internal reflection (TIR). In order to fabricate silica layer that has different optical properties, dopants like phosphorous, boron, and germanium are doped into each silica layer during its fabrication process. These dopants will affect the

atomic bonding of the silica layer and causes a change in refractive index, glass transitional temperature and other properties that play important role in a waveguide.

In terms of waveguide profiles, PLC waveguide is in planar form as its name indicates. The structure of PLC waveguide core layer can generally be divided into 4 categories. There are slab waveguides, deep ridge waveguides, channel waveguides and ridge waveguides. The cross-sectional geometrical structure of these waveguides is shown in Figure 1.1. While the structure of the core that viewed in z-axis; the wave propagating axis is depending on the function of the PLC waveguides. For example it has a Y-shape for a power splitter [6].

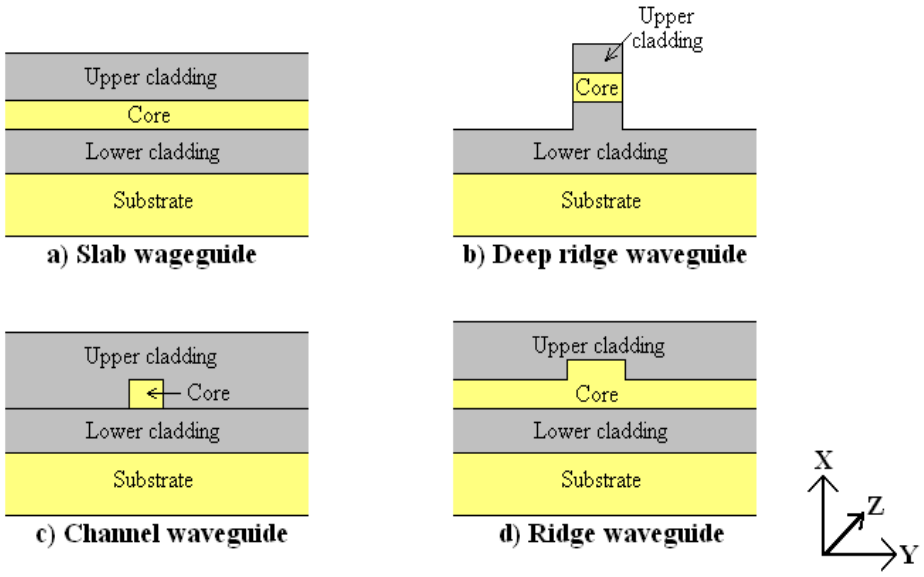

Figure 1.1: Types of waveguides structure with z-axis as light propagation axis.

1.3 Overview of silica on silicon PLC waveguide fabrication technique

The PLC waveguides fabrication processes can be generally separated into two. These two processes are fabrication of glass layer and waveguides definition. The common technique used to fabricate silica glass layer will be discussed in Section 1.3.1 while waveguides definition technique will be discussed in Section 1.3.2.

1.3.1 Fabrication of silica glass layer

There are various techniques that can be used for silica layer fabrication such as Plasma Enhanced Chemical Vapour Deposition (PECVD), Flame Hydrolysis Deposition (FHD) and sol-gel deposition (SGD). PECVD is developed for semiconductor industry and require radio frequency (RF) plasma source to initiate the chemical process between SiH_4 and O_2 or N_2O to form the silica layer. While for FHD, it is a technique based on the process of optical fibre preform fabrication. A high temperature oxy-hydrogen flame is generated, and vapour precursors like silicon tetrachloride ($SiCl_4$) and other dopant will undergo hydrolysis in the flame and form glass soot particles. The soot particles are then deposited uniformly on a silicon wafer. In both techniques, the refractive indices of the resulting silica film can be easily controlled by adding small amount of dopant like phosphorous and germanium. Besides, both techniques require thermal annealing process that reaches temperature above 1000^0C to consolidate the soot layer from the product of FHD or to reduce the concentration of Si-H bond from the product of PECVD. The uniformity of glass formed in PECVD process is much better than the glass formed by FHD process. However the PECVD glass deposition technique is much more time consuming compared to FHD deposition. On the other hand, the sol-gel deposition method is based on the

synthesis of glass via solution chemistry. Glass is directly formed from suitable chemical compound by chemical polymerisation. Hence it does not require high temperature in its process although it still requires sintering stages. Temperature of about 500^0C will be sufficient for this process. The drawback of this method is the difficulty to prevent cracking of the layer during its long sintering time [4, 6]. In this work, the silica glass layer is fabricated by FHD technique and its detail will be discussed in Chapter 3.

1.3.2 Waveguides definition

Currently, there are few techniques that can be used for waveguides definition. For example direct UV-writing, femtosecond direct writing and lithography plus etching. In terms of research purposes, direct UV-writing and femtosecond direct writing are more suitable. This is because these techniques do not require a parent mask in which the fabrication cost for a parent mask is very expensive. Hence it is more worthwhile in terms of fabricating new devices or prototypes for testing or verifying stimulation results. However, this technique requires expertise in optical alignment, stage automation for waveguides definition process and photosensitive glass layer. In general, the operation principle for this technique is to focus a UV beam or femtosecond beam with beam waist equivalent to the channel width onto the glass layer, and by traversing the beam or the glass to define the channel. When the glass layer is irradiated by the UV beam or femtosecond beam, defects are induced in the glass layer and cause changes in refractive index in the near IR region. Usually, the change of refractive index is positive compared to its surrounding glass layer and thus fulfil the requirement for TIR principle to guide light [4].

The second channel definition method is lithography plus glass etching. This technique is more suitable for mass production due to its ability to produce large number of identical devices per process, leading to very low fabrication cost per device. Besides, this technique does not require a photosensitive glass layer, expertise in optical alignment and stage automation. The drawback of this technique is the extra few processing stages that lead to the increase in fabrication errors and the large capital on dedicated, specified equipments for these processes. In general, the glass etching process requires a metal masks that is form by chromium or carbon that consist of the channel pattern. However, in order to transfer this pattern onto the metal mask, another layer of polymer called photoresist (PR) need to be spin coated on top of the metal mask. This polymer is responsible to gain the waveguides channel pattern from photomask during lithography process and then transfer the pattern onto the metal mask, so that the glass layer will have the identical pattern as the photomask after the etching process. In total, two stages of etching are required to etch the metal mask and the core layer.

1.3.2.1 Lithography

There are few different lithography techniques that can be used in waveguides definition. For example, optical lithography (photolithography), electron beam lithography and imprint lithography. The most common patterning technique used is the optical lithography because of it high throughput although it has low resolution compared to the other two techniques mentioned earlier. However, a pattern resolution of 150nm for non-contact type lithography is sufficient for waveguides fabrication with channel width of a few microns. For research or low volume production purpose, contact type photolithography with a

resolution of 0.8 micron using a common mercury lamp (I-line 365nm) as source is sufficient. In contact type photolithography, the UV light source is irradiating parallel onto the parent mask that makes mechanical contact with the photoresist in the mask aligner. For a positive photoresist, the area that is irradiated by the UV light will undergo chemical reaction like cross-link among the monomer molecule. The cross-linked molecule causes a change in property of the resist suitable for etching. This process is more commonly known as developing. The metal mask is exposed at this stage, leaving only the area where waveguides channel will form still covered by the PR. The PR will act as a temporary mask for metal mask etching, and the metal mask will be the hard mask for glass etching. In this work, contact type photolithography, with metal mask fabricated by direct current (DC) sputtering will be used and their detail will be discussed further in Chapter 3.

1.3.2.2 Etching

In wafer fabrication, etching refers to a process in which some unwanted part of a certain layer is removed from the wafer, i.e., either from the silicon substrate itself or from any film or layer of material on the wafer. There are two major types of etching: dry etching and wet etching.

Wet etching is an etching process that utilizes liquid chemicals or etchants to remove materials from the wafer. Areas not covered by the mask are 'etched away' by the chemicals while those covered by the masks are left almost intact. A simple wet etching process may just consist of dissolution of the material to be removed in a liquid solvent, without changing the chemical nature of the dissolved material. Wet etching is generally isotropic.

Isotropic means that the etching process proceeds in all directions at the same rate. On the other hand, an etching process that is not isotropic is referred to as anisotropic. For example, an etching process that proceeds in only one direction (e.g., vertical only) is said to be completely anisotropic. In waveguides fabrication, a high degree of anisotropy is desired in glass etching because it results in a more faithful copy of the mask pattern, since only the material not directly under the mask reacts with the etchant. Furthermore, wet etching is not practical for use in pattern images that have features measuring less than 3 microns due to it high bias properties. Other than the resolution limitations, there is a widespread use of wet etching because of its low cost, high reliability, high throughput, and excellent selectivity in most cases with respect to both mask and substrate materials. Moreover, automated wet etching systems add even more advantages like greater ease of use, higher reproducibility, and better efficiency in use of etchants.

In contrast to wet etching, dry etching process does not utilize any liquid chemicals or etchants to remove materials from the wafer, and generates only volatile byproducts in the process. The mechanism for dry etching can be through chemical reactions that consume the material using chemically reactive gas plasmas or physical removal of the material, usually by momentum transfer between gas molecules or a combination of both physical removal and chemical reactions. Plasma etching is an example of a pure chemical dry etching technique. On the other hand, physical sputtering and ion beam milling are examples of pure physical dry etching techniques. Lastly, reactive ion etching (RIE) is an example of dry etching that employs both physical and chemical processes. The type of glass layer used is also one of the factors that affect the choices of etching process used.

For example, silica layer is non-reactive hence RIE system is more suitable to be used. Moreover, dry etching systems are highly anisotropic. This is the reason why RIE is widely used in wafer fabrication although expensive machines like inductive coupler plasma (ICP) is required. A comprehensive study on RIE etching on silica glass layer was carried out in this work, and the detail or operating principle of RIE is discussed in chapter 2.

1.4 Objective

As mentioned in Section 1.1, passive devices are very important in FTTH network implementation. In fact passive devices can be considered as the major components used in such networks. As a result, fabrication of low loss passive devices has great market potential not only in local markets but also in international level. However, none of our local companies has acquired these technologies or are able to fabricate these passive devices with comparable specifications to the international standard. Hence, it is important for us as local researchers to acquire these fabrication technologies.

As mentioned in Section 1.3, the overall fabrication process of passive devices can be separated to a few categories like design and stimulation, glass fabrication, lithography for pattern transfer, glass etching, and alignment and packaging. In order to fabricate good devices, each of these fabrication steps must be optimised.

The glass etching process currently being used in University of Malaya does not produce the desired etching performance. The recipe used achieved an etching rate of about 200 nm/min but with low selectivity profile (less then 20). Under this condition, good passive

devices for example a splitter can not be fabricated. This is because a very thick layer of chromium hard mask is required to protect the glass channels in order to compromise the low selectivity effect. Increase in the chromium thickness is not feasible in terms of costing and technically it will lead to other problems like low quality pattern transfer, rough side walls, and faceting effect, which will be discussed in chapter 4. Therefore, optimization of the ICP process for silica glass etching is essential as part of the development for passive optical device fabrication in our facility.

There are several ICP parameters to be optimised in order to obtain good etching quality. These parameters are ICP power, bias power, operating chamber pressure, reactant gas composition, and reactant gas flow rate and working distance. These parameters directly define the property or the characteristics of the glass etching. A good etching must have characteristics of high glass etching rate with good selectivity of chromium to glass. The channels must display smooth side wall and perfect right angle of the side wall profile. Besides the above, the resultant sample must be free from polymerization.

In summary to obtain devices that will adhere to strict international standards, optimisation of the various ICP parameters is crucial. The result of such exercise is elaborated in chapter 4.

1.5 Thesis structure

This work has been structured as follows. In Chapter 2, an overview of ICP as dry etching process for silica-on-silicon is presented. It covers from the beginning of plasma definition

up to plasma generation by ICP and the mechanism of how the plasma particles etch the silica target. Furthermore, the channel etched profile and loading effect in the etched sample is also discussed. Lastly, it also covers the error analysis of few special terms that require calculation like etching rate and selectivity. While in Chapter 3, the experiment setup and the samples preparation step is discussed in detail. The preparation steps cover from deposition of silica soot by FHD, glass consolidation, hard mask deposition, photolithography and wet etching process. The entire results for ICP etching and its related discussion is presented in Chapter 4. In this chapter, optimization of the ICP machine and the criteria used to determine the optimised parameters is discussed. The final chapter concludes the works that has been carried out and suggestions of future works.

References

[1] Pearson, M.(June 2007). FTTx *Technologies: Planar Lightwave Circuits Revolutionize photonics*. Laser Focus World, 43, 6. Retrieved March 27, 2009, from http://www.laserfocusworld.com .

[2] TM showcases fiber-to-the-home (FTTH) technology delivering high-speed broadband access service from 10MBps up to maximum speed of 100Mbps to the home. (2007, July 17). TM Malaysia . Retrived March 27, 2009, from http://www.tmrnd.com.my.

[3] D.J. Mynbaev, & L.L.Scheiner (2001). Fiber-Optic Communications Technology. New Jersey: Prentice Hall.

[4] F.R.M. Adikan. (2007). Direct UV – Written Waveguide Devices. Unpublished doctoral dissertation, University of Sauthampton, Sauthampton.

[5] S.T. Jung, H.S. Song, D.S. Kim & H.S.Kim. (1999). Inductively Coupler Plasma etching of SiO_2 layers for Planar Lightwave Circuits. Thin Solid Film, 341, 188-191.

[6] M. L. Calvo, & V.Lakshminarayanan. (2007). Optical Waveguides:From Theory to Applied Technologies. Boca Raton:CRC Press Taylor & Francis Group.

CHAPTER 2

LITERATURE REVIEW

2.0 Inductively Coupled Plasma as dry etching process in silica-on-silicon waveguide fabrications

As mentioned in Section 1.3.2.2, dry etching was chosen to fabricate silica-on-silicon waveguide due to it anisotropic property. Among the techniques used in dry etching process, reactive ion etching generated by inductively coupled plasma (ICP) is more appropriate to be used due to its high etching selectivity and high ion energy property. This is because silica is a relatively inert material and requires significant amounts of ion energy to promote the etching process. ICP etching can be described as the selective removal of material in the gas phase usually under partial vacuum and plasma system. The plasma generated by ICP technique has high density of about $1x10^{11}$ cm^{-3} to $1x10^{12}$ cm^{-3}. The ion energy towards the wafer is independently from plasma generation ICP power but it is controlled by the RF bias that applied. Hence this technique is able to reduce the surface damage on the samples as compared to other plasma generation technique like capacitively coupled plasma. With operation chamber pressure of about 10mTorr, the ICP has significant mixing with mean free path of 1 cm, thus producing uniform plasma distribution. The details of plasma generation by the ICP system is discussed further in Section 2.1 while the study of plasma etching is discussed further in Section 2.2 [1-3].

2.1.1 Introduction to plasma

Plasma is defined as the fourth state of matter besides solid, liquid and gas. More than 99% of matter that exist in our universe is in the form of plasma. However, we live on earth in which plasma does not occur naturally. The accurate definition of plasma is given as a quasi-neutral gas of charged and neutral particles which exhibit collective behavior [2].

In order to explain the term quasi-neutral, let us imagine a group of gases that exist in a system. Due to natural collision among the gases, some gases will be excited or ionized. Note that the number of ions and electrons generated from the ionization process are the same and these charged particles will distribute themselves evenly in the system. This results in a system that is in balance and neutral. Now consider the system has been perturbed by adding in an extra electron. Now the system is in an unbalanced state and the electric field of the extra electron will attract the opposite charge particles and repel the same charge particles in the system. Eventually, ions will be attracted toward the extra electron, eventually surrounding the extra electron. Due to the positive charge property of the ion, the effect of the electric filed that causes by the electron will be "shielded" by the ion. The distance from the extra electron up to the point where its potential perturbation drops to 1/e of its initial value is called as Debye length, λ_b. The term quasi-neutral means the system is in neutral (number of ion equal to number of electron) and resistant to any perturbation either from concentration of charge arise or from any potential introduced by external factor. For an ionized gas system that is able to show the quasi-neutral property, the gas must be dense enough until the dimension of the system, L is much larger than the Debye length,

$$L >> \lambda_b \tag{2.1}$$

and the Debye length can be calculated by

$$\lambda b = \sqrt{\frac{KT_e \varepsilon_o}{n_e e^2}} \tag{2.2}$$

Where K is Boltzmann's constant, T_e is plasma temperature, ε_o is permittivity of free space, n_e is plasma density, and e is electron charge.

As discussed in the above paragraph, the charge particles in the system will induce electric field and this electric field will affect the motion of the other charged particles. The term collective behavior means that the motion of all charged particles is not only depending on local conditions but also depending on the state of the plasma in remote regions as well. Going back to the previous example, the concept of Debye shielding is valid if and only if there are enough particles in the charge cloud. When an external electric field applied, all the charged particles in the charge cloud will have the same reaction toward external field. In other words, all the charged particles in the charge cloud have the collective behavior toward the applied external electric field. In order for an ionized gas to shows the collective behavior effect, the number of particles N_D in the Debye sphere must much more greater than 1.

$$N_D >> 1 \tag{2.3}$$

where

$$N_D = \frac{4}{3}\pi\lambda_E^3 n_e \tag{2.4}$$

Besides the quasi-neutral and collective behavior, there are one more criteria that an ionize gas to fulfill in order to classified as plasma. This criteria, the plasma collision frequency, w must be greater than the collision frequency between the neutral particles. The collision frequency between the neutral particles can be calculated by inverting the mean time collisions between two neutral particles, τ. Hence the third criteria can be simplified as

$$w\,\tau > 1 \qquad (2.5)$$

Ionized gas system that fulfills all three criteria above then only can be classified as plasma [2, 4, 5].

2.1.2 Overview of plasma generation in ICP system

There are many methods that can be used to generate plasma. For example, direct current electrical discharge, radio frequency discharge, microwave heating plasma and pulsed plasma discharges. Among these discharge, radio frequency discharge that uses inductive effect is suitable for etching process and thus making it a widely accepted approach. This type of discharge has the advantage of able to generate higher plasma density as compared to other technique, and the electrode itself is located outside the chamber which can avoid erosion of the electrode by the reactant gases. Eventually this will increase the operational life time of the electrode and also able to reduce the contamination from the electrode element in the process.

The schematic diagram of a simple ICP system is shown in Figure 2.1. In general, the ICP system is in cylindrical shape and the diagram shown in Figure 2.1 is viewed from the radius plane. The ICP RF planar coil is located on the top of the chamber and connected to

RF source. The coils are separated from the chamber by dielectric material usually quartz or ceramic which depend on the etch target. The reactant gas was injected to the system from the side and extracted from the bottom of the chamber by turbo molecular pump. The operating chamber pressure is controlled by the gas extraction rate and the injection rate. When RF power is applied on to the coil, it will create a current flow in the coil alternately with the frequency of the RF source. The RF frequency is fixed at 13.56 MHz because this is the only frequency allocated to the industry and research by international communications authorities. Using other frequency range in the system will cause interference to other communication system like mobile phones, VHF broadcast band, or even aircraft communication bands.

Let us consider in the first half cycle of the RF source. When current, I passing through the coil, the current will create a magnetic field, B as shown in Figure 2.1 according to Ampere circuital law.

$$\oint_c B.dl = \mu_o I \tag{2.6}$$

Since the current is varying according to the RF frequency, hence the magnetic field generated will also vary accordingly. The time varying magnetic field will induce an electric field in the discharge region according to Faraday's law.

$$\nabla x E = -\frac{\partial B}{\partial t} \tag{2.7}$$

This induced electric field (in the opposite direction to the current of the RF coil) will drift the electrons in the chamber in azimuthal direction and ions in opposite direction. The drifted particles will collide with other particles including the neutral particles. As a result, energy transferred to the neutral particles and excited or ionized the neutral particle. Finally

discharge occurred and plasma formed. The general solution of equation 2.7 is approximated by Lieberman and Lichtenberg in 1994 as the form below,

$$E_{\theta,z} = E_{\theta,0} e^{-\frac{z}{\delta}} \tag{2.8}$$

$$E_{\theta,r} = fw\delta B_r \tag{2.9}$$

where δ is the skin depth of the RF plasma, typically 1-2 cm in plasma with electron density of $1x10^{11}cm^{-3}$ and B_r is the radial component of the magnetic flux. Equation 2.8 and equation 2.9 mean the azimuthal E-field, $E_{\theta,z}$ decays exponentially into the plasma region while in the radius direction, $E_{\theta,r}$ is proportional to B_r which is first increase with r then falls to zero at the wall. As a result, planar ICPs exhibit maximum power deposition in toroidal shape near the top window. This toroidally shape E-field will induces non-uniform etching rate in the wafer, hence the wafer is usually placed at a few skin depths below the dielectric window for better uniformity. While in the next cycle, the current flow in the opposite directed and creating magnetic field in the opposite resulted the charge particle drifted in the opposite direction and plasma maintained. Takes note that, E-mode discharge due to capacitive field was not discussed because the RF power applied is usually above 600W in which the break down in the azimuthal direction (h-mode) already occurs.

Now the plasma has effectively formed in the chamber. In the plasma system, due to the mobility of electrons being higher than the ions, the electrons will have a greater tendency to reach the surface of the system faster than the ions. These electrons will charge up the attached surface immediately and the surface will build up a net negative charge relative to the plasma. In other words, the plasma potential has an affinity to remain positive with respect to everything in the chamber. The negative-charged surface with negative potential

(usually known as the floating potential) will repel any late coming electrons and attract the ions. This effect is similar to the Debye sphere discussed earlier, and a layer of ions with a certain charge density will form in the surrounding area of the charged surface. This layer is usually known as a plasma sheath. Due to this effect, etching may occur. However, the ion attraction is (usually) not strong enough and results in no or slow etching process. In addition, the ionic attraction is random in all directions and will result in an isotropic etching property. When the negative bias power is applied, it will create an equipotential electric field that is tangential to the sample. This parallel electric field will further reduce the floating potential of the bias platform and direct the ions to bombard the sample vertically and resulting in an anisotropic etching in the sample. The mechanism of how the silica glass is removed or the chemical reaction between the reactant gas and silica glass was discussed in section 2.2. Take note that the bias power must be a negative potential. If a positive potential was applied, the plasma potential would rise to maintain the sheath in front of the bias platform, and the function of the original anode and the bias table would interchange, causing the sputtering to occur in the anode instead of bias platform [1, 2].

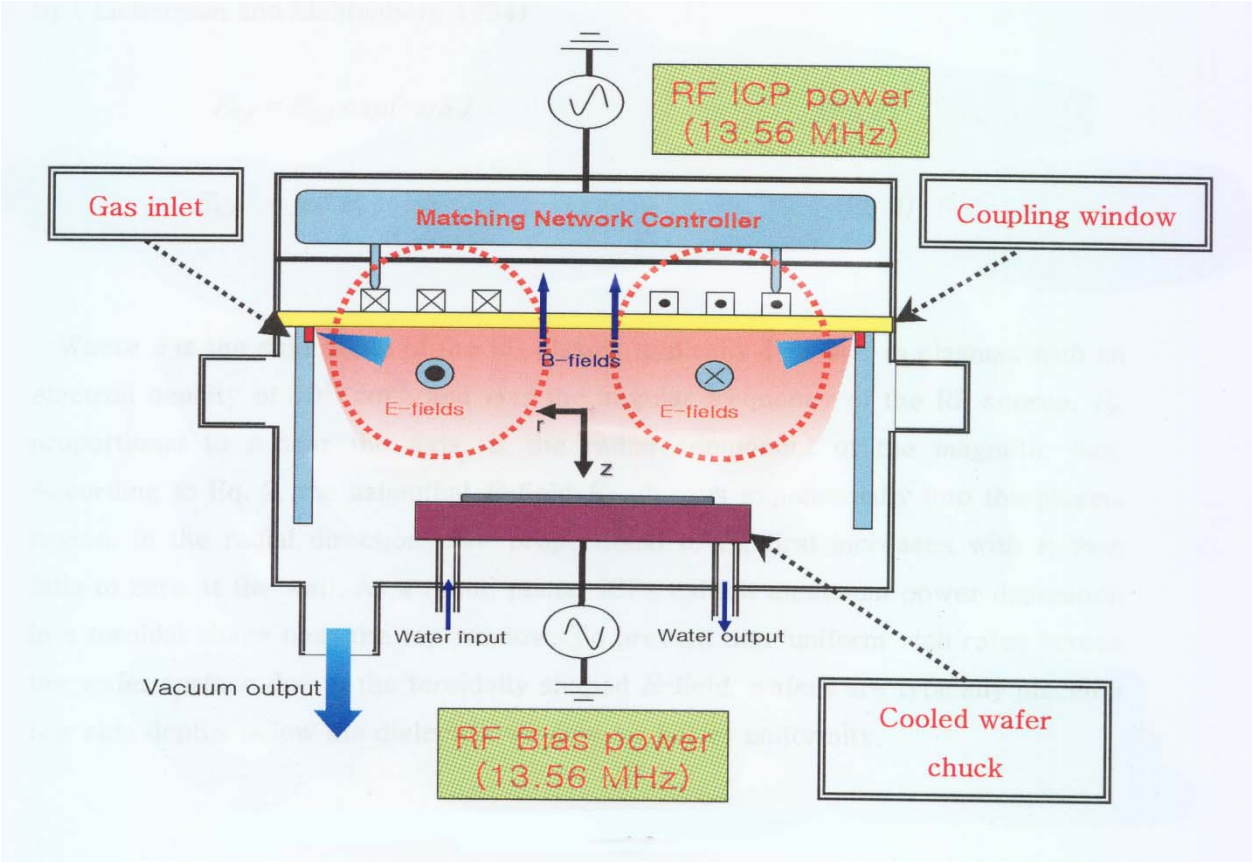

Figure 2.1: Schematic of ICP etching system [1].

2.2 Plasma etching

As mentioned in section 1.3.2.2, the mechanism of plasma etching can be purely through chemical reaction, purely physical bombardment or a combination of both. The mechanism of using purely chemical reaction gives a high etching rate and high etching selectivity between the target material and the mask. Unfortunately, this type of etching does not exhibit a high anisotropic property. This is because the chemical reaction takes place in any contacted surface including the horizontal direction and thus consumes a portion of the material covered by the mask. This phenomenon is known as undercutting. In PLC fabrication, it is important to achieve a high degree of anisotropy etching because a smooth and perfect vertical profile is required to minimize light scattering and maintain a collimated light beam when the etched side wall is used as a mirror surface [6]. The dry etching technique that uses physical bombardment to remove the target surface on the other hand, yields good anisotropic properties. Basically this technique uses highly energetic but chemically inert species or ions to collide then break the atomic bonding of the target surface in order to sputter out the atoms. The ions are usually driven out and accelerated by an electric field to strike exactly perpendicular to the target surface. Unfortunately, such a process is non-selective and it will attack the mask as well. This results in low selectivity between the targeted surface and the mask. Due to this reason, physical sputtering has never become popular as a dry etching technique for wafer fabrication.

A good balance between isotropy and selectivity can be achieved by employing both physical sputtering and chemical mechanism in a same dry etching process. Reactive ion etching (RIE) is one of the techniques that utilize both etching mechanisms. RIE, also

sometimes known as reactive sputtering etching (RSE) involves bombarding the target surface with highly energetic chemically-reactive ions. The bombardment with energetic ions will lead to the physical sputtering effect. Besides, these reactive species will partake in a chemical reaction with the target material to produce a highly volatile byproduct that can easily be pumped out from the system. This is the reason why RIE is widely used in PLC fabrication [3].

2.2.1 Types of reactant gas

The reactant gas used in dry etching must not attack the mask material over the material being etched as well as the material beneath the mask. In general, the criteria that is used to select the reactant gas are that it must have high selectivity against the mask material over the layer being etched, high selectivity against the material under the layer being etched, high etching rate towards the material being etched and excellent etching uniformity. Due to this reason, different types of target material must be used with different type of reactant gases.

Table 2.1: Typical etching gases for various kinds of films in dry etching processes [3].

Material	**Chemistry**	**Comment**
GaAs	BCl_3, Cl_2, HBr, $SiCl_4$	
InP	CH_4/H_2	Smooth, slow, room temperature passivation.
	Cl_2	No polymer formation, fast, high temperature required
Silica	CHF_3,CF_4, C_2F_6, SF_6, CHF_3 C_4F_8 (high density plasma)	
SOI	BCl_3, Cl_2, HBr, HCl	Slow, microelectronics
	C_4F_8 /SF_6	Medium etched rate, smooth

As shown in Table 2.1 several fluorocarbons such as CF_4, C_2F_6, C_4F_8, SF_6 and CHF_3 are commonly used in silica etching. These types of reactant gases are able to form fluorine based ions or free radicals in the plasma which are highly reactive to silica glass. The mechanism of the overall chemical reaction is discussed further in section 2.2.2 and the choice of reactant gas used in this work are discussed in section 4.1.9 [3].

2.2.2 Mechanism of ICP etching process

As mentioned before, the RIE technique consists of both physical and chemical etching. The mechanism of physical etching is simple. It is simply the sputtering of energetic ions onto the targeted surface. Virtually any material can be etched if the ion energy is high and the pressure is low enough for ejected matter to be thrown across the reactor with a few collisions. The etching rate for physical etching is related strongly to the ion current to the surface [7]. However, the mechanism of chemical etching is much more complicated and involves a few crucial steps. Firstly, the reactant gas is ionized and becomes the reactive species in the plasma, and then these reactive species will be diffused due to difference in concentration or directed onto the surface of the material being etched by the electric field. The reactive species will then undergo adsorption by the surface and a chemical reaction take places between the reactive species and targeted material. The byproduct of the chemical reaction is usually in the form of a light volatile species. These volatile species will be desorbed from the surface and finally diffused into the bulk of the gas [7]. Figure 2.2 summarizes the overall process.

The desorption of the reaction byproducts (step 5 in Figure 2.2) from the surface of the material being etched is equally important as the occurrence of the chemical reactions that consume the material. If desorption fails to occur, the etching process cannot take place even if the chemical reactions have been completed. Eventually, this will lead to re-deposition of by-products on the etched surface or passivation of the etched sidewall. As a conclusion, all the steps shown in Figure 2.2 must occur for the plasma etching process (due to chemical reaction) to be successful.

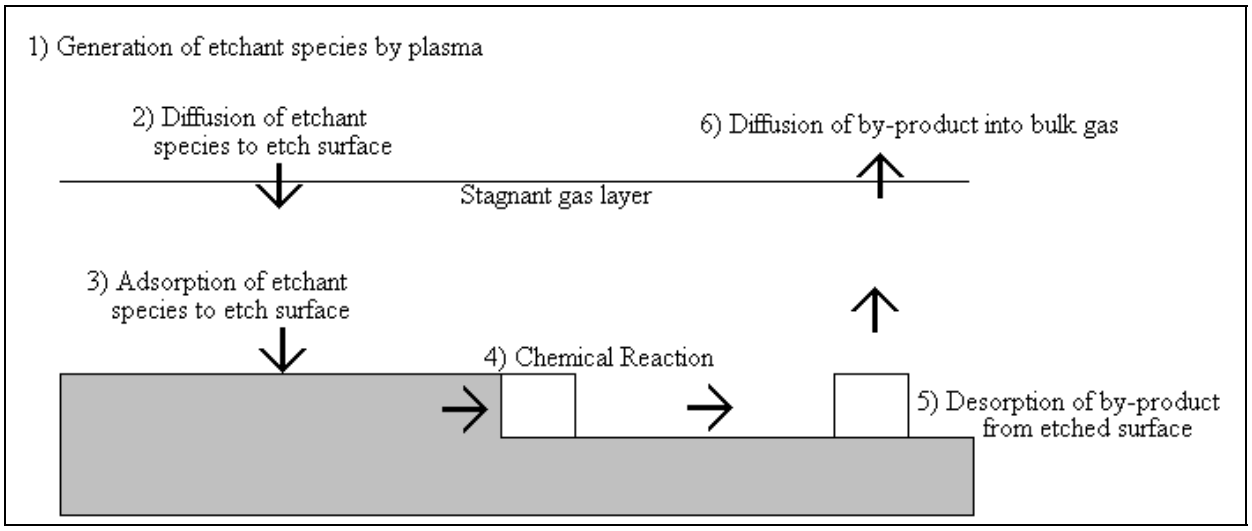

Figure 2.2: Mechanism of dry etching.

The re-deposition of by-products on the etched surface, also known as polymerization or passivation is detrimental to the etching process. Passivation refers to the re-deposition of the by product onto the channel side walls. Polymers on the etched surface will block the reactive species from making contact with the target surface and eventually halt the etching process while passivation might cause disturbance of the wave guiding in the channel or adhesive of the overcladding during deposition process. The effect of polymerization is discussed further in Section 4.2.1.

For silica glass etching, the targeted byproducts are SiF_4 and CO_2 which are light and volatile. However under incomplete chemical reaction processes, byproducts that are in the form of complete polymers may possibly form and lead to re-deposition as mentioned earlier [8].

2.2.4 Etched profile

Figure 2.3 shows several etch profiles that might result from dry etching. Figure 2.3a exhibits the ideal etch profile that is required of PLC fabrication. However, such a profile is difficult to achieve especially for high aspect ratio silica etching. Most of the time, the etched profile will consist of other etch profiles as shown in Figure 2.3b to Figure 2.3e. By choosing the optimal etching condition, this unwanted etched profile characteristics can be reduced.

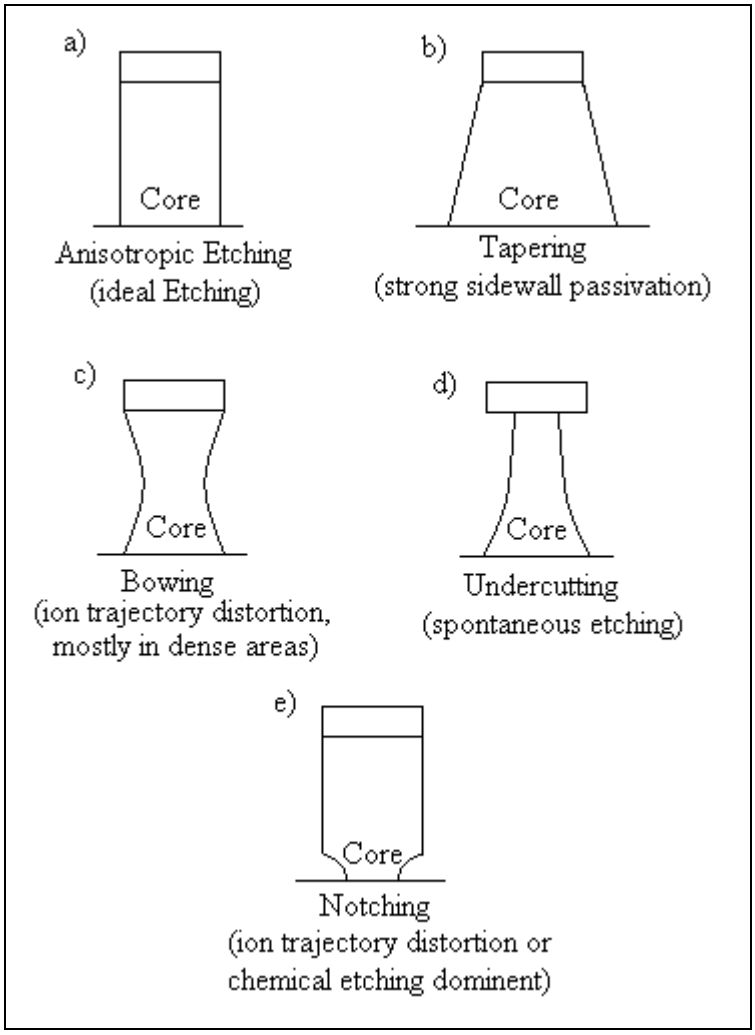

Figure 2.3: Several dry etching profiles

When physical etching is dominant in the etching process, tapering (slanted profile) trenching and mask erosion may occur. Tapering and trenching occurs due to the motion of the particles. For example when the particles colliding with the side wall initially may be scattered and in turn collide again at the bottom of the etching surface near to the channel. This results in trenching. The motion of particles that causes trenching is shown in Figure 2.5. Figure 2.4a and Figure 2.4b shows the actual view of trenching in PLC fabrication that is observed in this work. Besides, as mentioned before the energetic particles are non-selective and they might etch away the matter mask. Eventually the width of the channel mask gets smaller and smaller and this phenomenon is called mask erosion. Mask erosion will cause faceting in the glass etching. The effect of mask erosion in etching is shown in Figure 2.4c.

On the other hand, if the etching is chemically dominant, then it will usually lead to bowing, undercutting or notching. The reason behind this sort of etching profile is isotropic etching properties. As the etching rate in the horizontal direction will be equal to the etching rate in the vertical direction, the area that is not supposed to be removed (under the mask) will eventually being etched away. If this phenomenon is serious, complete undercutting may occur and the metal mask may just peel off from the surface [3, 7].

As a conclusion, the plasma etching mechanism consists of chemical etching and physical etching. By identifying the channel etched profile, which type of etching is dominant can be identified. Figure 2.5 summarizes the mechanism of etching and its effect on the sample.

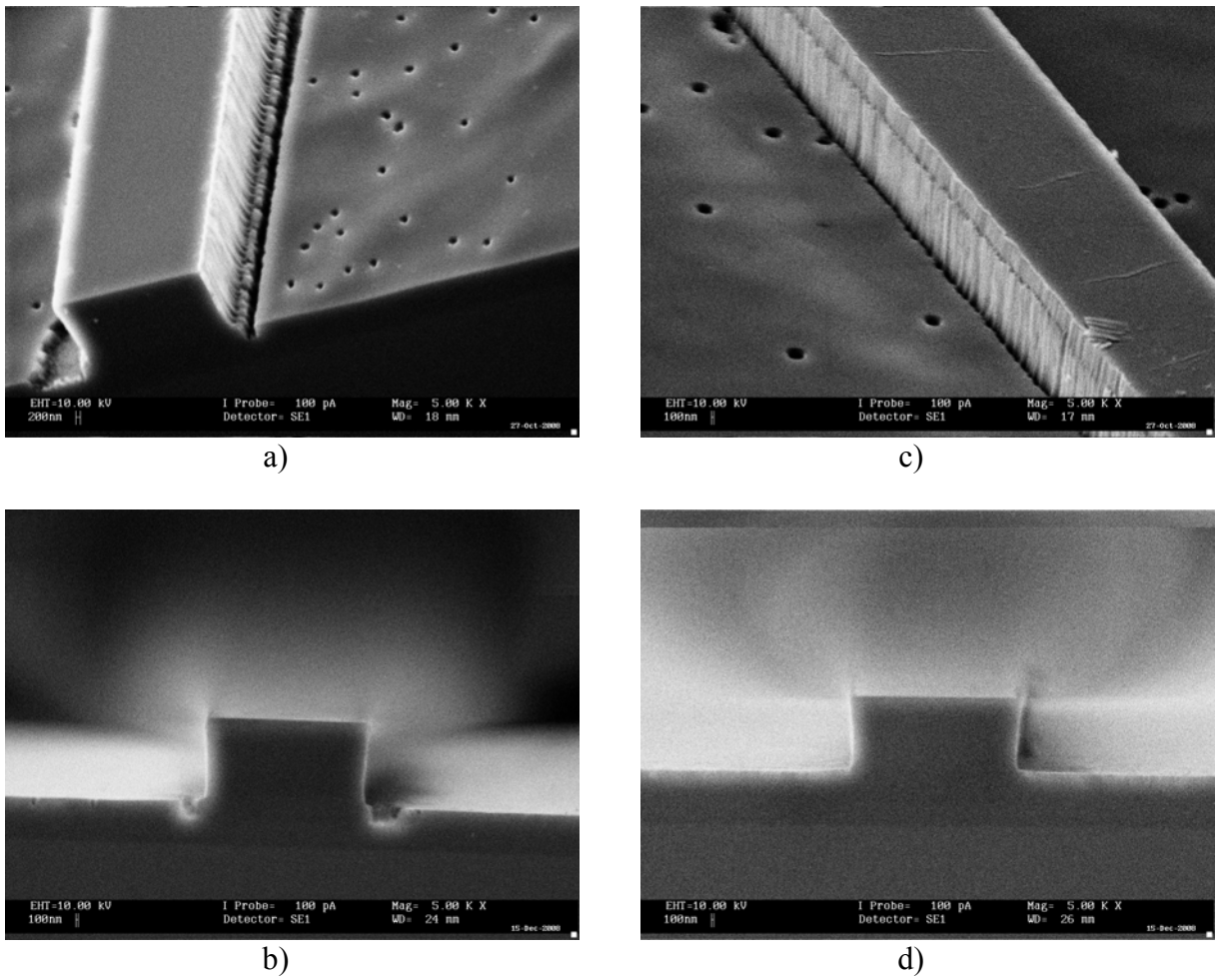

Figure 2.4: SEM images that shows etched profile of a) trenching (side view), b) trenching, c) mask erosion, and d) bowing.

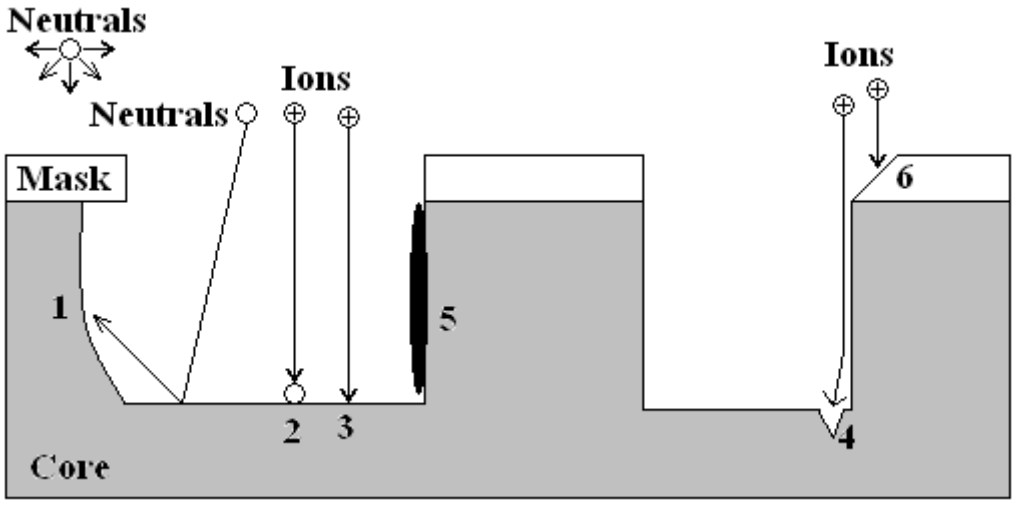

Figure 2.5: Mechanism of plasma etching

1. Chemical etching:	Spontaneous, isotropic and very selective.
2. Ion enhanced etching:	Neutrals and ions involved, ion energy needed to stimulate chemical reaction or to remove reaction products. Anisotropic and selective.
3. Physical etching:	Anisotropic and non-selective.
4. Trenching:	Caused by ion deflection from sidewalls (surface scattering or influence of electric field of charged mask / sidewall).
5. Sidewall passivation:	Deposition of non-volatile materials; etch by-products, surface reactions with certain feed gas additives, mask material.
6. Mask erosion:	Caused by ion bombardment / sputtering.

Due to the imperfection in anisotropic etching, the channel will have some deviation in terms of size from its expected dimensions (for example from the metal mask) as shown in Figure 2.6. This kind of deviation is called the critical dimension (CD). Critical dimension is a measure of how much the etch patterns width differs from the desired pattern dimension while the term critical dimension control describes the requirements and methods to transfer a critical dimension of a mask into the final dimension of the etched feature. A critical dimension control is a sidewall passivation thickness control either dense or isolated lines across the die, across the wafer, and wafer-to-wafer. In order to achieve good a critical dimension, anisotropy etching property plays an important role. The measurement of the degree of anisotropy etching, A is defined as

$$A = 1 - \frac{Horizontal\ etching\ rate}{vertical\ etching\ rate} \tag{2.10}$$

For purely isotropic etching A = 0 and A = 1 when it is purely anisotropic etching [3].

Critical dimension control becomes difficult as the aspect ratio of the pattern is higher. Aspect ratio is a term that relates the targeting etch depth, channel width and channel separation. Referring to Figure 2.6,

$$a + b = a' + b'' = a' + b'' \tag{2.11}$$

thus aspect ratio is defined as,

$$\text{Aspect ratio} = \frac{2C}{a + b} \tag{2.12}$$

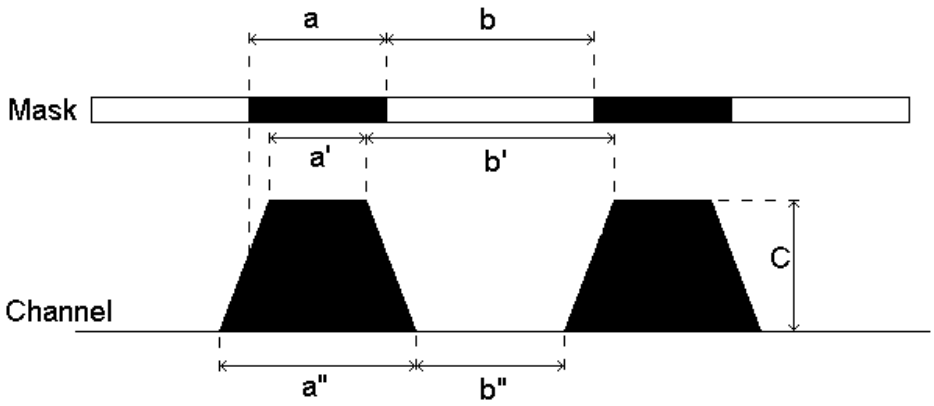

Figure 2.6: Definition of aspect ratio [9].

Besides critical dimension, there exists another term called the resolution. Resolution refers to the minimum achievable separation between channels where complete etching can be done. Usually, dry etching has a smaller resolution as compared to wet etching due to its anisotropic etching property. Critical dimension and resolution are important because it determines the quality of the circuits especially the minimum channel size and channel spacing [3].

2.2.5 Loading effects

Besides etching mechanism, the material of the etched surface and the pattern that is going to be transferred to the sample may also affect the etching property of the sample. Different materials have different atomic bonding energies; hence it will have different dissociation energies required to break these bonds. This results in different etching properties for various types of materials. For example, phosphorous or germanium doped silica will have different etching dependency even for the same amount of dopants. This effect is further discussed in Section 4.2.3.

As mentioned earlier, the pattern will affect the etching property of the sample. The scientific term for this is the loading effect. Examples of loading effects are macroloading, microloading and profile loading. Macro loading effects refer to the phenomenon where the average etching rate of the sample decreases as the total area of the wafer to be etched increases. The decrease in the etching rate is due to the consumption of reactive species since the concentration of reactive species is fixed in the plasma that is generated by a given fixed parameter. According to the Mogab model, the etching rate, ER is

$$ER = \frac{\beta\tau G}{1 + \beta\tau \frac{A_w G}{V}} \tag{2.13}$$

where β is the proportionality factor for the etching species, τ is the mean lifetime of the reactive species, G is the etchant generation rate, V is the reactor volume and A_w is the etchable area.

The microloading effect is almost similar to macroloading but it is comparing the local etching rate within a wafer. The etching rate is lower in a more dense area as compared to a less dense area as shown in Figure 2.7. This effect occurs due to the depletion of the etching species locally caused by the etching process itself [10].

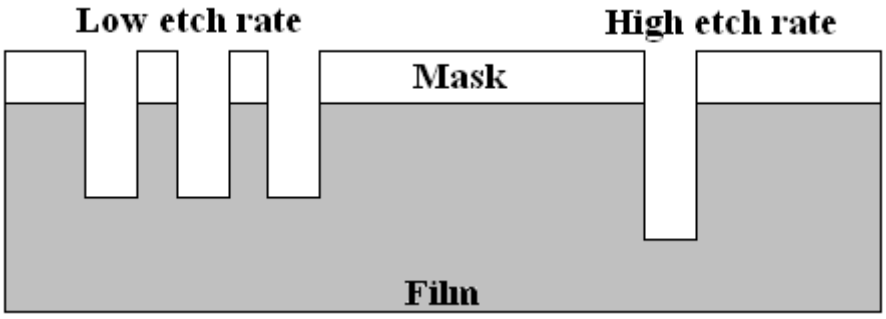

Figure 2.7: Etching rate dependency on feature concentration.

2.3 Etching rate, selectivity calculation and error analysis

Table 2.2: Symbol definition.

Symbol	Definition	Unit
T_{Cr}	Thickness of chromium hard mask	μm
T_{WCr}	Thickness of channel depth with remaining chromium (just after ICP process)	μm
T_C	Actual channel depth (after chromium wet etching)	μm
T_{ECr}	Thickness of chromium etched in the glass etching process	μm
E_C	Local glass etching rate	nm/min
E_{Cr}	Local chromium etching rate	nm/min
S	Local selectivity of chromium to glass etched	-
T_i	Total glass etching time	nm/min
Δ	Error of certain variable	-
$\bar{E}_C$	Average glass etching rate	nm/min
$\hat{S}$	Average selectivity	-

The plasma that is generated by a planar coil usually is in a donut (torus) shape, causing the etching rate and selectivity to be position dependent. As a result, averaging need to be conducted in order to obtain more accurate results. T_{Cr}, T_{WCr},T_C, ΔT_{Cr}, ΔT_{WCr}, and ΔT_C was measured by a surface profiler within the process at n (n=9) different areas distributed evenly within the sample. The local glass etching rate, E_c can be calculated by

$$E_c = T_c/T_i \tag{2.14}$$

and its error is given by:

$$\Delta E_c = \Delta T_c / T_i \quad (2.15)$$

The actual glass etching rate, $\bar{E}_C$ is calculated by averaging all nine E_c s at selected areas and its standard error can be calculated by:

$$\Delta \bar{E}_C = (\text{Standard deviation of n etching rate measurements}) / \sqrt{n} \quad (2.16)$$

Where n is number of measurement which is equal to 9 in this case.

In order to calculate selectivity, the chromium etching rate, E_{Cr} need to be calculated first. E_{Cr} is defined as:

$$E_{Cr} = T_{ECr} / T_i \quad (2.17)$$

where

$$T_{ECr} = T_{Cr} - (T_{WCr} - T_C) \quad (2.18)$$

Standard error for E_{Cr} can be calculated by:

$$\Delta E_{Cr} = \Delta T_{ECr} / T_i \quad (2.19)$$

where

$$(\Delta T_{ECr})^2 = (\Delta T_{Cr})^2 + (\Delta T_{WCr})^2 + (\Delta T_C)^2 \quad (2.20)$$

Finally, the selectivity, S can be calculated by

$$S = E_C / E_{Cr} \quad (2.21)$$

and by eliminating the time factor,

$$S = T_C / T_{ECR} \quad (2.22)$$

The standard error for selectivity, ΔS is calculated by

$$(\Delta S / S)^2 = (\Delta E_C / E_C)^2 + (\Delta E_{Cr} / E_{Cr})^2 \quad (2.23)$$

Similar to the actual glass etching rate, the actual selectivity is the average of 9 local selectivity measurements and its standard error is calculate by:

$$\Delta \hat{S} = (\text{Standard deviation of n local selectivity measurement}) / \sqrt{n} \quad (2.24)$$

Reference

[1] Maintenance and Operating Manual.(n.d). Korea:Hanvac Corporation.

[2] B. Chapman. (1980). Glow Discharge Process. New York: John Wiley & Sons.

[3] M. L. Calvo, & V.Lakshminarayanan. (2007). Optical Waveguides:From Theory to Applied Technologies. Boca Raton:CRC Press Taylor & Francis Group.

[4] F.Chen. (1997). Introduction to Plasma Physics. New York: John Wiley & Sons.

[5] J.R.Roth. (1995). Industrial Plasma Engineering. London:Institute of Physics Publishing.

[6] T.M.Hoa, Charles R. de Boer & Pasqualina M. Sarro. (n.d) Roughness Treatment of Silicon Surface after Deep Reactive Ion Etching. Retrived March 27, 2009, from http:// www.stw.nl/NR/rdonlyres/6A9E9428-9B60-42A2-A229-C6DDD618271D/0/pham.pdf.

[7] D.L.Flamm. (1990). Mechanisms of Silicon Etching in Fluorine and Chlrine Containing Plasma. Pure and Apply Chemistry, 62,(9),1709-1720.

[8] EzzEldin Metwalli & Carlo G. Pantano. (2003). Reactive Ion Etching of Glasses: Composition Dependence. Journal of Nuclear Instruments and Methods in Physics Research Section B: Beam Interactions with Materials and Atoms, 207 21-27.

[9] H. Miyajima & M. Mehregany. (1995). High-Aspect-Ratio Photolithography for MEMS Applications. Journal of Micromechanics system, 4 (4) 220-229.

[10] J. Karttunen, J. Kiihamaki, & S. Franssila. (2000). Loading Effects in Deep Silicon Etching. Proceedings of SPIE 2000, 4174 90-97.

CHAPTER 3

EXPERIMENTAL SETUP AND PROCEDURE

3.0 Introduction

The ICP machine that was used in this work is discussed in Section 3.1 while the sample preparation and requirement is discussed in Section 3.2

3.1 Inductively Coupled Plasma dry etching system

Figure 3.1 shows the ICP dry etching system in the Photonic Research Centre University of Malaya. The ICP system is fully automated. Several controllers manage the various component making up the system including turbo molecular pump power supply, throttle valve controller, mass flow controller, radio frequency (RF) power generator and air valve controller. All these controller are accessed by a laboratory personal via a graphical user interface.

Process gases like reactant gas, hydrogen, oxygen, argon, and nitrogen that flow in to the chamber are controlled by air valves and digital mass flow controllers. The operation range of the digital mass flow controller is in between 0 to 200 sccm (standard cubic centimetres per minutes) with intervals of 1 sccm. The pressure of the chamber is monitoring by pressure gauge like pirani gauge, ion gauge baratron gauge. During etching process, the

chamber pressure can be controlled by throttle valve and turbo molecular pump supported by a rotary pump. The ICP power and bias power were supplied by RF power supply. The maximum limit of RF power supply for ICP is up to 1000 W while 300 W for bias RF power supply. Matching circuit MC2 was used to match the impendent of the circuit in order to deliver maximum power to the system. Notes that, high reflected power will damage the RF power supplier. The load-lock chamber was used for load or un-load wafer to the main chamber. By using the load-lock chamber, minimum contact between the main chamber and the environment is ensured by reducing contamination.

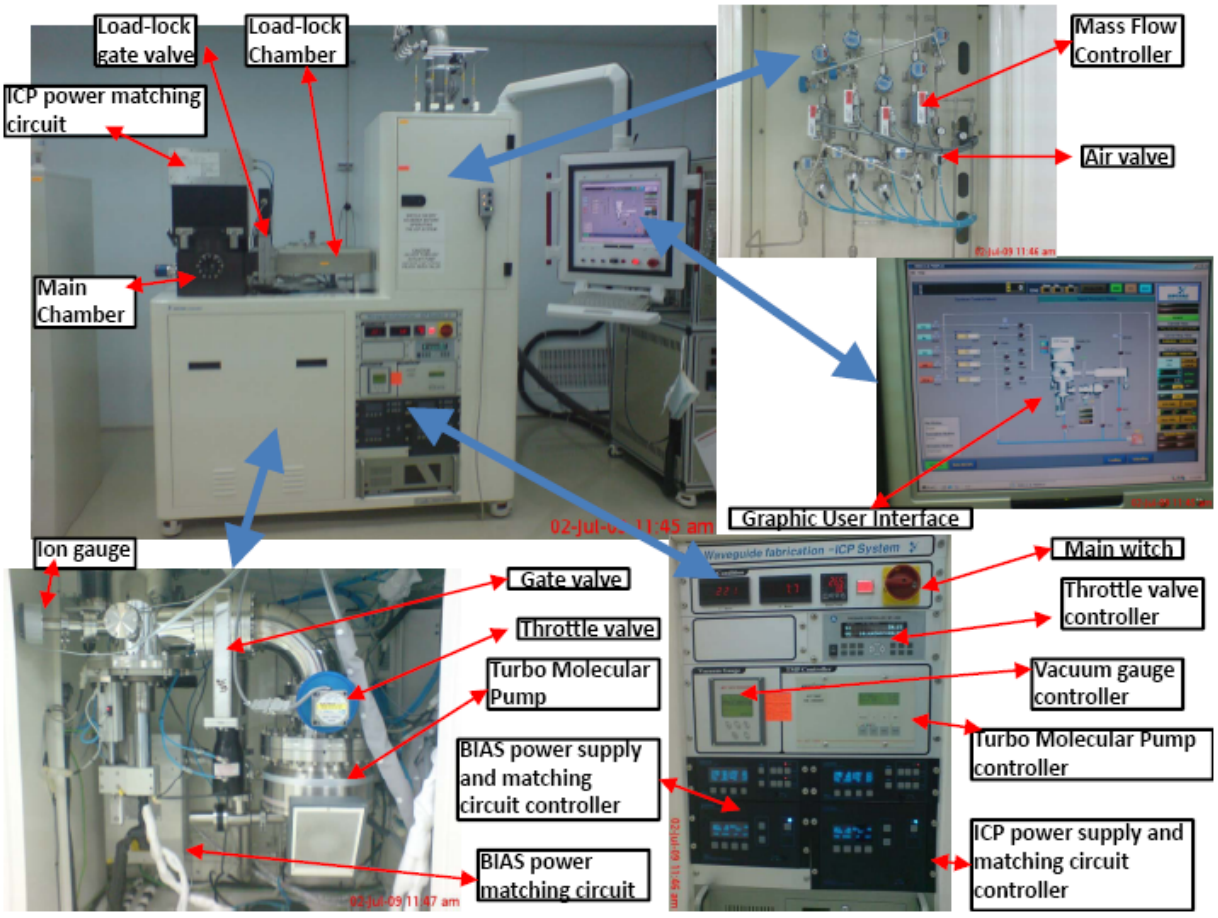

Figure 3.1: ICP dry etching system.

The product gases produced during the dry etching process will be sucked out through turbo molecular pump, and rotary pump to the dry scrubber. A dry scrubber system is an important supplementary component to filter the greenhouse gases such as fluorocarbon and hydrofluorocarbons. Figure 3.2 shows the actual view of the dry scrubber system.

Figure 3.2: Dry scrubber system.

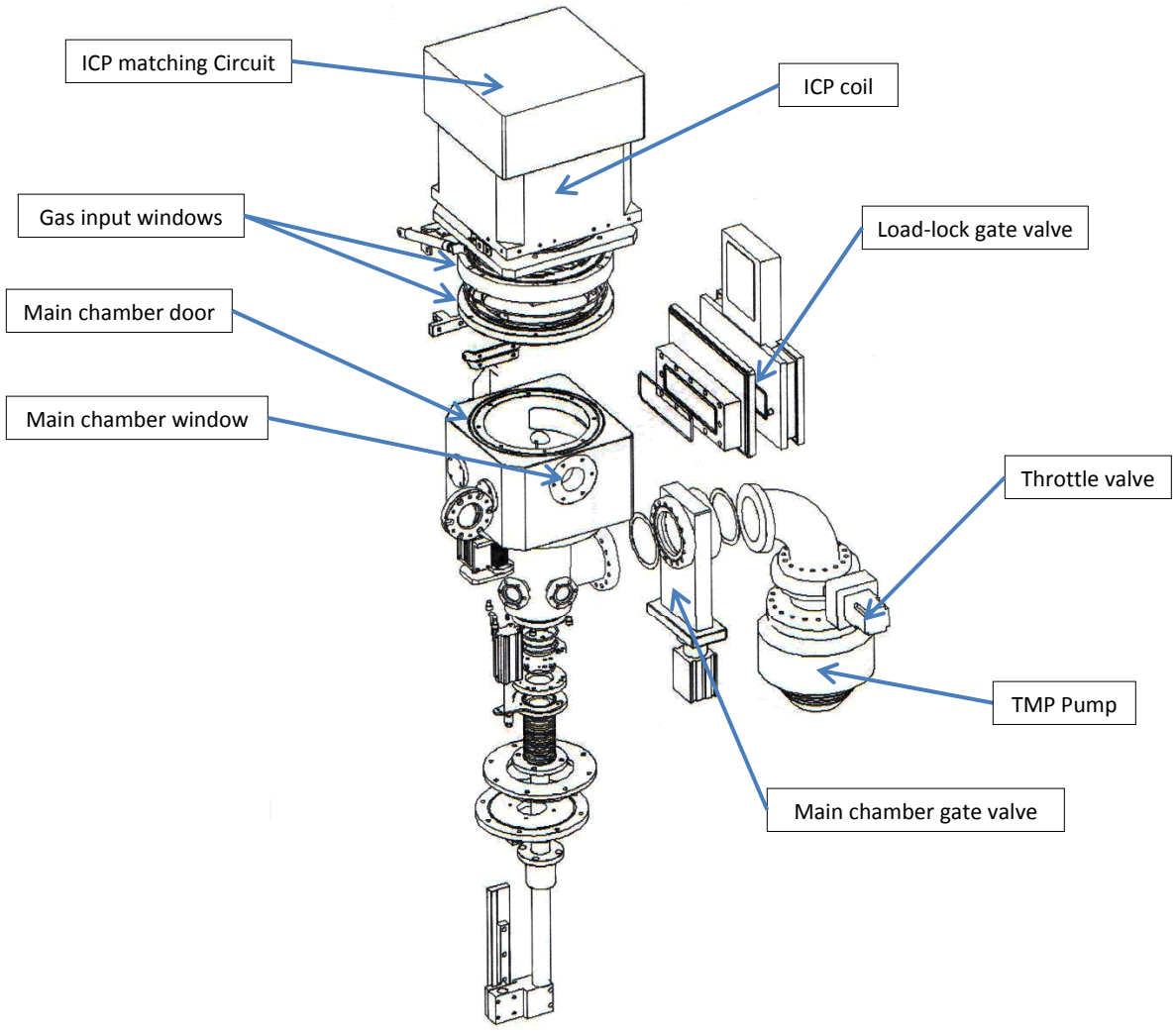

Figure 3.3: ICP main chamber design.

3.2 Experimental requirement and procedure

In this section, all related study on sample preparation for ICP glass etching is discussed at length. These studies include the study of fabrication environment and material requirement, the related sample fabrication process and surface study on the principle of those equipment that used in the fabrication process. The processes involved in sample fabrication consists of glass deposition by FHD, deposition of chromium layer as metal mask by DC sputtering, photolithography and chromium wet etching. All these preparation steps are required in order to determine the etching rate and selectivity accurately in the ICP process. Each of these processes is discussed separately in the next few sections. The summary of the sample preparation flow is shown in Figure 3.4.

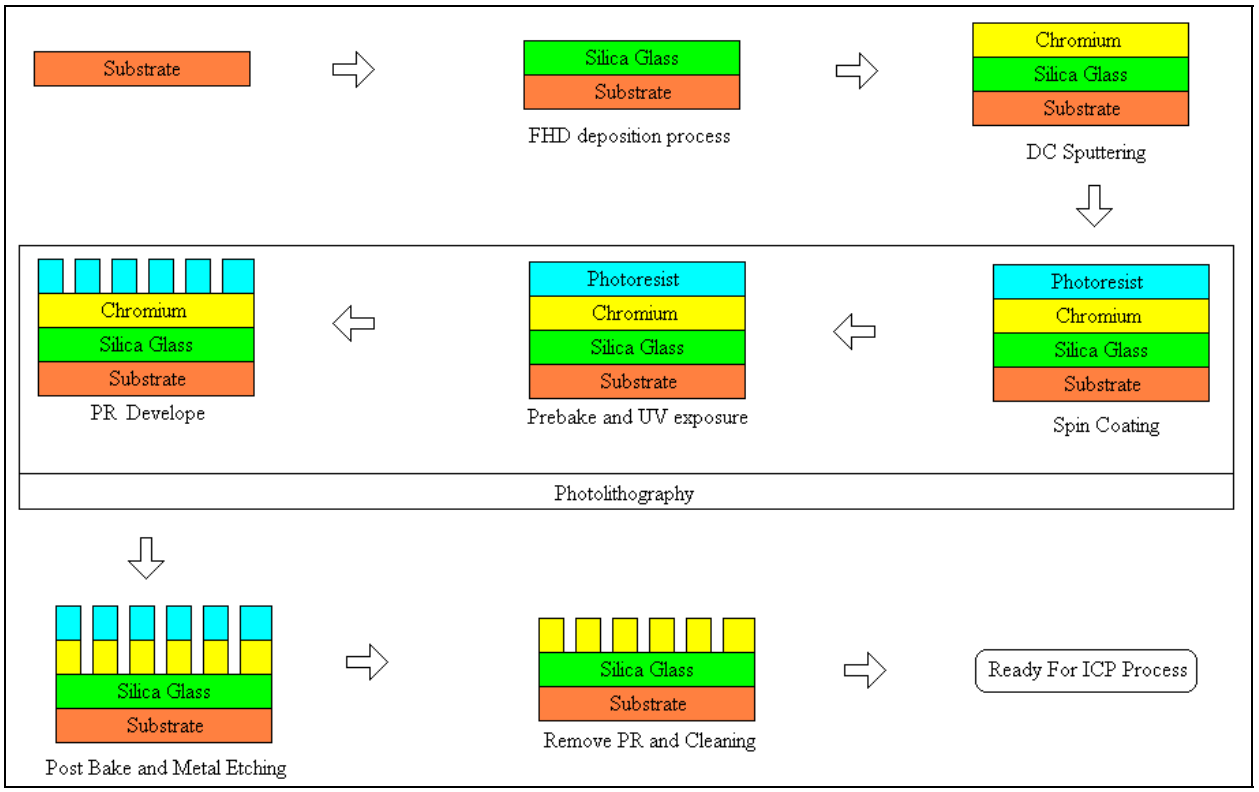

Figure 3.4: Summary flow of the sample preparation steps.

3.2.1 Fabrication environment

To produce good waveguides, fabrication environment must be taken into consideration. Dust particles on the sample during fabrication process such as photolithography can cause permanent defect on the sample. As devices become smaller, the requirements for contamination control become tighter. Therefore, a clean room is required. A clean room is a room in which the concentration of airborne particle is controlled. A clean room must be controlled and monitored very closely from construction to operation. Temperature, humidity, and particle count measurements must be conducted periodically to ensure the clean room is working properly according to the standard required. The clean room must be cleaned frequently by alcohol wiper and special vacuum cleaner. Every clean room user are required to wear lint free clean suits, overshoes, glove, hair cover and mask in the changing room and go though air shower room before enter the clean room.

The clean room in Photonic Research Centre UM is a 10k class clean room. The temperature of the clean room is fixed within 20 ^{o}C to 23 ^{o}C with humidity controlled in the range of 45 % to 55 %. A yellow room was also built within the main clean room area. This room is specially allocated for photolithography process where the light used is UV free. In additions, there are a few facilities installed in the clean room.

3.2.2 Substrate consideration

In order to fabricate a planar glass layer, a substrate is required. There are many materials that can be used as the substrate, for example commonly use are fused silica glass or silicon. The advantage of using fused silica glass as substrateis that it can be used as the under clad of the circuits. However, since the ICP glass etching process is applied onto the glass layer deposited on the substrate instead of the substrate itself, hence silicon substrate was chosen due to its availability and low cost. The requirements for the silicon wafer is summarised in Table 3.1.

Table 3.1: Silicon wafer requirement and specification.

Specification	Requirement	Description
Diameter	4 inch	Fixed by the fabrication machine
Crystal Orientation	110	Convenient for packaging
Buried Oxide	>1.5 µm	Required by the waveguides operating principle and FHD process [1]
Thickness	>1 mm	Required by the FHD process
Surface roughness	Optical grade	In order to fabricate flat silica glass film
Doping Type	P type/Boron	-
Resistivity	1 to 20 ohm	Required by ICP process

3.2.3 Glass deposition

The glass deposition method that was used in this work is Flame Hydrolysis Deposition. FHD is a popular method due to its high deposition rate, low production cost to gain a thick silica glass (from 1 µm to 400 µm) and ability to dope the silica matrix with dopants like germanium, phosphorous and boron with high precision. Dopants are important to manipulate the properties of the silica glass as summarised in Table 3.2. In the FHD process, the precursor gases like Silicon chloride ($SiCl_4$), phosphorous chloride ($POCl_3$), germanium chloride ($GeCl_4$) and boron chloride (BCl_3) were vaporized under bubbling technique by helium gas in their pure solvent and were hydrolyzed in a high temperature oxyhydrogen flame (1300-1500 ^oC) to form their corresponding oxides in the soot layers as refer to Table 3.2 for their chemical reaction respectively. The porous silica soot form were then be consolidated in furnace before it became hard transparent silica glass [2-5].

Table 3.2: Chemical reaction in the oxyhydrogen flame and effect of dopant on silica glass properties [2].

Material	**Chemical reaction in the oxyhydrogen flame**	**Effect on the silica glass**		
		Thermal Expansion	Melting point	Refractive index
Silicon	$SiCl_4(v)+2H_2O(v)\rightarrow SiO_2(s)+4HCl(v)$	-	-	-
Phosphorous	$2POCl_3(v)+3H_2O(v)\rightarrow P_2O_5(s)+6HCl(v)$	Increases	Decreases	Increases
Boron	$2BCl_3(v)+_3H_2O(v)\rightarrow B_2O_3(s)+6HCl(v)$	Increases	Decreases	Decreases
Germanium	$GeCl_4(v)+2H_2O(v)\rightarrow GeO_2(s)+4HCl(v)$	Increases	Decreases	Increases
H_2O was produce in the oxyhydrogen flame where $2H_2(v)+O_2(v)\rightarrow 2H_2O$				

In this work, the flow rates of the hydrogen and the oxygen in the oxy-hydrogen flame were both fixed at 5000 sccm. The flow rate precursor gases are set to 50 sccm, 35 sccm, 40 sccm and 30 sccm for $SiCl_4$, $POCl_3$, $GeCl_4$ and BCl_3 respectively. The soot is then consolidated in oxygen and helium rich environment with 1000 sccm and 2000 sccm flow rate respectively. During consolidation, outgassing will occur. Outgassing is a process where gases like water vapour that were trapped in the soot will be evaporated. This process is important in order to form high density glass. The purpose of consolidating in such environment is to avoid the inclusion of bubble during the outgassing process [6, 7] and remove the water vapour in the chamber so that the water vapour did not diffuse back to the glass. Water molecules that were trapped in the glass will increase the propagation loss due to OH absorption peak at 1380 nm. Although this absorption is not avoidable in glass but it can be reduced by consolidation under such environment. It is also worth noting that multi stage consolidation process with different ramp up time is applied in the consolidation process as shown in Figure 3.5. For example in the first stage, the sample was kept in 200 ^{o}C for dehydration purpose. At the second stage, the sample was kept in 850 ^{o}C for 30 minutes and this process is also known as pre-sintering process. During this process the dopants like phosphorous and boron will melt and fuse in to the silica matrix [8]. At the third stage, the sample was heated at 1270 ^{o}C for a short duration of 10 minutes. Finally, the glass is being consolidated at 1350 ^{o}C for an hour. In this stage, the silica soot will melt into viscous liquid form. The molten glass will slowly be quenched into a final transparent glass once the temperature is ramped down [8].

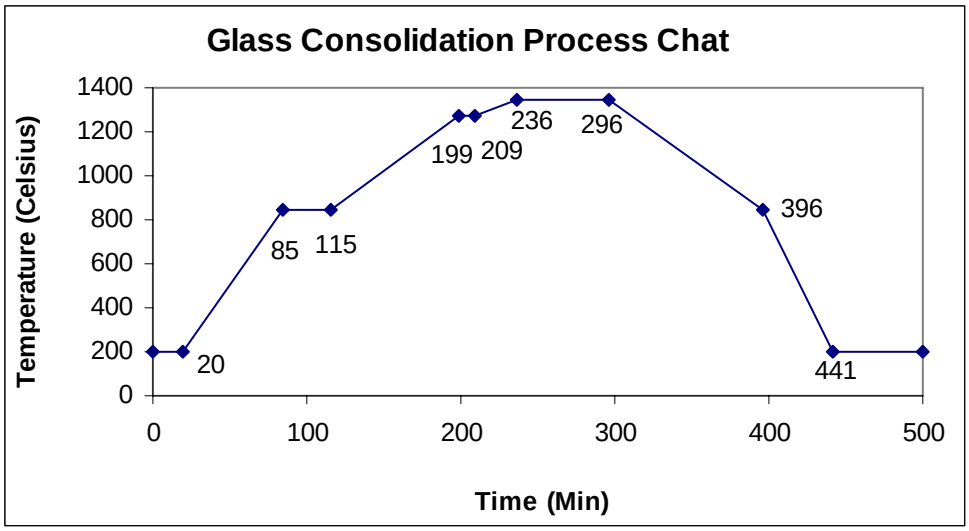

Figure 3.5: Glass Consolidation Process Chart.

The multi-doped silica glass formed using the above recipe has refractive index of 1.4530 ± 0.0003 at 1550 nm measured by prism coupling method. The thickness of the silica glass formed is around 5.5 ± 0.1 µm with average roughness, Ra about 17.0 ± 3 nm in a 0.2 mm X 0.2 mm region. The surface roughness profile of the silica glass film is shown in Figure 3.7. The propagation loss of the silica film from the prism coupling methode is about 0.980 ± 0.005 dB/cm in 1550 nm and the result is shown in Figure 3.8. The result of energy dispersive X-ray spectroscopy (EDX) composition analysis is shown in Table 3.3. The glass layer with property as mentioned above is used as the core layer in AWG fabrication in Photonic Research Centre UM and for consistency this glass fabrication recipe was used throughout the ICP optimization process. This is because different recipe will produce different optical as well as mechanical property and eventually will result in different ICP glass etching. This effect is discussed further in Section 5.2.

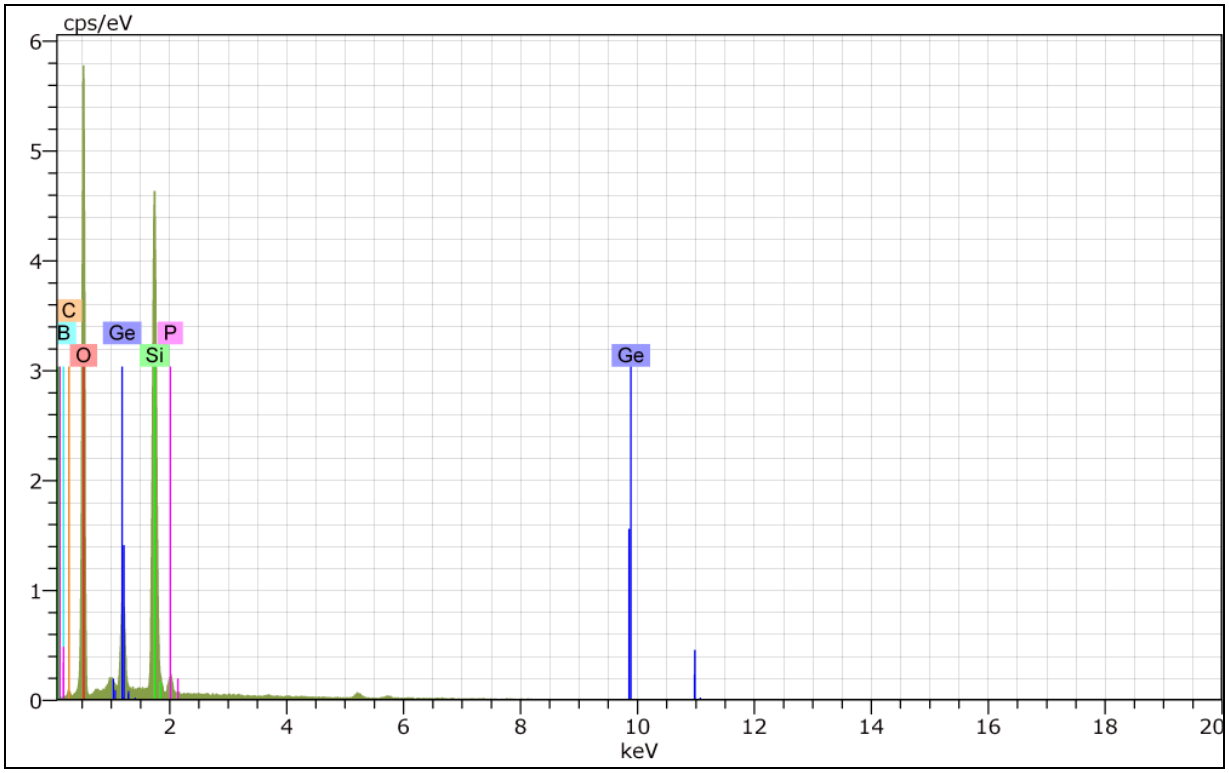

Figure 3.6: Composition analysis (graph) of the silica glass film by EDX.

Table 3.3: Summary of composition analysis of the silica glass film by EDX.

Compound	**Atomic %**
Silicon	17.32
Germanium	3.03
Phosphorous	0.80
Oxygen	72.83
Boron	6.02

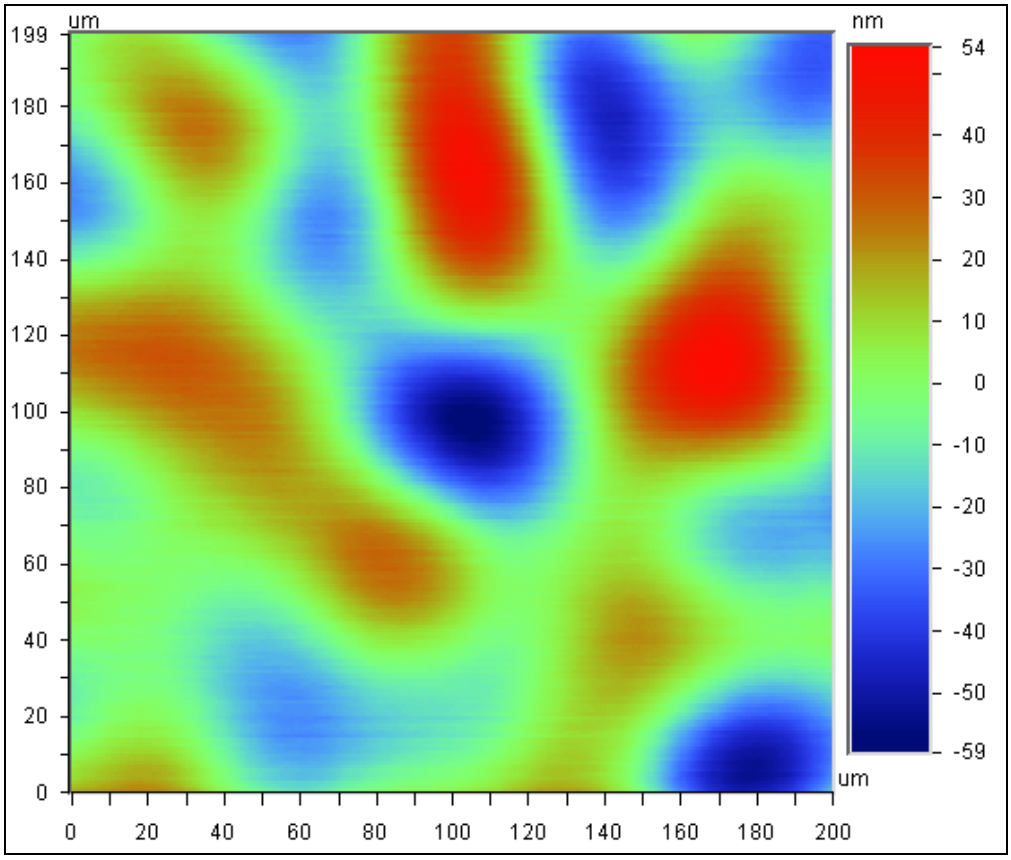

Figure 3.7: Surface roughness profile of the silica glass film.

(Average roughness,R_a is 17 ± 3 nm where Ra is defined as arithmetic average of the absolute values. Absolute values, Rt is 113nm in this case and it is defines as the range of the collected roughness data point or maximum height of the profile.

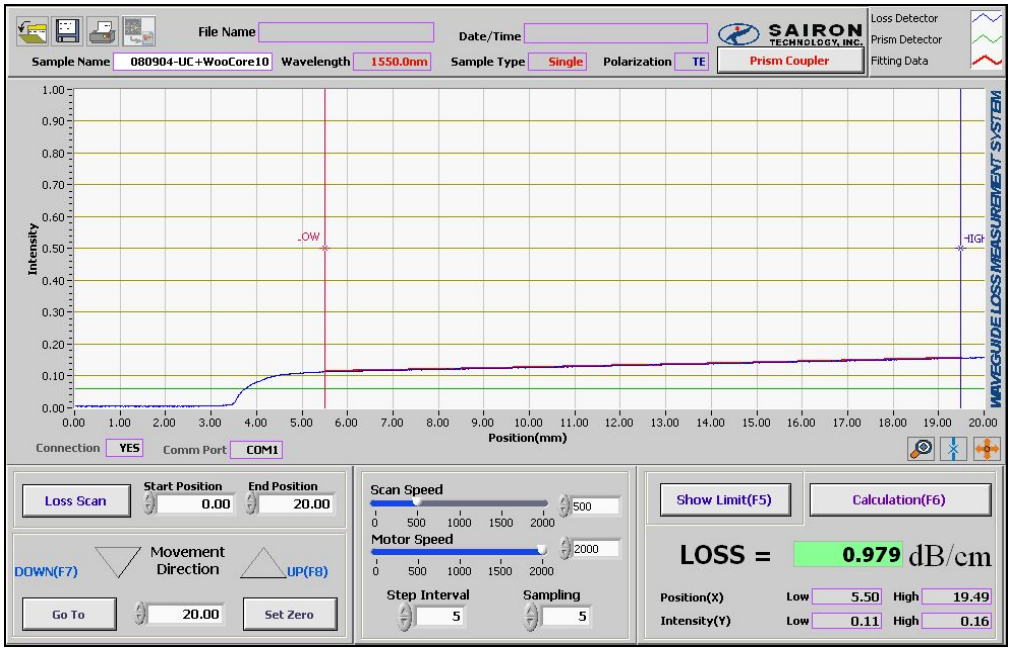

Figure 3.8: Propagation loss measurement from prism coupling technique.

3.2.4 Chromium deposition

In the ICP glass etching, the core (the wanted part) needs to be covered by a mask. The mask must be hard, non volatile, and chemically stable. Due to this reason, chromium was chosen. Chromium was deposited on top of the silica glass film by DC magnetron sputtering. In short, this process use the physical bombardment of plasma particle on to the pure chromium target (the cathode, purity is 99.99 %) to sputter out the chromium atom. The sputtered atoms are then deposited on to the wafer (anode).

Initially the sample was loaded into the working chamber through a load lock chamber. The chamber was then vacuumed to about 4×10^{-6} Torr. This step is important to minimise the impurity gas and water moisture in the chamber. Once the desired pressure was reached, purified 99.999 % Argon gas was supplied to fill the chamber. Any inert gas is suitable to

be used as ambient gas. However, since the sputtering process is basically a momentum transfer process, inert gas like helium or Neon are considered too light and will cause low energy transfer efficiency. Heavy inert gas like krypton are also not considered because there will scatter away the sputtered atoms that are moving toward the wafer although it is good in energy transfer. The operating chamber pressure was fixed at 6mTorr while the argon gas flow rate was fixed at 5sccm. Once the argon flow rate and chamber pressure are stable, the DC power supply voltage was increased slowly until glow discharge plasma was generated. The breakdown current was set at 0.8 A throughout the process. The breakdown voltage is depending on types of gas used, pressure of the chamber, and distance between the two electrodes. After the glow discharge was generated, the system required some time for the discharge to become stable, and this can be observed from the power supply reading. Within this period, the wafer was covered under a shutter to prevent deposition, which is referred to as pre-sputtering process. The purpose of pre-sputtering process is to remove the oxide layer or contaminants which cover the target surface [9]. After 9 minutes of deposition process, the DC power was reduced slowly to 0 V to stop the discharge process and cycle purge was conducted. In the cycle purge process, the system was disconnected from the pump and the chamber pressure was allowed to increase by flowing in the argon gas. Once the chamber pressure reaches about few mTorr, the argon gas supply was disconnected and chamber was connected to the pump followed by pumping down the chamber. This rapid pump down will create turbulence in the chamber and it will flush out the entire sputtered chromium atom which is harmful to humans. The cycle purge process was repeated at least 3 times before the sample was loaded out.

3.2.5 Photolithography

Photolithography is a process of transferring pattern of geometric shapes on a photomask to a thin layer of photosensitive material usually known as photoresist that covers the whole surface of a substrate wafer. The photoresist used in this work is PR-AZ1512 from AZ Electronic Material Company. This photoresist is sensitive to I-line (365 nm) with viscosity of 19 mPas. Its density is 1040 kg/m^3 and the surface tension is 32 N/km [10]. PR-AZ1512 is a positive type photoresist. It means that the area that was exposed to UV light will be removed during the developing process [11]. During the UV expose process, the UV irradiations will activate the crosslinking process among the polymer. The crosslinked polymer will be chemically stable and do not react with developer AZ726 MIF but for those un-crosslinked polymers, it will react with the developer and dissolve into the developer. Eventually, all the area that exposed to UV will be removed (etch away). Using this advantage, the pattern from the photomask can be transferred to the photoresist and the step is the most limiting factor to determine the side wall roughness and minimum feature size and other characteristic [12].

Photoresist was deposited on to the sample by using spin coating method. Spin coating is a very good method to deposit liquid based solvent on to a large surface area uniformly. The thickness of the coated film can be very thin up to submicron range with uniformity up to 5 Å [13]. This deposition method is cheap, fast, consistent and easy to handle. The thickness of the film deposited by this method is depending on the viscosity of the photoresist, spin time and spin speed (inversely proportional to square root of the spin speed). Hence the film thickness can be easily controlled by the spin speed. However, the spin speed must not

be slower than 1000 rpm. This is because the surface of the photo resist will not be smooth. The film smoothness is proportional to the spin speed. The only disadvantage of using spin coating method is that the approach is not environment friendly. This is because more than 90 % of the photoresist will be wasted in the spin coating process and photoresist is a hazardous material [11, 13, 14].

Before the photoresist deposition process begins, photoresist PR-AZ1512 needs to be heated to room temperature. This is because the viscosity of the photoresist is temperature dependent. Using a pipette, 3 ml of photoresist was dispensed on the sample wafer that was earlier placed on the spin coater. The pipette must be held as near as possible to the centre of the wafer surface to reduce the chances of trapping air or dust during the process. Air bubbles or dust that traps in the photoresist will cause defects in the photolithography process. The sample was then accelerated slowly to 100 rpm for 10 second with 10rpm/second ramp up speed. The purpose of this stage is to spread the photoresist toward the edge of the sample wafer and the ramp up speed need to be slow in order to provide the photoresist has sufficient time to spread and cover the whole wafer area. Then the sample was spun at 6000 rpm for 1 minute with total of 10 second ramp up time. During the second stage, the photoresist will undergo a thinning process due to centrifugal forces [15]. Finally, the rotation speed was ramped down to 0rpm with a 10 second ramp down time

After the spin coating, the photoresist will undergo prebaking. The purpose of this process is to remove solvent from the photoresist and increase resist adhesion to the wafer [11]. Prebake temperature and time are critical. The photoresist film cannot be too dry because

this will reduce the photosensitivity of the photoresist and eventually the resolution reduces [16]. Besides, the photoresist film will be difficult to develop completely or removed if it is over baked. Hence, prebake time is important and need to be optimise to achieve straight and near vertical sidewall profile [17]. This baking process can be done by using a oven or hot plate. However, hot plate is preferable due to its ability of keeping the temperature consistent throughout the whole working area. The optimum temperature is 100 ^{o}C with 2 minutes of baking time. After the prebake process, the sample must undergo UV exposure to obtain the pattern immediately.

The photolithography system come with a moveable stage that helps in the process of aligning the mask to the sample correctly to ensure good transfer of pattern. The whole set of UV mask alignment machine consist of high vapour mercury lamp, mercury lamp power supplier system, a 4 axis alignment system, shutter, shutter controller, and vacuum pump. The mercury lamp was placed on the top followed by shutter, photomask, sample, alignment system. The mercury lamp has broad band emission of 275 nm to 650 nm with peak emission at 365 nm (I-line). This wavelength is used to crosslink the photoresist. The sample was aligned properly with the alignment system to make contact with the photomask normally called as contact transfer method. They are two built in function in the alignment system to make a good contact between the photomask and sample. There are vacuum contact and hard contact. Hard contact uses physical mechanical force to push the sample toward the photomask while vacuum contact uses a vacuum pump to suck out all the gases between the photomask and sample so that they will contact closely. Usually hard contact will result in better resolution in pattern transfer but it may easily cause permanent

scratch on the photomask as compared to vacuum contact. Due to this reason hard contact is usually applied for smooth surfaces only. The function of the shutter is to control the dosage of UV irradiation onto the sample by controlling its opening time. The shutter opening time can be controlled in between 0 to 999 second with interval of 0.1 second. Usually 6 second is enough for the process. The total expose time is determine by the intensity of the UV light at the sample position and the UV dosage required by the photoresist.

After the UV exposure process, the sample undergoes the developing process immediately. Under this process, the sample was immersed into the developer (AZ 726 MIF) for about 30 second. The immersion duration is important. If the develop time is too short, the unwanted area may not completely removed while too long will cause jagged edge in the channel or the wanted part also be removed by undercut process.

Before the wet etching process can be carried out, the sample needs to undergo a postbake process. The purpose of this process is to further stabilize the photoresist and improve the adhesion during wet etching [11]. In the postbake process, the sample was heated on a hot plate (100 ^{o}C) for 2 minutes.

After photolithography process, the photoresist comprise of feature pattern was now printed on top of the sample and the sample is ready for chromium wet etching in order to transfer these feature pattern to the chromium layer.

3.2.6 Metal wet etching

Wet etching is a purely chemical etching process. It has the advantages of high etching rate, high selectivity, suitable for mass production, less possibility of damaging the substrate and cheaper because do not require expensive machines like ICP. Unfortunately, it has limitation of isotropic etching profile, poor process control, large volume of chemical waste, not suitable for small feature device, and easily cause contamination [12, 18]. However, for chromium film that thinner than 500nm, the isotropic property is in the acceptance level [19]. Hence, wet etching was chosen for chromium etching.

In the chromium wet etching process, the sample was immersed in chromium etchant (Cr 7s) and then shake it for about 4 minutes. Basically, chromium etchants are a mixture of perchloric acid ($HClO_4$), ceric ammonium nitrate ($(NH_4)_2Ce(NO_3)_6$) and water. Perchloric acid is a strong acid and therefore it used to stabilise the ceric ammonium nitrate, while ceric ammonium nitrate is a strong oxidizer and will oxide the chromium to form chromium nitrates according to the chemical formula (1).

$$3(NH_4)_2Ce(NO_3)_6 + Cr \rightarrow Cr(NO_3)_3 + 3(NH_4)_2Ce(NO_3)_5 \qquad (3.1)$$

Chromium nitrate is relatively darker than chromium. Hence once the sample was immersed into the chromium etchant, the wafer surface will slowly turn dark. When the etching process was completed, the chromium was then completely removed and exposed the silica glass with pattern. Silica glass is shiny than chromium nitrate, hence this observation can be a reference for the operator to determine the completeness of the etching process [20, 21].

3.2.7 Substrate cleaning

Substrate cleaning is an important step in order to avoid polymerization during ICP dry etching process. Initially, the sample was dipped into the photoresist stripper, and swept with tipped gently. This process was repeated by using acetone, methanol, and iso-propanol. Then the sample was rinsed in deionised water for about 1 minute and blow dried as fast as possible by using nitrogen gas. Finally, the sample was put into an oven (130^{o}C) for dehydration purpose for about 10 minutes.

3.2.8 ICP glass etching

Before the sample undergoes ICP glass etching, the height or thickness of the chromium pattern, T_C need to be measured. This value is needed to determine the selectivity of the chromium to glass during ICP etching process. The height of the chromium can be measured by a surface profiler. For averaging purpose, 9 selective points in the wafer were measured.

In the ICP glass etching process, initially the wafer will be loaded in to the load lock chamber, The chamber is then pumped down to about few mTorr before the sample is loaded into the main chamber. Using a Turbo Molecular Pump, the main chamber is then pumped down to at least $4x10^{-}6$ Torr. This process is important for the chamber dehydration and reduces unwanted gas particles in the chamber during process. Once the required pressure was reached, the reactant gas was filled into the chamber with the desired flow rate and the pressure of the chamber will be fixed to the required value via a throttle valve. The ICP power and bias power were then applied after the chamber pressure and

flow rate was stable. The etching time was recorded immediately, once the bias power was applied. When the etching process was completed, the bias power was disconnected followed by disconnecting the ICP power, and reactant gas flow. Before the sample was removed, the chamber needs to undergo cycle purging process that is similar to the DC sputtering.

The channel height before, T_{WC} and after, T_C chromium wet etching was measured. For accuracy purpose, the similar selective point that chosen when measure T_{Cr} was measured by surface profiler.

References

[1] T.H.Kim, H.K.Sung., J.W.Choi & K.H.Yoon. (2003). Effective Silicon Oxide Formation on Silica-on-Silicon Platforms for Optical Hybrid Integration. ETRI Journal, 25 (2).

[2] G.C. Choon, M.J.Jeong., & T.G.Choy. (1999). Characterization of Boronphosphosilicata Glass Soot Fabrication by Flame Hydrolysis Deposition for Slica-on-Silicon Devices Application. Journal of Material Science 34 6035-6040.

[3] Y.T.Kim, S.M.Cho, Y.G. Seo, H.D.Yoon, Y.M.Im, S.J.Suh, & D.H.Yoon. (2003). Refractive Index Control of Core Layer using PECVD and FHD for Silica Optical Waveguides. Journal of Surface and Coating Technology,171.

[4] S. Garcia-Blanco & J.Stewart Aitchison. (2005). Direct Electron Beam Writing of Optical Devices on Ge-Doped Flame Hydrolysis Deposited Silica. Journal of IEEE, 11(2), 528.

[5] L. Zhang, X.Wang, W. Xie, T.Hou & Y.Zhang. (2004) . Characterization of Ge-Doped Silica Film with Low Optical Loss Grown by Flame Hydrolysis Deposition. Journal of Material Science & Engineering B, 107,317-320.

[6] A.Kilian, J.Kirchhof, B.Kuhlow, G.Przyrembel, and W.Wischmann. (2004). Birefringence Free Planar Optical Waveguides Made by Flame Hydrolysis Deposition (FHD) through Tailoring of the Overcladding. Journal of Lightwave Technology, 18 (2),193.

[7] S. Sakaguchi. (1995). Behavior of closed pores formed in consolidation process for silica soot precursor. Journal of Non-Crystal line Solid, 189 43-49.

[8] S. Sakaguchi, (1994). Consolidation of GeO_2 soot body prepared by flame hydrolysis reaction. Journal of Non-Crystal line Solid, 171 228-235.

[9] B. Chapman. (1980). Glow Discharge Process. New York: John Wiley & Sons.

[10] Material Safety Data Sheet AZ 1512 Photoresist. (2005). AZ Electronic Material.

[11] Gary S.May & Costas J. Spanos. (2006). Fundamentals of Semiconductor Manufacturing and Process Control. [s.l.]: Wiley-IEEE Press.

[12] M. L. Calvo, & V.Lakshminarayanan. (2007). Optical Waveguides:From Theory to Applied Technologies. Boca Raton:CRC Press Taylor & Francis Group.

[13] S.J.Han, J.Derksen, J.H.Chun (2004). Extrusion Spin Coating:An Efficient and Deterministic Photoresist Coating Methode in Microlithography. IEEE Transactions On Semiconductor Manufacturing, 17 (1), 12.

[14] Spin Coat Theory. (n.d.). Columbia University. Retrived March 27, 2009, from http://www.clean.cise.columbia.edu/process/spintheory.pdf.

[15] J.H.Tortai. (2004). Modeling of Ultra Thin Resist Film Structure After Spin-Coating and Post-Application Bake. Microelectronic Engineering, 73-74, 223-227.

[16] Alexei L. Bogdanov.(n.d.). Use of SU-8 Negative Photoresist for Optical Mask Manufacturing. University of Lund, Sweden.

[17] Vempati Srinivasa Rao, V.Kripesh, W.Y. Seung, & Andrew A O Tay. (2006). A Thick Photoresist Process for Advanced Wafer Level Packaging Applications Using JSR THB-151N negetive tone UV Photoresist. Journal of Micromechanics and Microengineering, 16 1841-1846.

[18] S. Franssila. (2004). Introduction to microfabrication. England: John Wiley & Son.

[19] D.Shin. & J.H.Eo. (2005) Plasma Etching Characteristic of Ge-B-P doped SiO_2 Film for Waveguides Fabrication. Ceramic Processing Research, 6 345-350.

[20] Technical information of Chromium etching. (n.d.). Microchemicals. Retrived March 27, 2009, from http://www.microchemicals.com/technical_information/chromium_etching.pdf.

[21] Meterial Safety Data Sheet (MSDS) of Cr-7S. (n.d.). Syantek Corporation Retrived March 27, 2009, from http://www.clean.cise.columbia.edu/msds/CR-7S.pdf.

CHAPTER 4

OPTIMIZATION OF THE ETCHING PROCESS USING ICP

4.0 Introduction

In this chapter, the result of basic characterization study on ICP is discussed. All possible variables in the ICP process are comprehensively investigated. The optimum parameters for glass etching process using our ICP machine (HVI-620 from Hanvac Corporation) were then obtained based on the basic characterization results. The criteria that were used to determine the optimized parameters are summarised in

Table 4.1. Details of these criteria are as follow.

Table 4.1: Criteria that were used to determine the optimum ICP parameter.

Criteria	Description
Etching rate	Fast
Selectivity	High
Side wall roughness and vertical profile	Smooth and perfectly rectangular
Channel cleanliness	Clean and without polymerization

Etching rate – The higher the etching rate, the shorter the time required to etch a certain amount of depth of the target material, hence improving the process throughput. Besides, shorter etching time will result in a lower temperature being induced onto the sample during the etching process. This will prevent residue PR on the sample from being hardened.

Selectivity – A higher etching selectivity can reduce the chromium mask layer thickness, using less chromium during DC sputtering process, and requiring less etchant to be used during wet etching process. In addition, wet etching of a thinner chromium layer will yield a smoother side wall.

Side wall roughness and vertical profile – Smooth side wall and perfect vertical profile is required to minimize light scattering and maintain collimated light beam when the etched side wall is used as a mirror surface [1]. Some literatures use the term line edge roughness instead of side wall roughness. Channel side wall roughness is defined by the root mean square (RMS) deviation and its correlation length. Roughness dominated by vertical striation also induces polarization dependence loss (PDL). Besides, it may induce crosstalk between the channel [2].

Channel cleanliness – Contaminations such as polymerization and etched product re-deposition that surrounds the waveguide channel will affect the waveguiding performance. This is because contaminations have different refractive index which will change the effective refractive index of the waveguide. As a result, this will induce propagation loss in the channel.

4.1 Characteristics of the ICP

There are 6 basic variables in the ICP machine. In order to optimize the ICP glass etching process for PLC fabrication, all these variables are studied comprehensively and discussed in this chapter. These 6 variables are ICP power, bias power, operating pressure during etching, reactant gas flow rate, gas composition used, and working distance of the sample in the chamber. As an initial reference to optimize each parameter, the default parameters used are shown in Table 4.2. These values were suggested in the ICP machine manual.

Table 4.2: Default setting of ICP machine in glass etching process.

ICP Parameter	**Set Value**
ICP Power	880Watt
Bias Power	65Watt
Pressure	10mtorr
Flow	30sccm
Gas	C_2F_6
Working distance	0 cm (refer to Section 4.1.3)

4.1.1 ICP Power optimization

The actual RF power that is delivered into the plasma system is known as effective ICP Power. An ideal case, the effective ICP power should be equal to the ICP power applied by the RF power generator. However, in practice, there always exist some RF power that is reflected back onto the generator although a matching network is being used to reduce RF power reflection. The value of the reflected power is different for each particular process. Besides, the reflected power also varies during an etching process although by only a small magnitude. Hence the effective ICP power is not constant and difficult to determine for each process. In order to simplify the process, an acceptance level was introduced. It is observed that the amount of reflected power usually gets lower along the etching process. In other words, the reflected power is highest when the plasma is initially generated. Using this observation as a reference, the initial value of the reflected power in every process was kept below 2% of the applied ICP power. For example, when 880 W ICP power was applied, the initial reflected power must be lower than 17 W. In the case of the reflected power exceeding the 2% level, the etching process will be terminated and the plasma generation procedure repeated.

The acceptant level of 2% was determined based on a series of tests done earlier. Plasma was generated using the conditions mentioned in Table 4.2 and the initial RF reflected power recorded. This process is repeated 45 times. The mean value of the initial reflected power to applied power ratio is 1.6% with standard deviation of 0.35%. Hence, the acceptance boundary of 2% was chosen by taking into consideration the standard deviation of the repeatability measurement. With this acceptance level introduced, the term ICP

power will be used throughout this work to refer to the effective ICP power with an error of 2%. As the maximum ICP power generation is 1000 W, experiments involving the variation of ICP power was carried out with a minimum interval of 20 W (2% of 1000 W) to avoid overlapping to the neighboring values.

In the course of this study, it was observed that the etching rate is lower at the center of the sample as compared to its side. This is believed to be the effect of the RF coil structure which generates plasma with a "donut" distribution profile, a positional variation of the plasma density. Hence, to obtain a mean value of the etching rate, the average etch depth was measured on 9 evenly distributed points on the sample with their uncertainties calculated using error analysis as shown in Section 2.3.

The effect of ICP power on the etching rate is shown in Figure 4.1. The graph shows that the etching rate increased as the applied ICP power increases. The etching rate increases from 180 nm/min to 240 nm/min when ICP power is set to 720 W and 900 W, respectively. This observation is expected as the ICP power is responsible for plasma generation. As the applied ICP power increases, more energy is delivered into the plasma system. The number of plasma molecules generated in the chamber is increased accordingly. In other words, the density of the plasma in the chamber is increased as the applied ICP power increases. When the plasma density increases, the chances of particles bombardment on to the sample will be higher. This will then increase the etching rate. However, above a certain ICP power (900 W in this case) as shown in Figure 4.1, the etching rate starts to decrease. This is because when ICP power is applied above this point, the mean free path of the plasma

molecules is too short [3] that the collisions between the particles become more frequent than the plasma particles bombardment onto the sample. In other words, the average time required for a particle to travel onto the sample is longer than the average plasma collision time. This reduces the number of plasma particles in contact with the sample surface as well as their energy at the time they reach the sample surface and consequently reduces the etching reaction.

Figure 4.2 shows the etching selectivity as ICP power is varied. Selectivity is constant around the value of 20 with an R-squared value of the data distribution near to zero (about 0.05). This shows that the selectivity is not affected by the ICP power or the variation is too small to be identified using current measurement tools. This result does not agree with a previous study by Jung. In his report, the selectivity has a similar increasing trend as the applied ICP power increases [3].

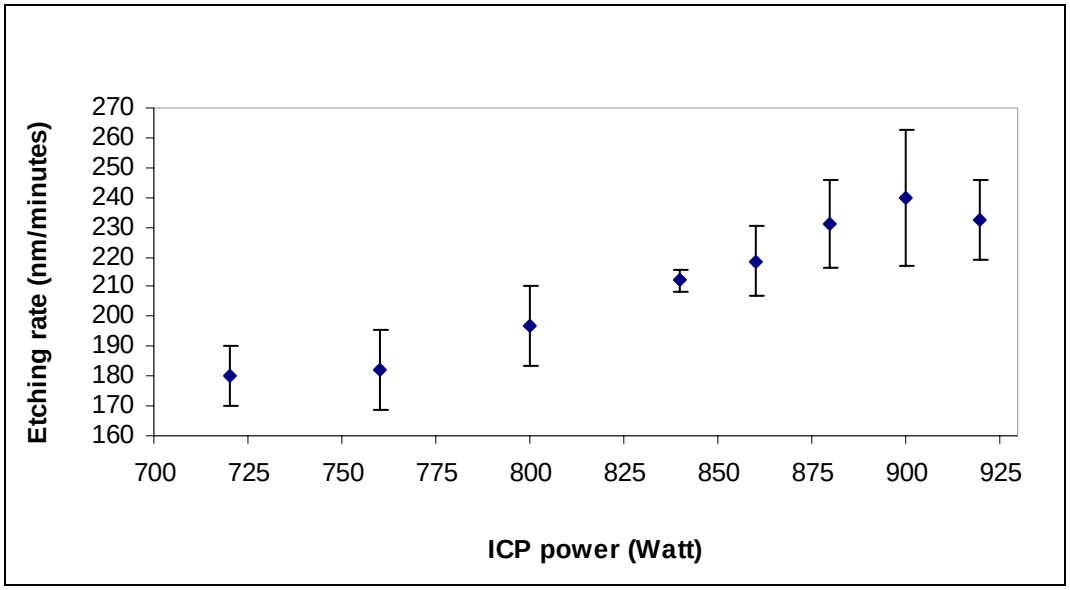

Figure 4.1: Glass etching rate against ICP power under default etching conditions as shows in Table 4.2.

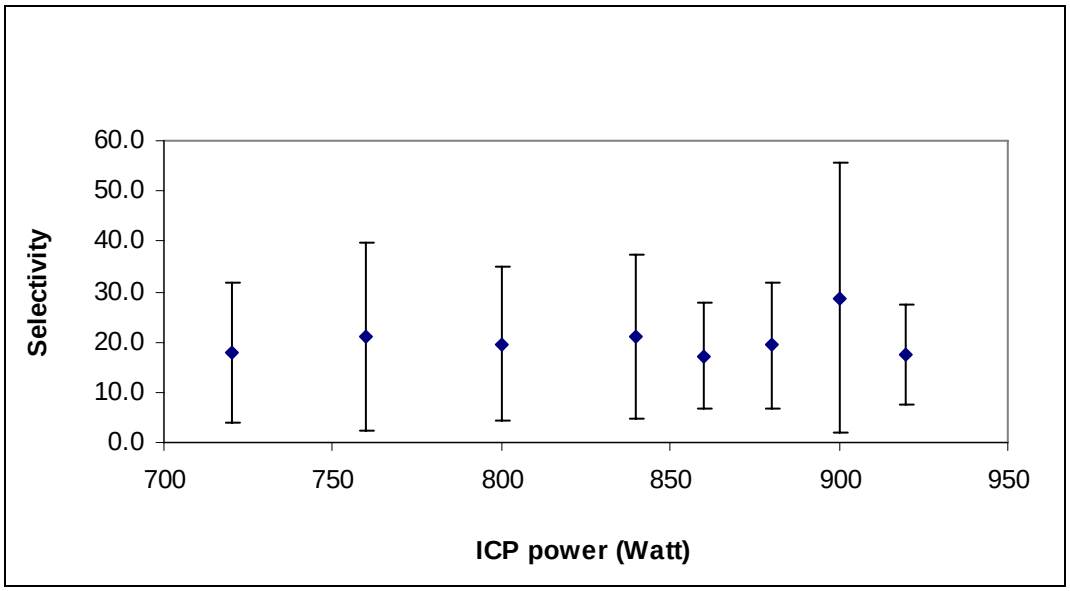

Figure 4.2: Selectivity of silica glass etching to chromium against ICP power under default etching conditions as shown in Table 4.2.

Selectivity is defined as the ratio of glass etching rate to chromium etching rate. When selectivity is constant as the glass etching rate increases, it means that the chromium etching rate is also increased. It is suspected that the etching mechanism with the current ICP parameters was dominantly physical etching (this phenomenon is further discussed in Section 4.1.3 and 4.1.6). This causes the increase in plasma density to directly increase the frequency of bombardment of the particle onto the sample and hence causes the etching rate of both glass and chromium to increase (constant selectivity). While in Jung's work, it is suspected that the chromium etching rate was constant as the applied ICP power increases. The etching condition for his work is more dominantly chemical etching. Hence, increasing plasma density will only increase the probability of the glass layer being etched while the etching rate of the chromium layer remains constant.

As a conclusion, the most suitable ICP power is 900 W, as it gives the highest etching rate about 240nm/min. Higher etching rate reduces the total process time. The advantage of fast etching is cost saving in general and technically it also has some advantage on the sample. As the plasma particle bombarded onto the sample, he sample heats up. If the sample is too hot when etching time is long, the PR residue on the sample may harden and becomes difficult to be removed by the ICP etching process or conventional PR remover. As a result, this will cause permanent contamination on the sample. Sample contamination is discussed in more detail in Section 5.1.

4.1.2 Consistency test

Plasma generation can be easily performed by many techniques like ICP or DC discharges. However, the reproducibility of plasma that has exactly same properties is difficult. This is because plasma is affected by many factors besides all the controllable parameters like ICP power, chamber pressure etc. One of the factors that are not controllable or difficult to control is the temperature of the chamber, the amount of impurities in the chamber, and chamber sidewall cleanliness. Moreover, chamber cleaning is usually carried out after a series of processes or after a period of operation. In general, the etching rate will degrade beyond the optimum operating period, because the chamber side wall becomes dirtier as the number of processes increases. In order to study this effect, a series of consistency tests were conducted following chamber cleaning by carrying out two etching processes per day continuously in a week. Note that chamber cleaning is usually conducted weekly and at most 2 etching processes were carried out in a day due to time spent to cool down the temperature of the system and to pump down the chamber. It is worth pointing out that 30 minutes of oxygen ashing process was conducted before each etching process. Ashing process helps to remove the photoresist residue and fluorocarbon based by-product of etching in the chamber [4].

Figure 4.3 shows the etching rate of the 12 measurements taken in this consistency test series. The graph clearly shows that measurement number 7 is extremely higher than other measured values. This shows that the machine may produce abnormal etching conditions, and the probability of this condition occurring is about 8.33%. Besides, the standard deviation of the remaining 11 measurements in this series (the outlier has being excluded)

is about 7.28 nm/min which is about 3.1% error in the mean measurement. This shows that the reproducibility of the machine in the test period was good [5].

Based on the above observation, the ICP machine is reliable and consistent within the testing period. A set of etching processes for a variable optimization must be conducted in a same batch (same testing period) in order to obtain consistent results. This is because the machine may show a slightly different behaviour for different batch of processes.

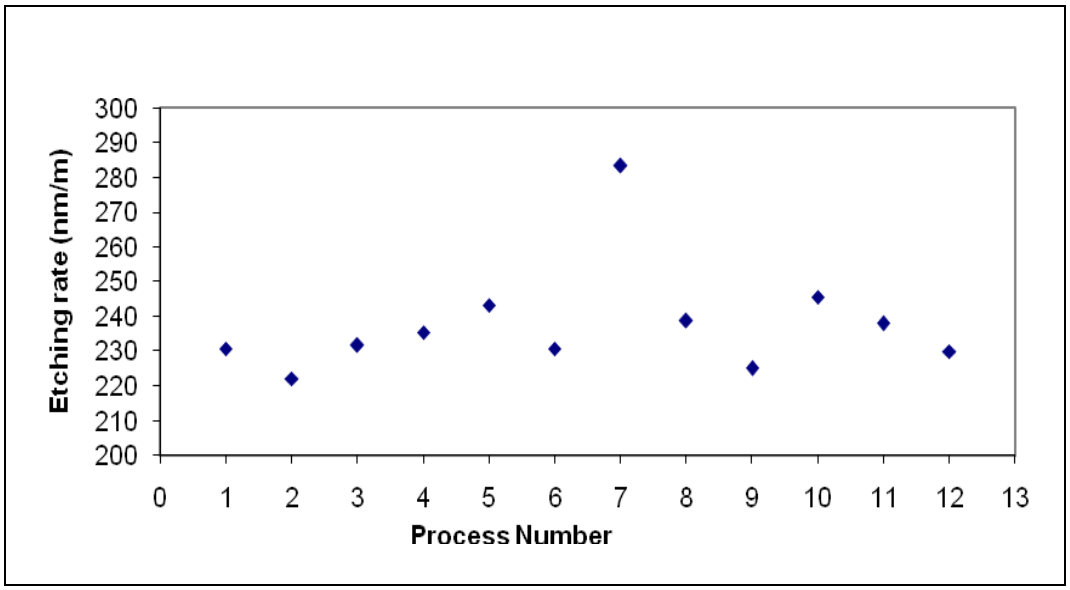

Figure 4.3: Consistency test, glass etching rate for 12 etching processes using default ICP etching conditions.

4.1.3 Working distance optimization

Working distance is referred to as the position of the sample wafer with respect to the plasma source. However plasma does not have a discreet boundary and it is difficult to measure the exact position inside a close chamber. Hence, a reference point needs to be defined. The possible working position lies between the bottom surface of the ceramic slab that separates the ICP coil and plasma chamber and the vertically adjustable substrate holder. The distance between these two positions when the substrate holder is at its lowest position is taken as zero reference point while the vertical position of the substrate holder is indicated by the height (in cm) the holder is raised.

Figure 4.4 shows the glass etching rate of the sample with respect to the wafer's vertical position. In general, the graph shows an increasing trend in the etching rate as the position increases until it reached maximum at the position of 5 cm. The etching rate increases from 210 nm/min at the reference position to 300 nm/min at position 5cm. The lower the sample position, the farther the sample is from the plasma cloud hence lessening the number of energetic particle that are able to perform the etching process to reach the sample under the same bias condition. As a result, the etching rate varies in such a trend before it reaches the maximum. However, after the maximum peak, the etching rate starts to decrease. This might be due to sample penetration into the plasma cloud and causes distortion in the plasma cloud, hence the total plasma particle that are able to reach the sample surface is decreased.

Figure 4.5 shows the selectivity of glass to chromium etching rate ratio as sample working distance is varied. In general, the graph shows a slightly increasing trend in the selectivity as the working distance increases. This means that the selectivity was affected by the variation of the sample working distance. At the zero reference point, the value of selectivity is lowest and only about 11. The reason for the low selectivity is suspected to be due to the working distance is too far from the plasma cloud. With the longer working distance, the plasma particles are able to gain more kinetic energy under the same applied bias power as they reach the sample surface. Hence it is expected that the physical etching is dominant at this working distance. That was the reason why the assumption that the physical etching is dominant was made in Section 4.1.1. Please refer to Section 4.1.6 for further discussion regarding physical etching. As the working distance increases, the sample now is nearer to the plasma cloud. Hence the bias accelerating effect was reduced and resulted in the decrease of chromium etching rate. Decrease in the chromium etching rate coupled with the increase in glass etching rate will increase the selectivity since selectivity is defined as the ratio of glass to chromium etching rate.

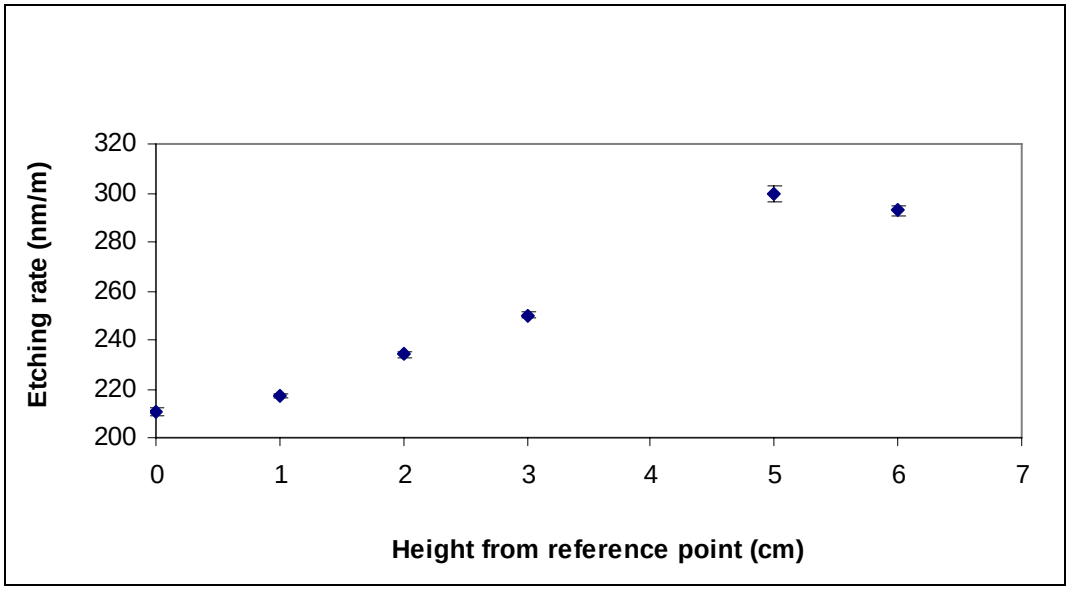

Figure 4.4: Glass etching rate against height from the zero reference point under default ICP etching conditions.

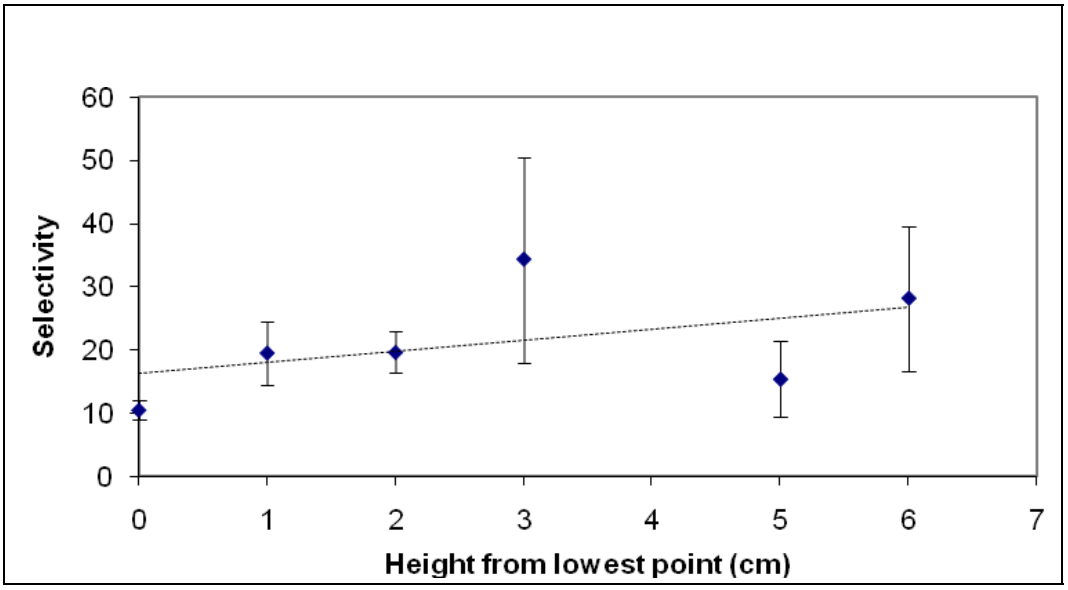

Figure 4.5: Selectivity of silica glass etching to chromium etching against height from the zero reference point under default ICP etching conditions. (Dotted line is for indication purpose only)

As the ICP power optimization reported in Section 4.1.1 was carried out with working distance set at zero reference level (0 cm), re-optimization of ICP power is necessary at the optimized working distance (5 cm) to study its effect on the optimization of ICP power. This is because the sample is now placed nearer to the plasma cloud. The smaller travelling distance of plasma molecules to the sample together with the bias power applied causes stronger capacitive effect. Hence it is expected that the optimized value of ICP power will shift towards the lower power range in order obtain the same plasma condition as optimised in the 0cm substrate position. As shown in Figure 4.6, the optimized value for ICP power has downshifted to 880W. In general, the distribution shows the same trend as Figure 4.1. But in term of the etching rate, the highest etching rate increases from about 240nm/min in Figure 4.1 to about 300 nm/min in Figure 4.6 which is about 20.8% of increment.

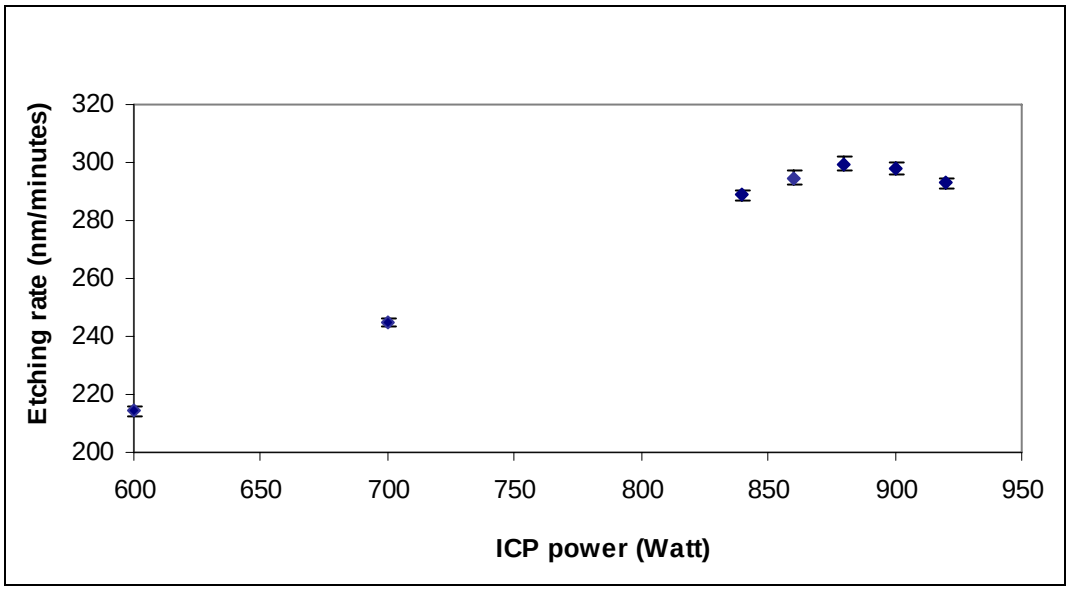

Figure 4.6: ICP Power Optimization under default etching parameter except the working distance is set at the optimized value (5 cm).

After these series of optimization, the default setting of the ICP machine was reset as shown in Table 4.3.

Table 4.3: New default settings of ICP machine 1.

Parameter	**Set Value**
ICP Power	880 Watt
Bias Power	65 Watt
Pressure	10 mtorr
Flow	30 sccm
Gas	C_2F_6
Working distance	5 cm

4.1.4 Effect of ICP Power on sample surface

As mentioned earlier, ICP Power controls the density of the plasma [6]. Besides, ICP dry etching uses the combined mechanisms of physical bombardment and chemical reaction to remove the target material [2]. Hence it is expected that surface damage will be more obvious as the density of plasma increases by increasing in ICP power. A very rough etched surface may have the problem of low adhesion during the over cladding deposition. SEM images of surface damage for various ICP powers are show in Figure 4.7.

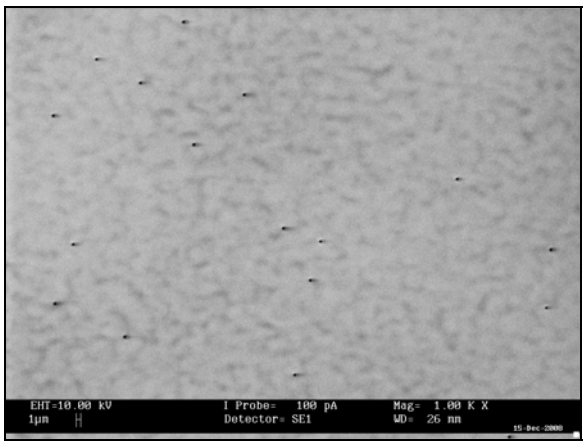

a) 600 W

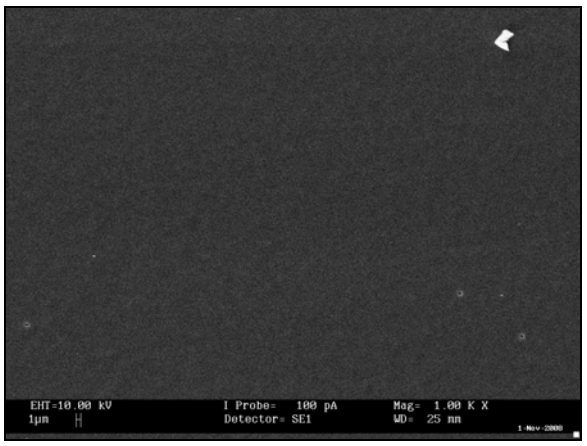

d) 860 W

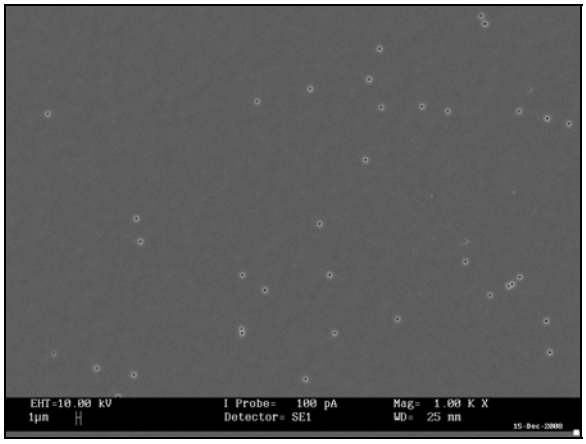

b)700 W

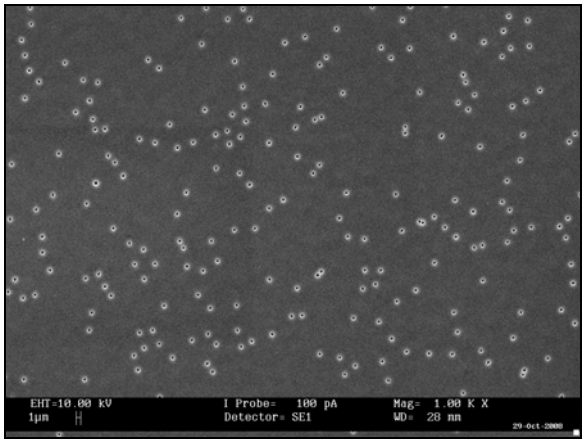

e) 880 W

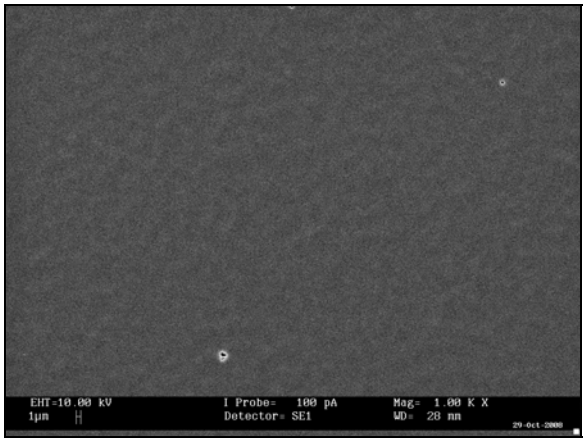

c) 840 W

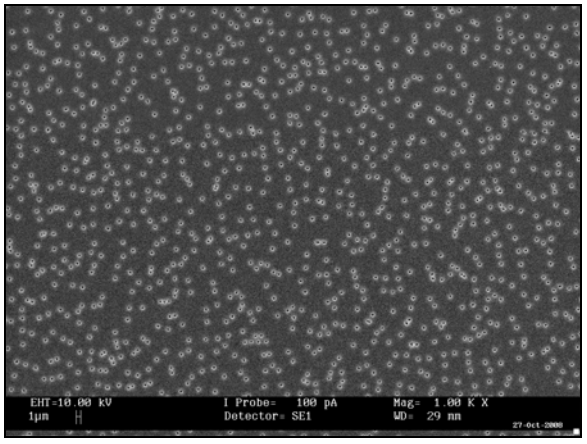

f) 900 W

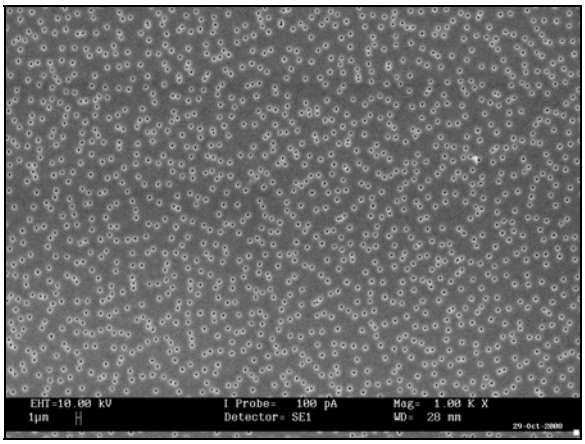

g) 920 W

Figure 4.7: SEM Images of surface damages for various applied ICP Power.

In general, the sample surface when ICP power is set below 860 W is very smooth and no pinhole damage is observed. In this region, the etching process was suspected to be dominantly chemical etching with no or minimal physical etching effect. When ICP power is set at 880 W and above, there are many pinhole damages. In fact the concentration of pinhole seems to be increasing as the power increases. In this region, the etching process is mix between physical bombardment and chemical reaction and finally the physical etching will become the dominant effect. The mechanism of the pinhole formation on the sample during etching process is proposed in Choi's work [6].

For a more quantitative study, pinhole density is measured using the particle count function in ImageJ software. Initially, all images are crop into the same size at 1024x680 pixels. Then a threshold was set to allow the program to identify the pinholes on the image. This step is important because it will affect the number of pinhole count and the pinhole size. However, this threshold setting is quite subjective, different user may set different values. Hence this process needs to be repeated several times to obtain an average value. Finally,

the particle count function was applied. Usually, a pinhole is defined only when there are more than 5 adjacent pixels within the threshold value. This is because some small areas (< 5 pixels) may also be darker and coincidently fall in the range of threshold value, thus being wrongly counted as pinholes. In addition, the function "exclude on edge and hole" was chosen in order to avoid miscounts in pinhole size. The result of this analysis is shown in Figure 4.8 and Figure 4.9. Both graphs show the similar characteristic mentioned earlier. The number of pinhole count shown in Figure 4.8 shows an exponentially increasing number of pinhole damages on the sample up to an ICP power of 880 W. Above 880 W, the gradient of the curve points to a possible saturation effect. Hence, for ICP power of 920W and above, physical etching is believed to be dominant.

Glass etching is still possible via pure chemicaly etching. However, pure chemical etching is usually isotropic which is poor for pattern transfer [7]. Besides that, the etching rate is very slow, leading to inefficiency in fabrication production especially for silica glass which still requires physical etching to initialise the etching process [8]. Hence the optimize ICP power must consists of a certain degree of physical etching with minimum defect on the sample surface. As a conclusion, the optimal power setting is 880 W because the plasma generated by this value causes the minimum surface area defect on the sample which is only about 2.5% as shown in Figure 4.9. Note that, this optimized value is the same as the etching rate optimization value determined earlier in Section 4.1.3. In order words, both criteria either based on etching rate or surface damage leads to the same optimized ICP power of 880 W.

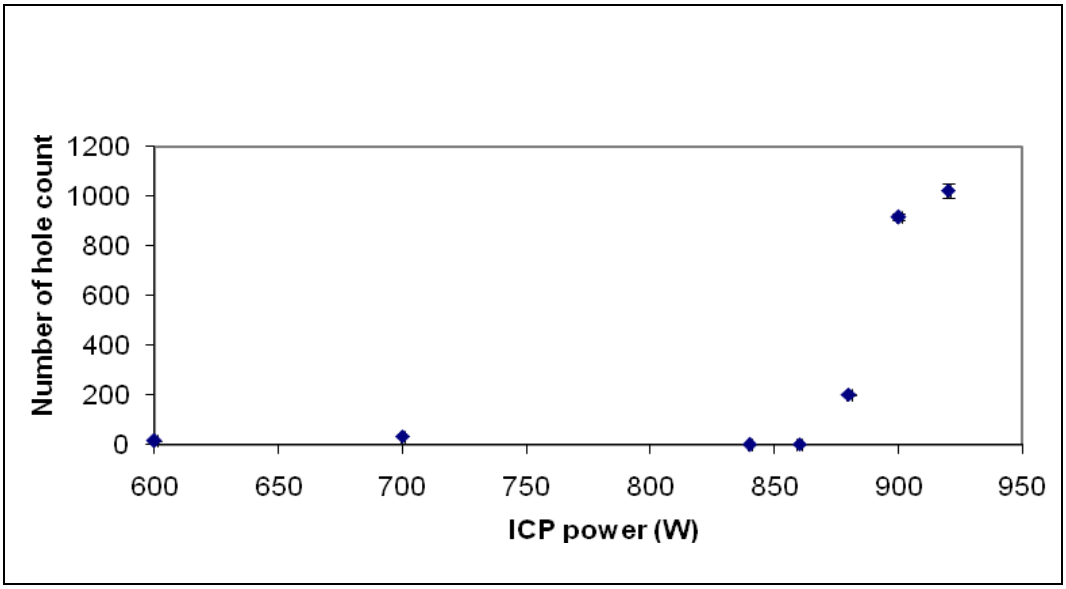

Figure 4.8: Total number of pinhole count against applied ICP power under default ICP etching condition as shows in Table 4.3.

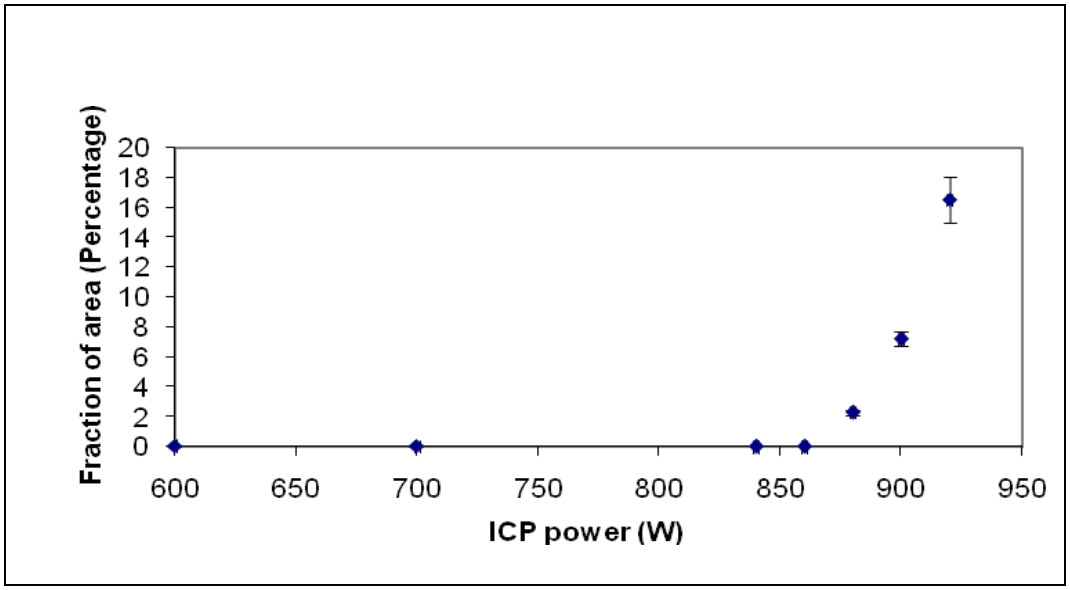

Figure 4.9: Fraction of area that is covered by pinhole defects in the image against applied ICP power under default IPC etching condition as shown in Table 4.3.

4.1.5 Bias Power optimization

Bias power is very important in ICP etching. It provides a negative equal potential electric field that attracts the plasma particles to bombard onto the sample surface [9]. Hence if the supplied power is too low then the particles will not be directed on to the sample and causes isotopic etching which will lead to slanted side wall. On the other hand, if the applied bias power is too high, the capacitive effect between the ICP coil and the bias coil will disturb the plasma condition. Furthermore, the plasma particles will gain extra energy to bombard onto the sample which will lead to the dominance of physical etching rather than chemical etching.

As in the case of ICP power determination in Section 4.1, the effective bias power is difficult to determine. Hence the term bias power is used to represent the effective bias power throughout the thesis. The acceptance level of the reflected bias power was set at 2 W. This value was chosen based on a test done earlier. In this test a set of 45 data were collected. The average reflected power is 0.84 W with standard deviation of 0.88W. Hence by taking the average value plus a standard deviation (1.72 overestimated to 2), the acceptance level was set in that value. Note that, the matching circuit controller only gives integral value in the reflected power, hence the value of the standard deviation that calculated earlier is slightly higher than usual.

Figure 4.10 shows an increasing trend of etching rate as the applied bias power increases. The etching rate increases from 170 nm/min at bias power of 25 W to about 300 nm/min at the bias power of 65 W. This result is expected because the higher the bias power, the more

energy the particles will gain. These highly energetic plasmas will bombard harshly on the sample surface and cause the glass layer to be removed faster.

On the other hand, selectivity dropped from the highest value of about 40 at 20 W of bias power to 16 at 65 W of bias power as shown in Figure 4.11. Decrease in selectivity while glass etching rate increases indicates that the chromium layer was etched at a higher etching rate. Chromium is not reacting with the reactant gas, hence the only reason that causes the chromium layer to be etched is through physical etching. Higher bias power leads to higher ion energy. This ion energy will cause the physical etching to be more significant and causes the decrease in selectivity.

Although faster etching rate is better for the fabrication process, no test was done at bias power higher than 65 W. This is because the selectivity at bias power of 65 W is too low (about 16) as shown in Figure 4.11. Selectivity lower than 20 is not suitable for silica waveguide etching application as a minimum etch depth of 6 μm is required. The minimum chromium layer thickness required for selectivity of 20 is about 300 nm, which is, according to Park, the maximum chromium layer thickness that can produce a smooth sidewall after the chromium wet etching [10]. Hence the optimize value of the bias power must below 45 W in which the selectivity is higher then 20.

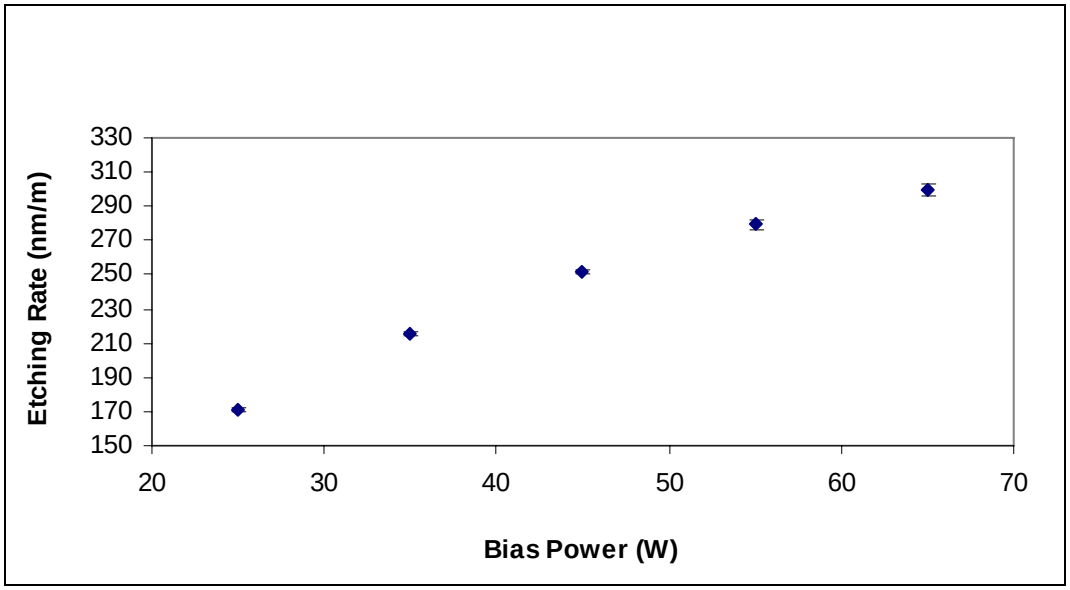

Figure 4.10: Glass etching rate against applied bias power under default ICP etching condition as shown in Table 4.3.

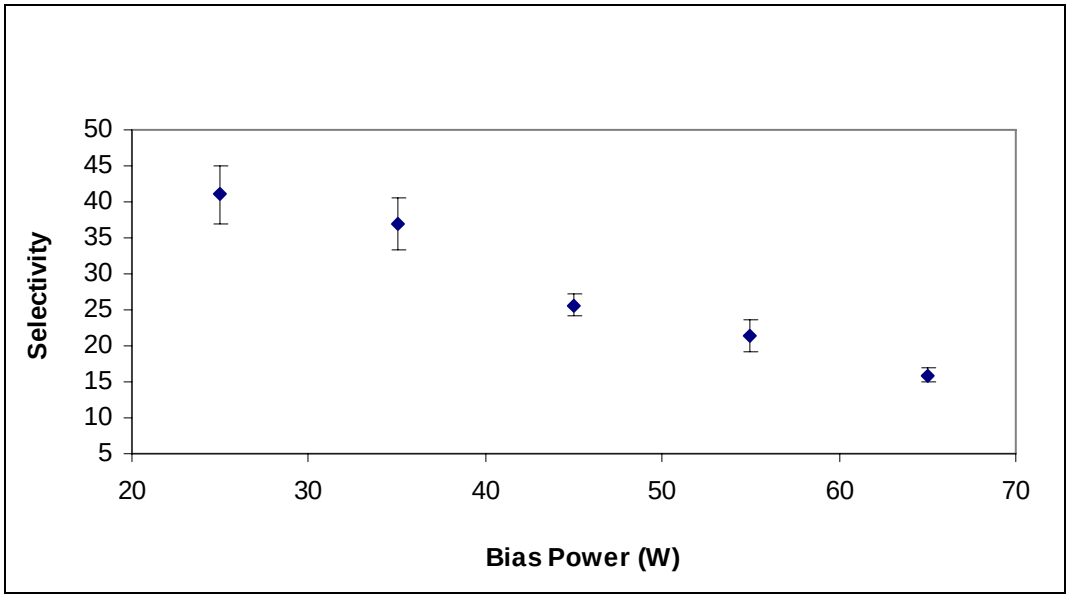

Figure 4.11: Selectivity of silica glass to chromium etching for various applied bias power under default ICP etching condition as shown in Table 4.3.

4.1.6 Effect of Bias Power on sample surface

Similar to the effect of ICP power on the sample surface studied in Section 4.1.4, the bias power will also cause defects on the sample surface [3] as shown in Figure 4.12. In general, there are no observable pinhole damage on the sample surface for applied bias power of 25 W and 35 W. This is because chemical etching is dominant at these bias powers. When bias power is set at 45 W, the pinhole effect started to appear but is not obvious compared to the surface for bias power 65 W. This is because at the bias power 45 W, the degree of physical etching is small while it is dominant at bias power of 65 W. Statistically, under the same degree of pinhole damage, the number of pinhole count on the sample that etched under bias power of 65 W is 140 counts per sampling area while in sample that etched under bias power of 45 W is just only 1 counts per sampling area. The size of sampling area is 1024X690 pixels and 8 pixels corresponding to 1 μm.

After the bias power optimization work, the default setting of the ICP machine was reset as shown in Table 4.4.

Table 4.4: New default settings of ICP machine 2.

Parameter	**Set Value**
ICP Power	880 Watt
Bias Power	45 Watt
Pressure	10 mtorr
Flow	30 sccm
Gas	C_2F_6
Working distance	5 cm

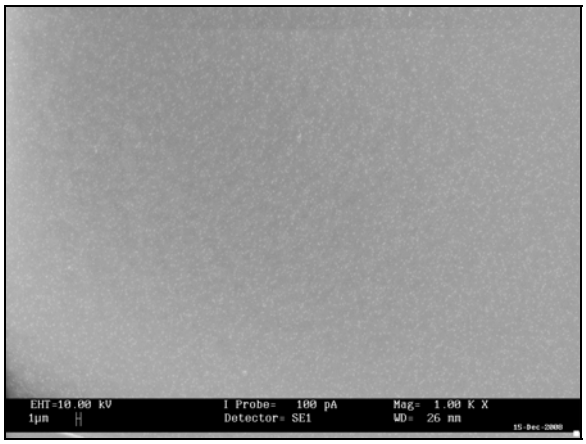

a) 25 Watt

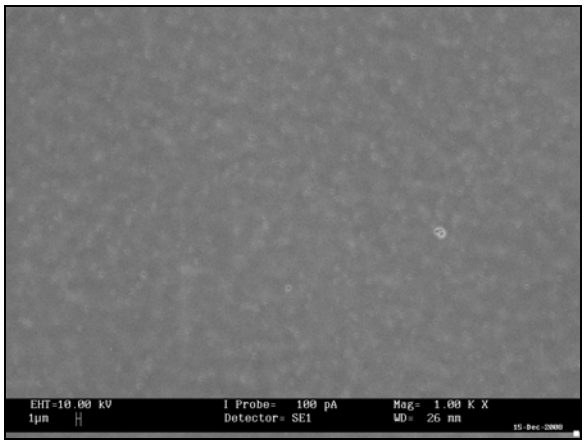

c) 45 Watt

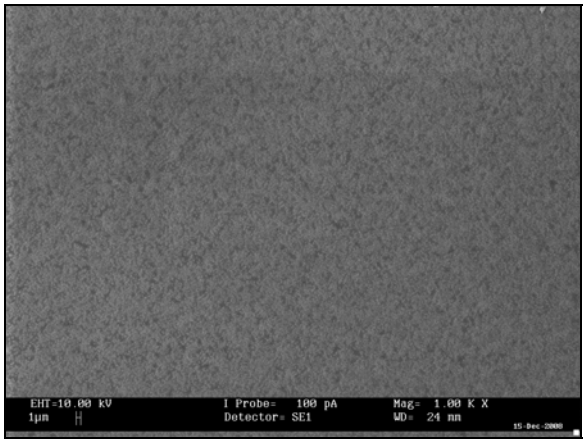

b) 35 Watt

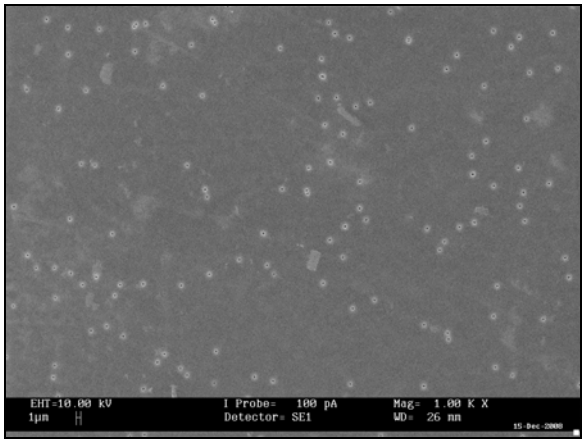

d) 65 Watt (before optimazation process)

Figure 4.12: SEM images of surface damages for various applied bias power.

4.1.7 Pressure Optimization

ICP glass etching is a type of RIE etching hence its operating chamber pressure is around 10mTorr to 100mTorr with ion energy of about 100eV. The advantages of this etching technique are its good selectivity and anisotropic etching. Operating chamber pressure near the lower end of 10 mTorr is known as high density plasma system and this pressure range is suitable for silica glass etching. This is because silica glass is not reactive and requires certain degree of physical etching to initialise the process. Moreover, for this range of operating chamber pressures, the process produces higher etching rate and good anisotropy etching. While operating chamber pressure near to 100 mTorr is also known as plasma etching and this operating range usually gives very good selectivity but with low anisotropic etching characteristic. This operating pressure range is not suitable for optical waveguides fabrication due to its low anisotropic property [9].

Figure 4.13 shows the variation of glass etching rate and the selectivity as the operating chamber pressure is varied from 6.5 mTorr to 14 mTorr. At pressure below 8 mTorr, etching rate increases with increasing pressure. This is because the lower the operating chamber pressure, the longer mean free path the ions travel. The ions will gain more energy before hitting the sample. It is also suspected that higher order of ionization may occur in this pressure region. Hence, this phenomenon resulted in higher etching rate but also causes the decrease in selectivity [3]. Unfortunately due to the limitation of the extraction rate of the turbo molecular pump, the chamber pressure cannot operate below 6.0 mTorr with 30sccm of reactant gas flow rate and therefore no test was done below 6mTorr. At operating chamber pressure of 8mTorr and above, the collision between the particles is

more frequent since higher operating chamber pressure means more particles in the chamber. This will generate more plasma particles which is desirable in etching process. Hence the etching rate shows an increasing trend. On the other hand, the selectivity also shows an increasing trend for operating pressure from 8mTorr to 12 mTorr. Again this is because the average plasma energy is slightly reduced as the pressure increases due to the reduced time for the plasma particles to gain accelerating energy before colliding with neighbouring particles.

Note that the flow rate of input reactant gas is fixed at 30 sccm, hence in order to create higher pressure in the chamber, the gas extraction flow rate need to be reduced. As a result, this causes the gas to stay longer in the chamber. The term that refers to how long a particle stays in the chamber is known as residence time. Longer resident time will allow the reactant gas to have longer time to gain energy from the ICP power. However, longer residence time will induce polymerization on the sample surface. This is because if the resident time of the reactant gas is too long, the silica glass layer that is sputtered out from the glass layer in the form of carbon based compound have a higher chance to re-deposit onto the sample. It is observed that polymerization occur for both samples etched under operating chamber pressures 12 mTorr and 14 mTorr. In fact, polymerization already start occur at the centre of the sample that etch under 10 mTorr. However, due to the averaging effect (9 points that distributed evenly across the sample was taken in calculation as mention in Section 2.3) in etching rate calculation, it would not effects much on the average results. In general, polymerization on the sample surface will block the etching

process, slowing the etching rate as shown in Figure 4.13. As a result, the selectivity decreases since the glass etching decreases.

The optimized pressure range is between 10mTorr to 12mTorr depending on whether selectivity or etching rate is chosen as the determining factor. Although post treatment to remove polymerization can be carried out by oxygen ashing [4] or by using conventional stripper, these additional processes will complicate the fabrication procedure and are time consuming. Hence operating chamber pressure above 14mTorr was not chosen. While are polymerization still occur in the 12 mTorr operating chamber pressure sample, it is believed that this can be reduced by increasing the input reactant gas flow rate. This approach is discussed further in the next section.

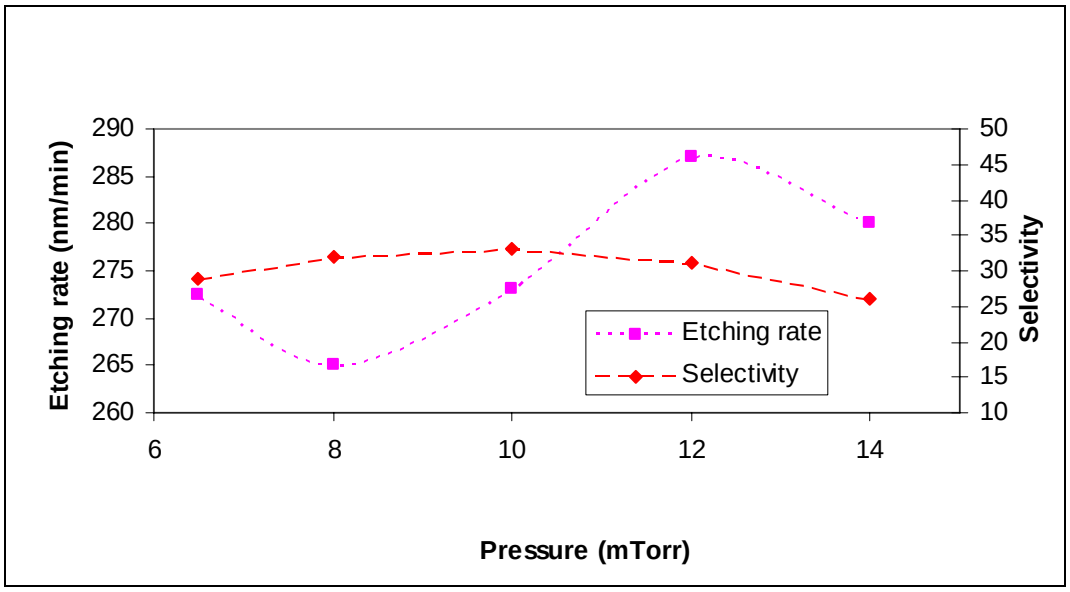

Figure 4.13: Glass etching rate and selectivity against operating chamber pressure under default etching condition as shown in Table 4.3.

(Error bars were not included for easy viewing. Trend lines are for indicative purpose only.)

4.1.8 Flow rate optimization

The operating chamber pressure and the flow rate of the reactant gas directly affect the resident time of the reactant gas. For example, in a fixed flow rate, the resident time is proportional to the pressure, while in a fixed pressure system resident time is inversely proportional to the input gas flow rate. As mentioned at the end of Section 4.1.7, polymerization on the etch sample at a fixed operating chamber pressure of 12 mTorr is expected to reduce by applying higher input reactant gas flow rate. Figure 4.14 shows the image taken for samples that were etched under various input reactant gas flow rates. Note that polymerization is easier to identify in images taken using camera flash in which the white coloured areas are the surface affected by polymerization. The clean area is observed as optical fringes, which show up more obvious in images taken without camera flash. For sample etched under 30 sccm flow rate that is shown in Figure 4.14b, it is clearly observed that polymerization only occur at the centre of the wafer while the side of the sample wafer is free from polymerization (refer to the image shown in Figure 4.14c). The local polymerization dependent phenomenon was suspected to be related to the design of the chamber. (Please refer to Section 3.1 for the chamber design). In the current chamber design, the input reactant gas flows into the chamber from the small holes distributed evenly at the top section of the chamber side wall while the gas was extracted from the bottom of the chamber. Hence under this operating chamber pressure of 12 mTorr with input reactant gas flow rate of 30sccm, the new fresh reactant gas has lower chances to reach the centre of the wafer before there are extracted by the vacuum pump. In other words, the resident time for the gas at the centre of the wafer is expected to be slightly longer than the resident time of the reactant gas at the side of the wafer and this cause

polymerization to occur at the centre of the wafer. For 35 sccm of input reactant gas flow rate, the new fresh gas now are able to reach to the centre of the wafer. However, in general the resident time is still too long hence polymerization still occurs on the whole wafer as shown in Figure 4.14d. The optimum flow rate of input reactant gas is 40 sccm. This is because samples etched in this condition are free from any polymerization as shown in Figure 4.14e. However, polymerization will reoccur with higher flow rates as shown in Figure 4.14f. This is because at higher flow rate like 50 sccm, the resident time is too short and the reaction will produce un-reacted carbon species [3]. Moreover it is observed that polymerisation is more serious at the side of the wafer instead of at the centre of the wafer. It is suspected that the fresh reactant gas was able to reach the centre of the wafer by the gas injection since the flow rate was high but the un-reacted carbon species causes the polymerization to occur especially at the side.

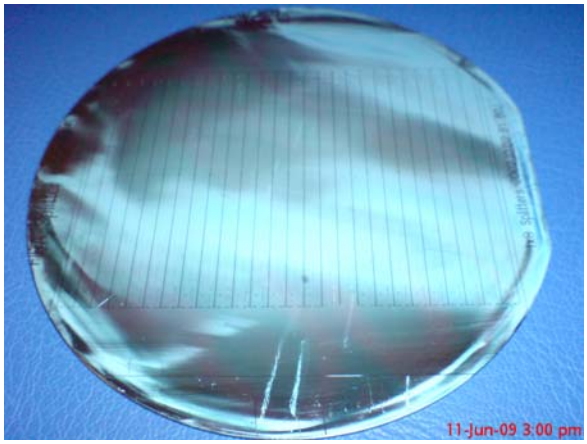

a) 25 sccm

d) 35 sccm

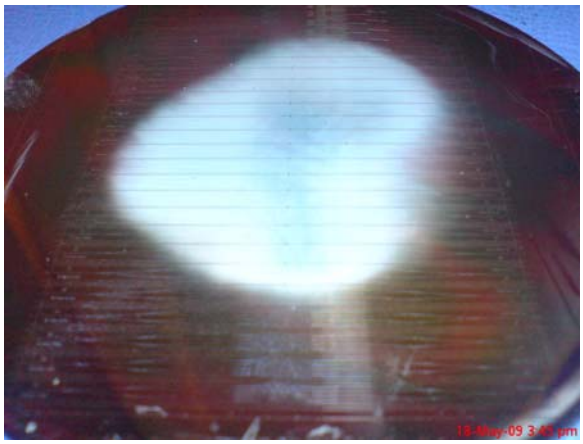

b) 30 sccm

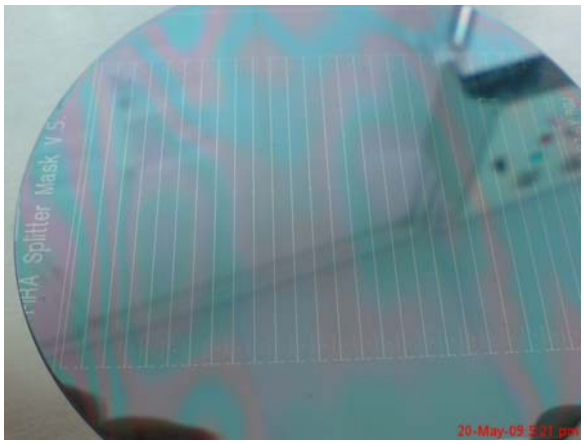

e) 40 sccm

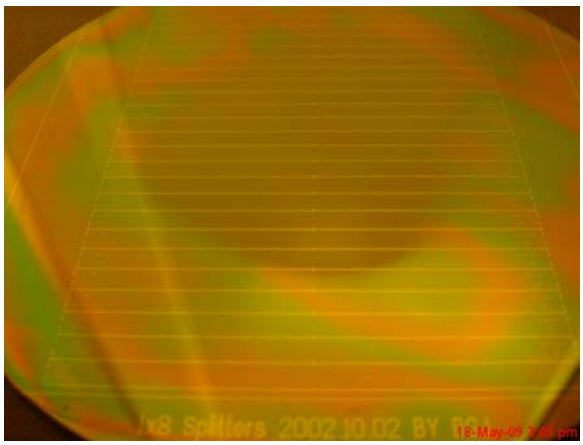

c) 30 sccm

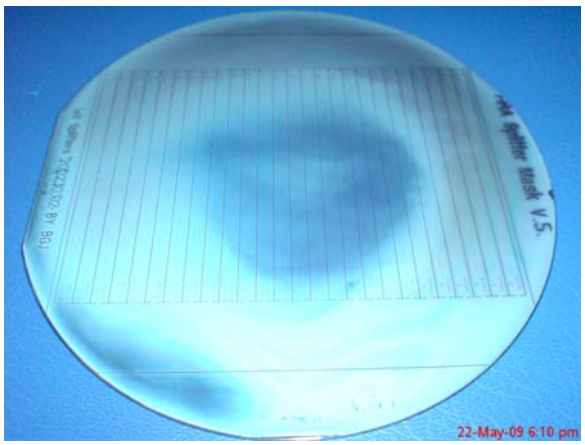

f) 50 sccm

Figure 4.14: Sample images after ICP process with various flow rate of reactant gas under default etching condition as shown in Table 4.3 except the chamber pressure was set at 12 mTorr.

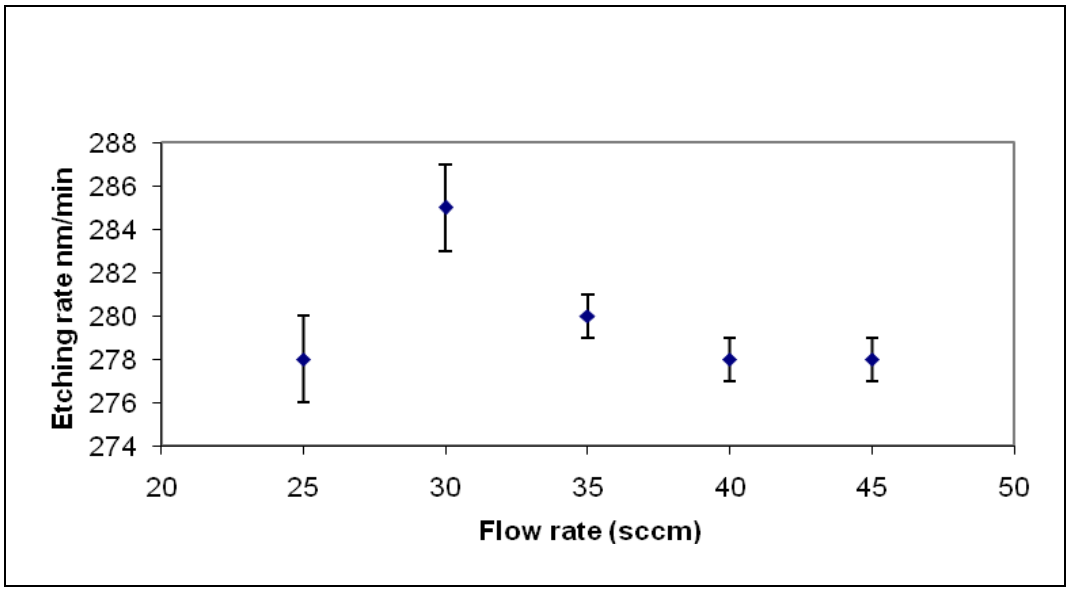

Figure 4.15: Glass etching rate against flow rate of input reactant gas under 12mtorr vacuum pressure with other default settings as shown in Table 4.3.

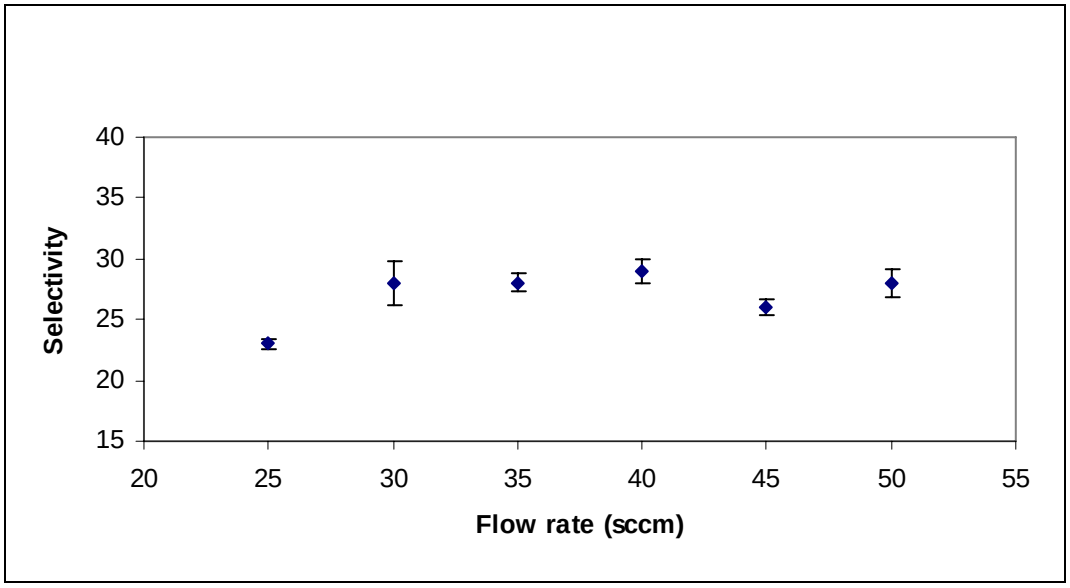

Figure 4.16: Selectivity of silica glass etching to chromium for various reactant flow rates under default settings as shown in Table 4.3 with 12mTorr operating chamber pressure.

The results of etching rate for samples that were etched under 12 mTorr of chamber pressure for various input reactant gas flow rates are shown in Figure 4.15. As mentioned earlier, the samples that were etched under 40sccm flow rate of reactant gas displayed a clean polymer-free surface, but it has a minimum etching rate of just about 278 nm/min. It is suspected that the resident time of the reactant particle at this flow rate when other conditions such as pressure was fixed, is most suitable for silica glass etching. For input reactant gas flow rate lower than 40 sccm, although it will increase the plasma energy and hence the etching rate like the sample that etched under 35 sccm and 30 sccm reactant gas flow rate. However, increase in the plasma energy will also induce polymerization and the etching process will be hack finally and causes the etching rate to decrease as in the case of 25 sccm reactant flow rate. The selectivity of silica glass to chromium etching under this condition is shown in Figure 4.16. In general, the average selectivity is for the range of input reactant gas flow rate tested is about 28 with standard deviation of 2.2. This shows that variation in reactant gas flow rate does not result in a significant effect on the etching selectivity.

The etching rate for the optimum flow rate (sample without polymerization) is 278 nm/min at 40 sccm. This value is almost equal to the etching rate for sample etched at 10 mTorr operating chamber pressure with 30 sccm reactant gas flow rate as shown in Figure 4.13 in the pressure optimization study. Hence it is expected that lower chamber pressure with a correspondingly lower reactant gas flow rate will result in the similar etching rate with higher selectivity. This is because the results discussed earlier show that the reactant gas flow rate does not cause any effect on selectivity, and samples etched at 10mTorr operating chamber pressure with 30 sccm reactant gas flow rate results in the highest selectivity as

shown in Figure 4.13. Therefore, input reactant gas flow rate optimization was carried out at 10 mTorr operating chamber pressure and the result is shown in Figure 4.17.

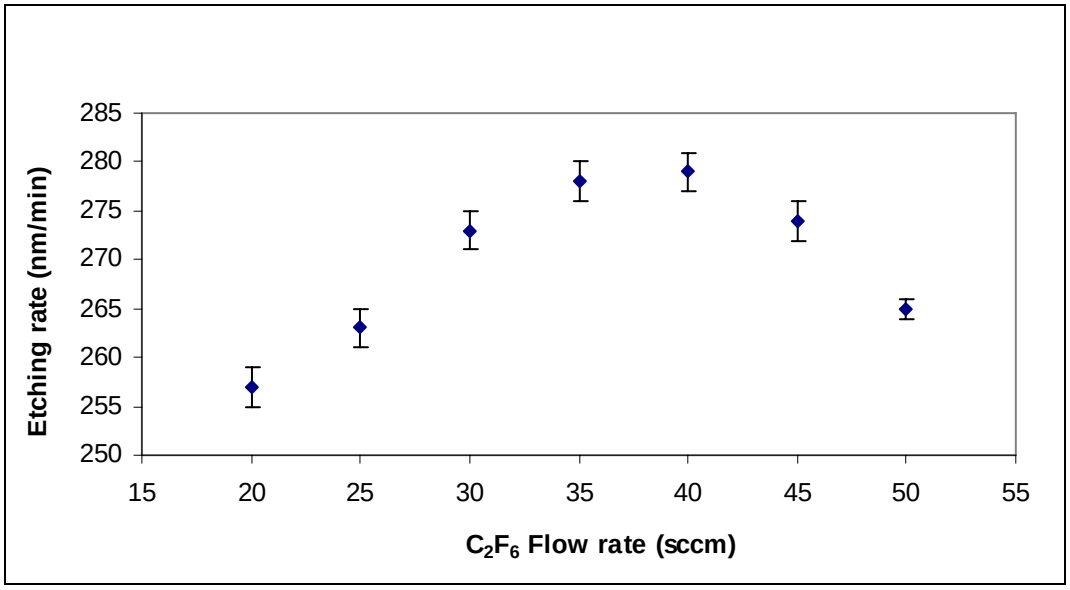

Figure 4.17: Glass etching rate against flow rate of input reactant gas under default ICP etching conditions as shown in Table 4.4 (10 mTorr).

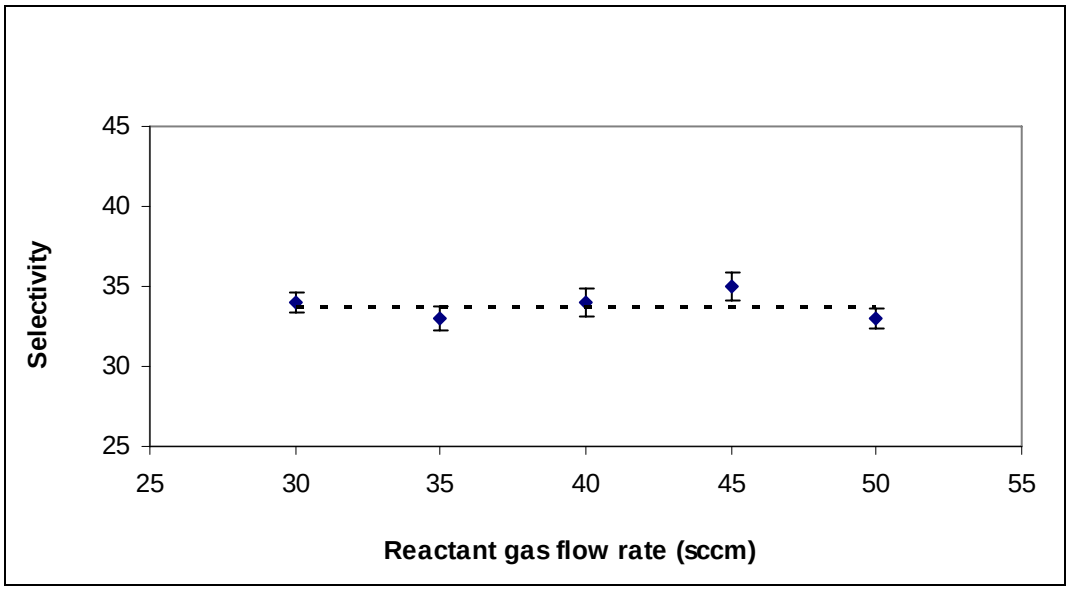

Figure 4.18: Selectivity of glass to chromium etching against flow rate of input reactant gas under default ICP etching conditions as shown in Table 4.3 (10 mTorr). (Trend line is for indicative purpose only)

In general, all samples etched at 10 mTorr operating chamber pressure from 20 sccm to 50 sccm input reactant gas flow rate did not produce serious polymerization effect as shown in Figure 4.14. In fact, the polymer layer was very thin that it cannot be observed with bare eye and this thin layer of polymer is somewhat beneficial for etching process. The detail of this effect will be discussed further in Chapter 5. Furthermore, lower operating chamber pressure mean higher plasma energy but lesser number of plasma particles. This condition might just be enough and suitable for etching compared to operating chamber pressure of 12 mTorr in which the plasma particles is in excess. Although excess in plasma particle results in higher etching rate, desorption of the by-product from the sample surface might not be efficient enough and causes polymerization occurrence.

As mentioned in the previous paragraph, desorption process for the by-product is believed to be sufficient in the operating chamber pressure of 10 mTorr. Under this condition, the optimum reactant gas flow rate that results in the highest etching rate is in the range of 35 sccm to 40 sccm. For reactant gas flow rate higher than 40sccm, the resident time for plasma particle is too short and leads to the presence of un-reacted carbon species in the chamber and finally reduces the etching rate. On the other hand, for reactant gas flow lower than 35sccm, the resident time is too long and the plasma could not supply enough fresh plasma particles for the etching process.

4.1.9 Gas composition optimization

Many fluorocarbon based gases can be used as reactant gas. These include, CF_4[6, 8], CHF_3[6, 11, 12], C_4F_8 [6, 12], and C_2F_6. In their work, Choi stated that the selectivity and polymerization are decreased as the fluorine to carbon (F/C) ratio of the reactant gas decreases (i.e. $F/C_{CF_4} > F/C_{CHF_3} > F/C_{C_4F_8}$) [6]. For example, CF_4 has a F/C ratio of 4 while C_4F_8 has a F/C ratio of 2. He also mentioned that the roughness of the glass after etching process are highest with C_4F_8 gas, followed by CF_4, while etching with CHF_3 produced the smoothest surface among the three gases. The fact that gases with lower F/C ratio are preferred for silica glass etching and that only C_2F_6 and CF_4 gas were available during the time of this research, meant that C_2F_6 was chosen to be used in this work.

During the etching process, small amounts of other gases like oxygen [11], argon [8] and hydrogen [13] may be added into the process to change the etching characteristics. For example, adding argon gas in the etching process will increase the degree of physical etching. However, this usually only applies to etching with light reactant gas like CF_4. Reactant gases like C_4F_8 or C_2F_6 themselves are heavy enough to provide a small degree of physical etching during the process. Adding oxygen into the etching process will enable the removal of polymerization simultaneously during the etching process. The oxygen radicals will oxidise the polymer to form light gases like carbon dioxide. However, adding oxygen gas into the etching process will cause the etching selectivity to decrease, while polymerization can be prevented by choosing the optimized etching process parameters, or by performing post treatment process like ashing or wet etching by polymer stripper to remove the polymerization. This effect will be further discussed in the next section. In this

study, only addition of hydrogen into the etching process was studied, while other gases like argon and oxygen were not investigated due to their negative effect on the etching selectivity.

4.1.9.1 Effect of adding hydrogen in the etching process

Low etching selectivity is caused by the relatively high etching rate of the chromium mask during the etching process. There are two processes during ICP etching which will increase the etching rate of chromium mask. The first is the physical etching [13]. It is induced by the application of bias power during ICP etching to achieve anisotropic etching. Physical etching is non-selective and will etch away both chromium mask and silica glass but with different etching rates. The difference in the etching rate depends on the materials bonding energy. However, this difference in physical etching is relatively small for chromium and silica. Therefore, physical etching causes significant removal of the chromium mask during ICP etching. The second is the chemical etching of chromium by oxygen radicals produced as by-product during the glass etching process. Tonotani reported that during silica glass etching, oxygen radicals in the etching system will oxidize the chromium to form CrO_x ($2 \leq x \leq 3$) [14]. These compounds are light and may evaporate from the mask surface. When the silica glass was etched by hexafluoroethane gas, by-product consisting oxygen compounds are released [15]. This oxygen based by-product may be ionized by the RF power source to form oxygen radicals and eventually result in the removal of the chromium mask. This type of etching may be prevented by eliminating the oxygen radical before it reacts with the chromium mask. By adding hydrogen into the plasma system, the liberation of oxygen during glass etching can be offset [9]. It is believed that hydrogen gas introduced

during glass etching process will react with the oxygen radicals to form water molecule and prevent the etching of chromium mask by these radicals, thereby increasing the etching selectivity.

Figure 4.19 shows chromium mask etching rate and selectivity of glass to chromium etching against the amount of hydrogen added in the etching process. It can be seen that the chromium mask etching rate reduces from about 8.5 nm/min to 5.5 nm/min and saturates at 5.5 nm/min while the selectivity of glass to chromium etching increases from 33 and saturates at 47 as the amount of hydrogen added increases from 0% to 31.4%, respectively. Moreover, Figure 4.20 shows the comparison of glass etching rate to selectivity of glass to chromium etching against the amount of hydrogen added in the etching process. The glass etching was highest at about 278 nm/min when no hydrogen is added into the system but reduces to about 255 nm/min and was maintained at this value as hydrogen gas was added with the compositions mentioned earlier. Increase in the hydrogen flow rate will shorten the resident time of the gases in the system because the gas extraction rate need to be increased in order to maintain the pressure of the system at 10mTorr. Short resident time will create un-reacted carbon species and eventually reduces the glass etching rate as shown in Figure 4.17.

The same effect is observed when only C_2F_6 gas is used in the etching process. Figure 4.17 shows the variation in etching rate as the C_2F_6 reactant gas is varied from 35 sccm to 50 sccm without addition of hydrogen gas. The glass etching rate reduces from 278 nm/min to 264 nm/min when C_2F_6 flow rate is increased from 35 sccm to 50 sccm. Therefore, glass

etching rate has a strong dependency on process gas flow rate regardless of whether hydrogen is introduced in the etching process. On the other hand, the etching selectivity is maintained at 33 when C_2F_6 gas flow rate is varied as shown in Figure 4.18. This shows that chromium etching rate decreases at a similar rate as glass etching rate with with different total gas flow rate when only C_2F_6 gas is used in the etching process. Therefore, without the addition of hydrogen gas, the etching selectivity can only be maintained but not improved, as in the case of hydrogen addition.

As a conclusion, by adding a small amount of hydrogen gas (about 30% of total gas) in the plasma etching system the selectivity of glass to chromium etching was increased. The selectivity was increased from 33 with no hydrogen addition to about 47 when 30% of hydrogen was added to the etching process. However, the etching rate was reduced by 23 nm/min and maintained at 255 nm/min when hydrogen is introduced in the etching process. ICP etching with only C_2F_6 gas also shows a decrease in glass etching rate when the gas flow is increased. However, selectivity is maintained at 33 for all gas flow rate. Therefore, introduction of hydrogen during ICP glass etching process improves the etching selectivity by more than 40% with a small penalty on glass etching rate.

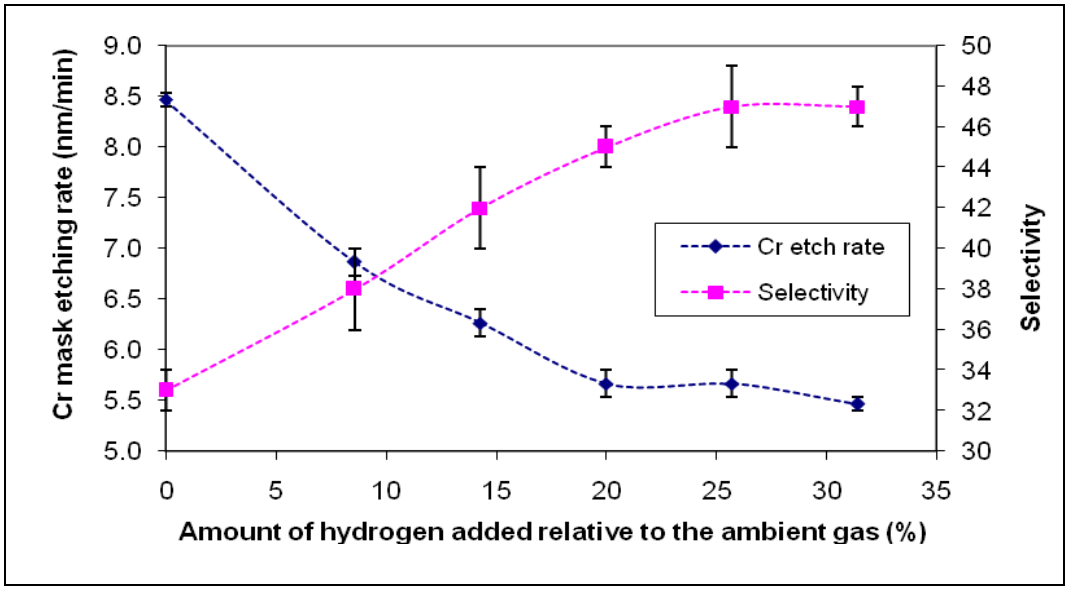

Figure 4.19: Chromium mask etching rate and selectivity against amount of hydrogen added in plasma etching. (Trend line is for indicative purpose only)

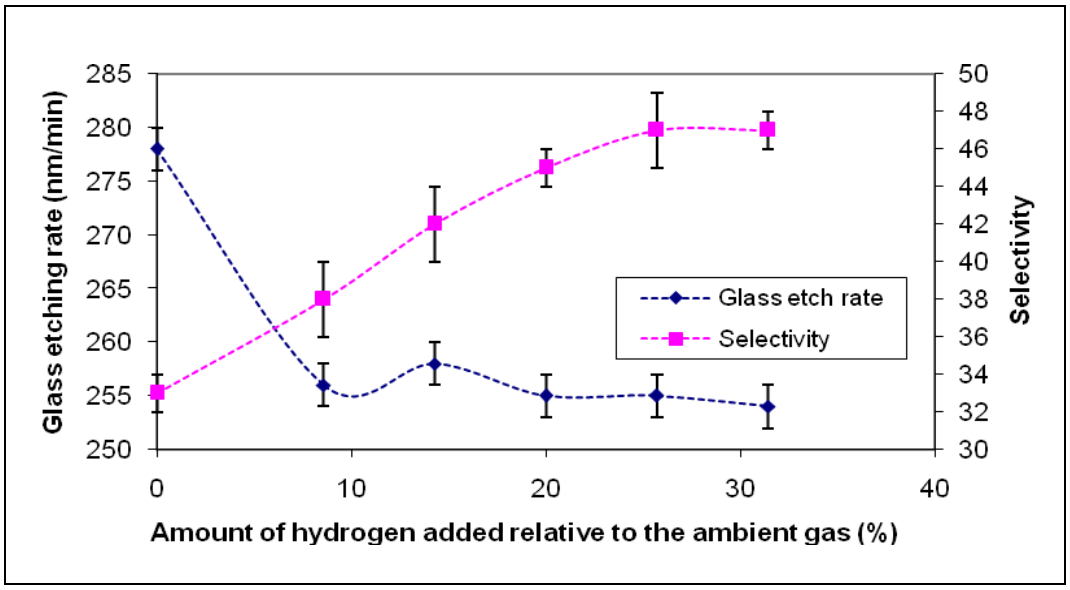

Figure 4.20: Glass etching rate and selectivity against amount of hydrogen gas added in plasma etching. (Trend line is for indicative purpose only)

4.1.10 Critical dimension & Resolution

Error analysis of critical dimension and resolution are important in etching process. Critical dimension refers to how much the etch patterns width differs from the desired pattern dimension while resolution refers to the minimum achievable separation between channels where complete etching can be done. Error analysis is important because it determines the quality of the circuits especially the minimum channel size and channel spacing. Besides, these two parameters should be taken into consideration during photomask fabrication in order to offset these errors. Error analysis can be measured by using the error analysis scale printed on the photomask as shown in Figure 4.21.

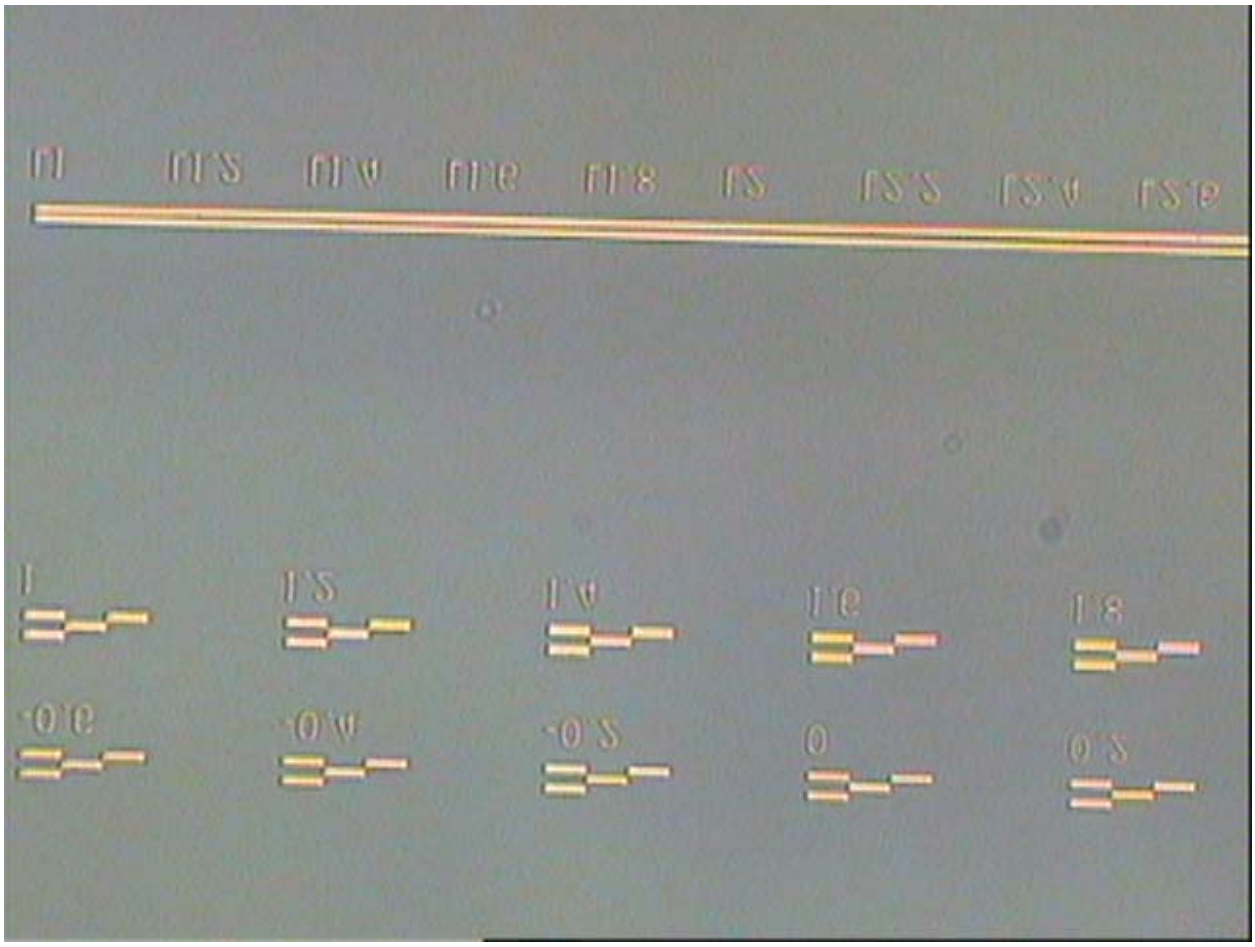

Figure 4.21: Error analysis scale on photomask.

Under optimum photolithography process done in a previous work, the pattern of photoresist itself has a critical error of 0.4 μm with average resolution of 1.2 μm as compared to the photomask. These results are shown in Figure 4.22. This means that the photoresist channel patterns is 0.4 μm smaller compared to the channel dimensions on the photomask. Additionally, the minimum spacing between two channels where complete etching was achieved is 1.2 μm.

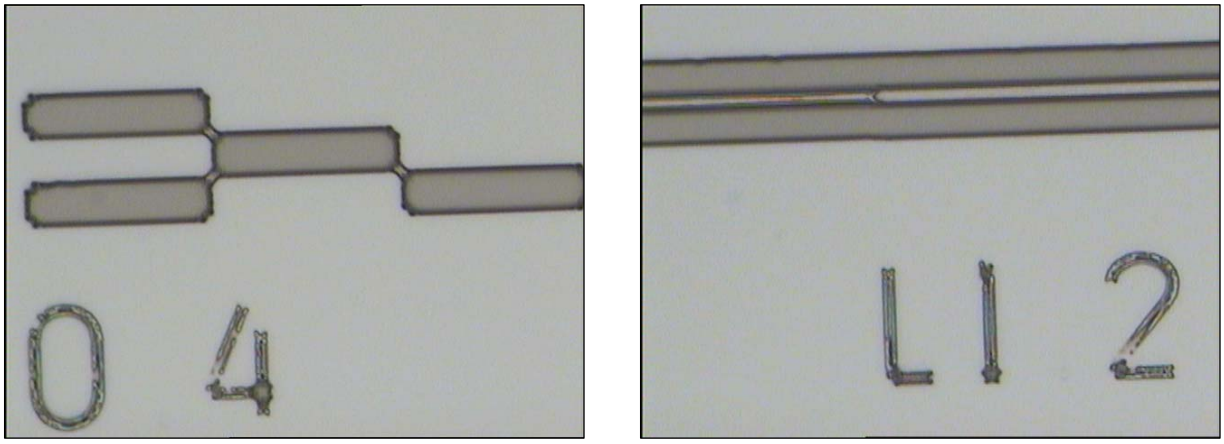

A) Critical Dimension B) Resolution

Figure 4.22: Error analysis of photoresist pattern.

On the other hand, after the chromium wet etching was conducted, the resulting chromium channel pattern has an average critical dimension of 0.8 μm while the resolution is maintained at 1.2 μm. Comparing the critical dimension of photoresist and chromium mask, the critical dimension of chromium mask increases about 0.4 μm. The reason for the large increase in critical dimension of chromium mask is due to chromium wet etching. Wet etching is isotropic etching and causes the critical dimension increases. While after ICP glass etching, the critical dimension was reduced by 1 μm with the resolution still maintained at 1.2 μm. The small increase in the critical dimension with a consistent

resolution after the ICP process is expected. This is because ICP glass etching is anisotropic. By right, the glass layer would have the same critical dimension as the chromium mask. However, the faceting effect on the chromium mask during wet etching process cause increase in the critical dimension. Faceting effect will cause the chromium pattern to be trapezium in shape instead of a perfect rectangular shape. Trapezium shape that has the property of larger area in bottom surface than the upper surface in the chromium layer will be transferred on to the silica layer due to anisotropic ICP etching. As a result, the critical dimension for silica glass layer is larger than the chromium layer. In order to reduce the faceting and minimize the critical dimension, reactive ion metal etching process is used to replace wet etching. Unfortunately in Photonic Research Centre University Malaya, we do not have this facility. Therefore, under optimum conditions, the pattern that the glass layer gain after all three etching processes are always smaller by about 1 μm with 1.2 μm resolution as compared to the pattern dimensions on the photomask.

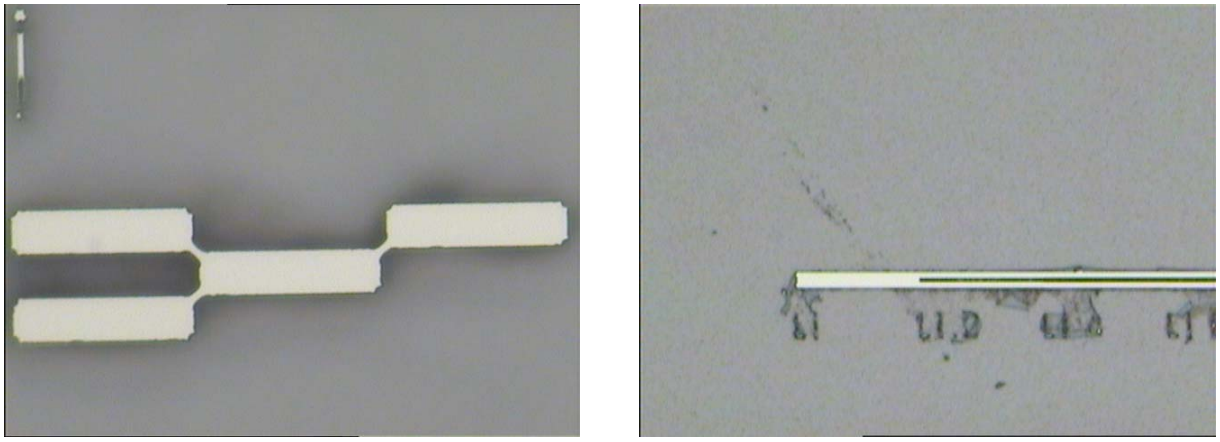

a) Critical dimension b) resolution

Figure 4.23: Error analysis of glass pattern after ICP process.

4.1.11 The plasma ring effect

4.1.11 The plasma ring effect

The plasma in the ICP machine is generated by a coil as shown in Figure 4.24. Since the coil is in circular shape (the plane of the coil is considered as the x-y plane), the distribution of the plasma in the x-y plane below the coil will form a “donut” shape. Viewed in the z-axis, it will be in a cone shape where the divergence end is furthest away from the coil. Hence, the density of the plasma is less compact in the centre as compared to the outer position. This distribution is suspected to give some effect on to the etching process.

Figure 4.24: ICP hollow copper coil. Water is flowed in the coil for cooling purposes.

In order to study the effect of plasma shape on the etching process, a test was conducted. In this test, the etching rate (by measuring the etch depth of each dicing line) across the whole

4 inch wafer was measured. The result is shown in Figure 4.25. The x-axis is an arbitrary unit that represent the position of dicing lines in an axis across the diameter of the wafer. The spacing between each dicing line is about 3 mm. In general, it has a "U" shape etching rate trend across the wafer. Higher etching rate is observed at the side of the wafer. The difference between the maximum etching rate and minimum etching rate is about 17nm/min. Moreover, the "U" shape trend was maintained when the ICP power was varied while bias power fixed at 65 W. The only difference is that the opening of the "U" might slightly be different. For lower ICP power, the "U" shape is open wider, it mean that the etching rate has smaller in different as across wafer. In order to study this effect, the regression function in the Excel program was used. The distribution of etching rate for each ICP power was fixed into a second order polynomial which has the general form of

$$AX^2 + BX + C \qquad (4.1)$$

Coefficient A is determines the opening of the polynomial graph. For example, a lower A value will lead to a wider graph opening. Using these advantages, each value of coefficient A for various ICP powers was determined and shown in Figure 4.26. In general, the distribution of etching rate across the whole wafer has a narrower opening at ICP power of 880W and becomes broader as the ICP power increases or decreases from this value.

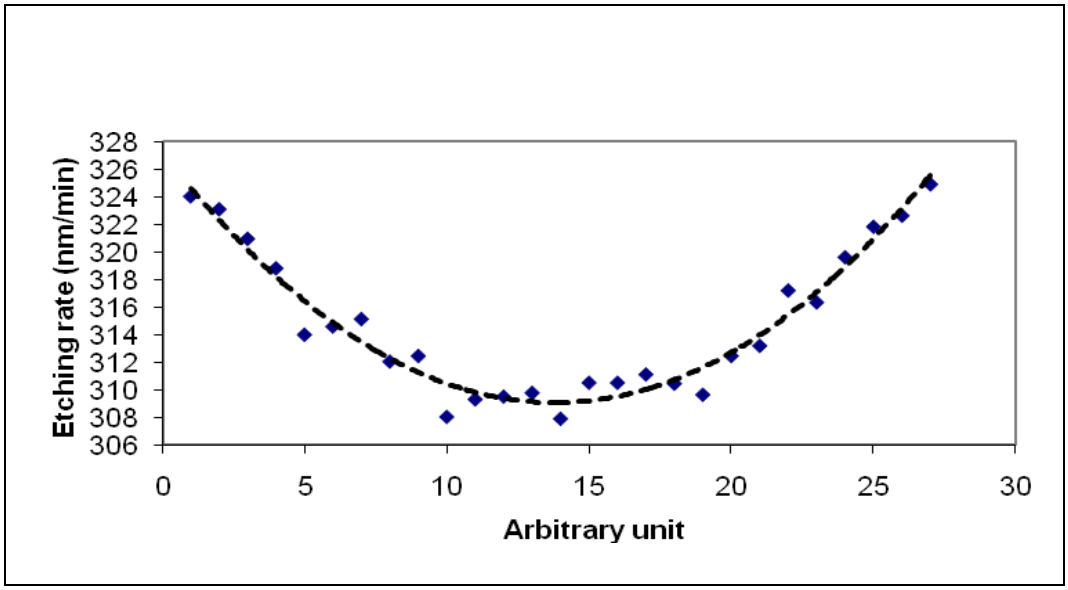

Figure 4.25: Effect of plasma shape on sample with bias power 65 W and other default ICP etching conditions as shown in Table 4.3. (Trend line is for indicative purpose only)

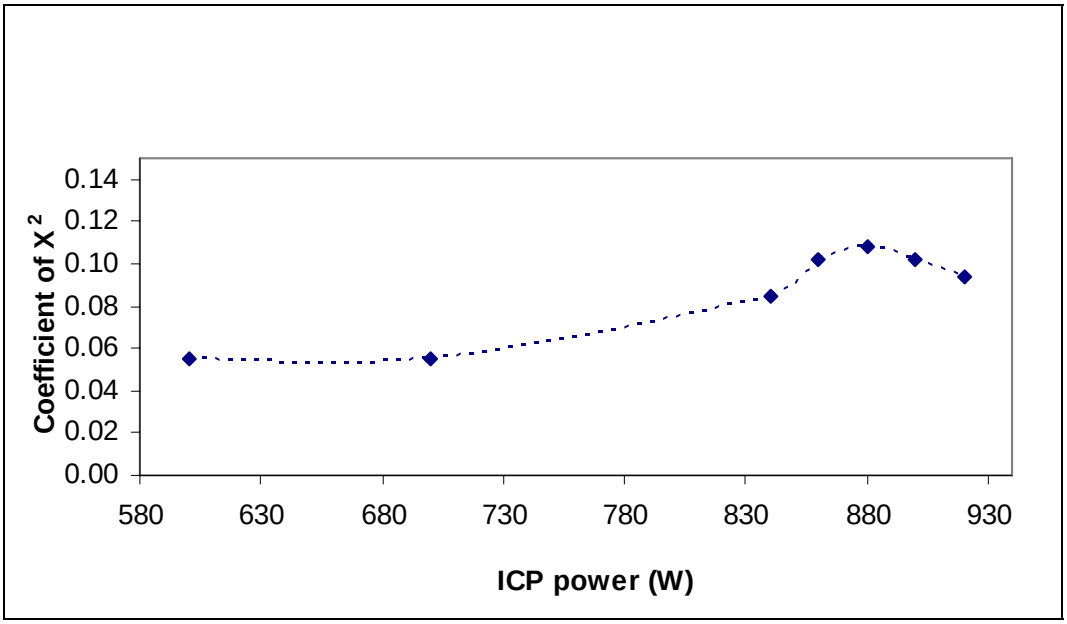

Figure 4.26: Coefficient values for X^2 in a regression fit of etching rate distribution for various ICP powers. (Trend line is for indicative purpose only)

The distribution of etching rate across the wafer for fixed ICP power but with various bias powers has a different characteristic as compared to variation in the ICP power. Figure 4.27 shows this effect and in general, the distribution trend changes from a "U" to a flat line as the bias power reduces. This is reasonable because as the bias power reduces, the etching process progress more towards isotropic etching hence reducing the plasma shape effect. Moreover, it is observed that the distribution was tilted. We suspect that it is due to the orientation of the bias coil. It is suspected that the bias coil is not fixed horizontally and was titled slightly. The left side is slightly higher than the right side and causes the left side of the wafer to etch faster due to stronger bias effect. However, for high bias power like 65 W, this difference is small and non-observable.

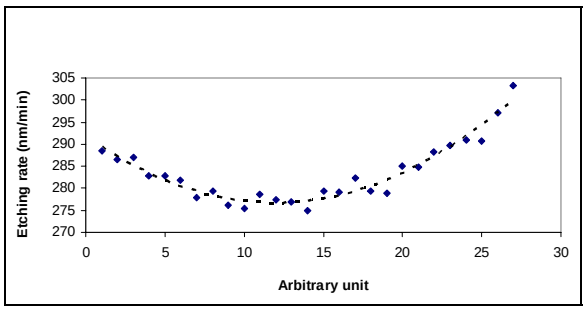

a) Bias power 55 W

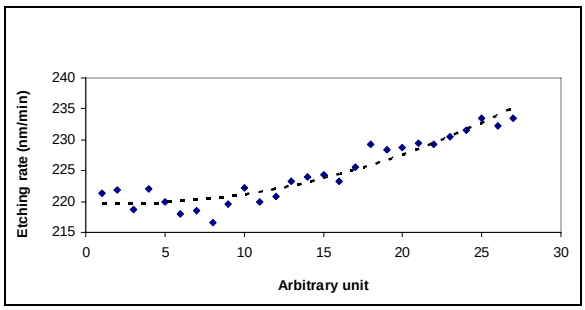

c) Bias power 35 W

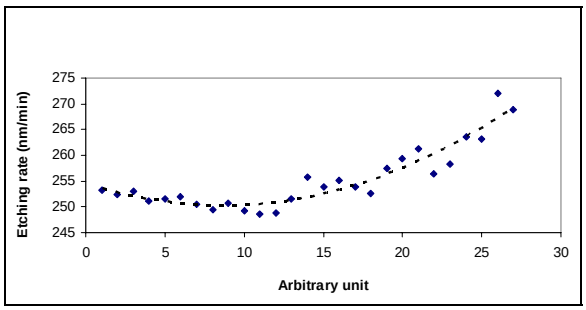

b) Bias power 45 W

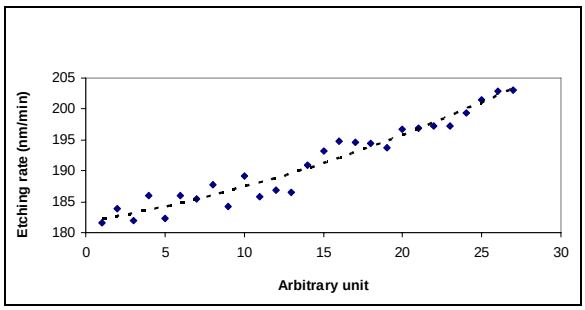

d) Bias power 25 W

Figure 4.27: Distribution of etching rate across the wafer for various bias power under default etching conditions as shown in Table 4.2. (Trend line is for indicative purpose only)

4.1.12 Summary of optimization process

As a summary of the optimization work that has been discussed in Section 4.1, the optimized parameters for silica glass etching for the current ICP machine are shown in Table below:

Table 4.5: Optimized parameters for silica glass etching process.

ICP Parameter	**Optimized Value**
ICP Power	880 Watt
Bias Power	45 Watt
Pressure	10 mtorr
Gas	C_2F_6 and H_2
C_2F_6 gas Flow	35 sccm
H_2 gas flow	9 sccm
Working distance	5 cm

The silica samples etched under these optimum etching conditions have display high etching rate of about 250 nm/min with good selectivity of about 45. For example, in a common 8 μm etch depth splitter fabrication, 35 minutes of glass etching process with chromium mask thickness of 200nm is sufficient. Furthermore, samples etched under these conditions with good handling in it pre-preparation steps are clean and free from any polymerization. Polymerization or contamination in the sample was further discussed in Section 5.1. Moreover the etched surface morphology, display minimum surface damage due to the small degree of physical etching which is avoidable. The channels that were etched under these optimized etching parameter has acceptable side wall angle and the

good sidewall roughness as compared to other tested parameter. Channels that almost in perfectly rectangular shape is important in waveguiding principle. The critical dimension of the channels is about 1 μm with resolution of 1.2 μm which is the best among the tested parameter. In term of etching rate uniformity, the sample has a low etching rate different in between the centre of the sample and the outer circumference of the sample due to the plasma ring effect. This different is just about 16nm/min and it corresponds to about 0.55 μm different between these two areas in 35 minutes of etching process.

The optimize parameters that shown in Table 4.5 are suitable for silica glass which only contain dopant likes phosphorous, boron, and germanium especially with the composition that shown in Table 3.3. Different composition or addition of other dopants such as Erbium in to the silica glass layer will cause deviation in the etching property. This deviation might require some minor turning in the ICP parameters to compromise the effect. For example, a higher reactant gas (C_2F_6) is required when erbium was doped in to the silica glass in order to obtain polymer-free etched surface. However, this will slow down the etching rate and also reduces the etching selectivity. The effect of dopant dependent in the silica glass etching process is further discussed in Section 5.3.

References

[1] T.M.Hoa, Charles R. de Boer & Pasqualina M. Sarro. (n.d) Roughness Treatment of Silicon Surface after Deep Reactive Ion Etching. Retrived March 27, 2009, from http://www.stw.nl/NR/rdonlyres/6A9E9428-9B60-42A2-A229-C6DDD618271D/0/pham.pdf.

[2] M. L. Calvo, & V.Lakshminarayanan. (2007). Optical Waveguides:From Theory to Applied Technologies. Boca Raton:CRC Press Taylor & Francis Group.

[3] S.T. Jung, H.S. Song, D.S. Kim & H.S.Kim. (1999). Inductively Coupler Plasma etching of SiO_2 layers for Planar Lightwave Circuits. Thin Solid Film, 341, 188-191.

[4] S.B.Kim, H.Seo, Y.Kim, & H.Jeon. (2002). Remote RF Oxygen Plasma Cleaning of the Photoresists Residue and RIE-Related Fluorocarbon Film. Korean Physical Society, 41 247-250.

[5] D.S. Rawal, V.R.A., H.S.Sharma, B.K.Sehgal, & R.Muralidharan, (2008). A Reproducible High Etch Rate ICP Process for Etching of Via-hole Grounds in 200 μm Thick GaAs MMICs. Journal of Semiconductor Technology and Science, 8 (3) 244.

[6] D.Y.Choi, J.H.Lee, D.S.Kim, & S.T.Jung. (2004). Formation of Plasma Induced Surface Darmage in Silica Glass Etching for Optical Waveguides. Journal of Applied Physics, 95 (12),8400-8407.

[7] S. Franssila. (2004). Introduction to microfabrication. England: John Wiley & Son.

[8] D.Shin. & J.H.Eo. (2005) Plasma Etching Characteristic of Ge-B-P doped SiO_2 Film for Waveguides Fabrication. Ceramic Processing Research, 6 345-350.

[9] B. Chapman. (1980). Glow Discharge Process. New York: John Wiley & Sons.

[10] K.H.Park, S.Lee, K.H.Kwon and J.H.Moon. (2001). The effect of CF_4 and CHF_3 gas on the etching characteristics of Er-doped glass. Material Science Letter, 20 565-568.

[11] L.B.Zhou, F.G.Luo, & M.C.Cao. (2005). Study of the Plasma Etching Process for Low-loss SiO_2/Si Optical Waveguides. Thin Solid Film, 489,229-234.

[12] T.Akashi & Y.Yoshimura. (2006). Deep Reactive Ion Etching of Borosilicate Glass Using an Anodically bonded silicon wafer as an etching mask. Journal of Micromechanics and Microengineering, 16, 1051-1056.

[13] J.D.Chinn, I.Adesida, E.D.Wolf & R.C.Tiberio. (1981). Reactive Ion Etching for Submicron Structure. Journal of Vacuum Technology, 19, (4) 1418-1422.

[14] J.Tonotani, S.I. Ohmi, & H.Iwai. (2005). Dry Etching of Cr_2O_3/Cr Stacked Film During Resist Aashing by Oxygen Plasma. Japanese Journal of Applied Physics, 44, 114-117.

[15] EzzEldin Metwalli & Carlo G. Pantano. (2003). Reactive Ion Etching of Glasses: Composition Dependence. Journal of Nuclear Instruments and Methods in Physics Research Section B: Beam Interactions with Materials and Atoms, 207,21-27.

CHAPTER 5

MORE ON ICP

5.0 Introduction

There are few investigations into areas that are related to the ICP process was conducted in this study and the result of this study is discussed in this chapter.

5.1 Contamination

A clean surface is important in PLC fabrication especially after the ICP glass etching. This is because contamination will affect the light propagation due to differences in the effective refractive index from the expected or designed value. Contaminations during ICP etching are usually in the form of polymeric material adhering to the substrate surface. Therefore the term polymerization is used to refer more precisely to contamination formed during ICP process. Beside polymerization, plasma induced surface damage (PISD) or plasma induced damage (PID) refers to pinhole shaped damages on the sample surface during ICP dry etching process. For general simplification, PSID, PID and polymerization will be referred generally as contamination in this work.

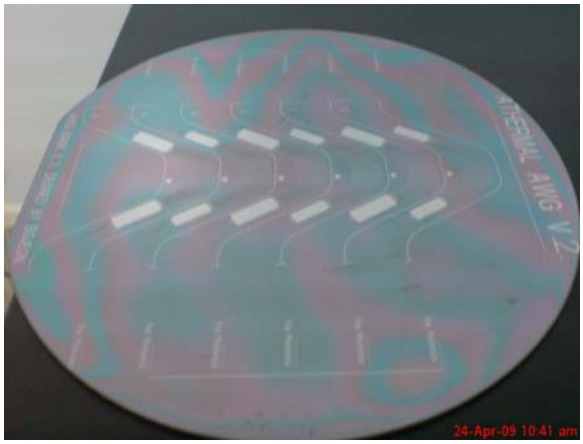

a) Digital camera

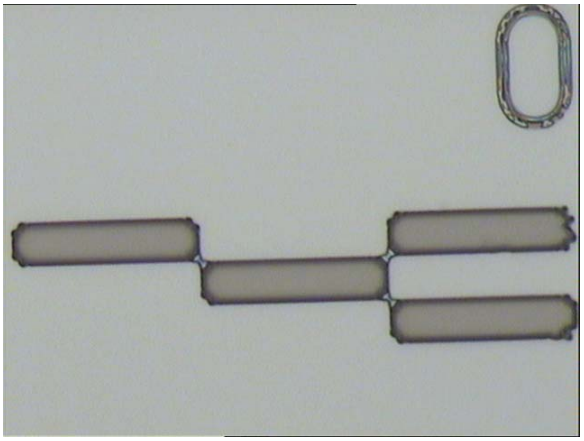

b) Microscope

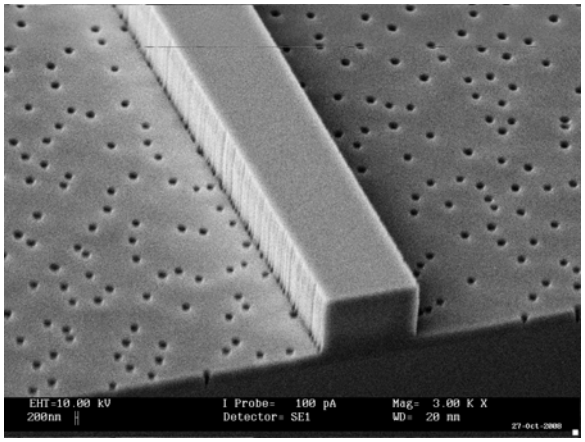

c) SEM Image with mild PSID effect

Figure 5.1: Example of clean surface images taken using a) camera, b) microscope and c) SEM image with mild PSID effect.

In the camera image shown in Figure 5.1a, a very clean surface is observed. In fact, the optical fringes caused by the in-homogeneity of the glass layer can also be observed. This phenomenon is usually used as pre-determination to check whether the sample is free from contamination. This determination method is quite accurate unless the contamination formed is a very thin layer until it cannot be observed by bare eye or it occurs only in a certain small area. Figure 5.1c shows the example of SEM image for a clean side wall channel with mild PSID effect. Note that, a very thin layer of polymer formed on the wafer

are good for etching process as reported by Shin [1]. However, Shin did not mention the optimum thickness in his work. The basic etching mechanism must be understood in order to appreciate why a thin layer polymer is good for etching.

As mentioned in chapter 2, the etching mechanism consists of several steps shown below:

1) Generation of reactive species in plasma;
2) Diffusion of these species to the surface of the material being etched;
3) Adsorption of these species on the surface;
4) Occurrence of chemical reactions between the species and the material being etched, forming volatile by-products;
5) Desorption of the by-products from the surface; and
6) Diffusion of the desorbed by-products into the bulk of the gas.

For a successful etching, all the steps above must be fulfilled. Contamination occurs due to the inefficiency of step 5 or step 6. If the by-products formed are not able to desorbs from the layer, then a layer of polymer will form on top of the sample surface and it will hack the etching process. On the other hand, if the diffusion process in step number 6 is incomplete, the by-products may redeposit back onto the sample surface and hence polymerization occurs. However for a good etching process, step 4 needs to be efficient in order to allow sufficient chemical reaction. The plasma particles, usually in polymer form, need to be adhered on the wafer surface for a certain amount of time before the desorption process takes place. A certain thickness of polymer deposited on the wafer is sometimes preferable for etching process as reported by Shin [1]. If the thickness of the polymer is too thin, it will slow down the etching process due to insufficient amount of volatile species. It

is suspected that this phenomenon shows in operating chamber pressure optimization under Section 4.1.7 where the etching rate of sample that etched under 12mTorr which has polymerization is higher than 10 mTorr sample which free from polymerization. However, the etching rate decreases again for samples etched under operating chamber pressure, of 14mTorr. This is because if the polymer is too thick, then the polymer layer will prohibit further etching process by weakening the plasma particle.

In general, the source of contamination can be grouped into 3 categories. There are contamination caused by the mis-handling of sample before ICP etching, by the ICP etching process itself, and the behaviour of the glass layer itself.

5.1.1 Contamination caused by mishandling of sample before ICP etching process

The reason for this contamination to occur is the existent of certain contaminants that sticks on the surface of the sample before the etching process. This contaminant may not react with the etchant gas to form volatile by-product, blocking the diffusion of the by-product from the sample surface. The sources of this contamination are in the lithography process. For example, after wafer cleaning, if the remaining water is not dried on the surface quick enough, the contaminant in the water will stick onto the wafer after the water droplet dried. Hence the resulting contamination after ICP etching usually shows a shape similar to the water mark as shown in Figure 5.2a, and Figure 5.2b. During the substrate cleaning process for the sample shown in Figure 5.2c, a water droplet from the researchers' glove was accidentally dropped onto the wafer. This water droplet is believed to have transferred micro particles on the glove onto the wafer and cleaning the wafer again with standard cleaning procedure was not able to completely remove these contaminants. As a result, this causes contamination as shown in Figure 5.2c. The contamination shown in Figure 5.2d originates from the glass consolidation process. The rectangular mark on the sample is similar to the mark on the silicon substrate holder that holds the sample during the consolidation process. Whether the contaminant originates from the silicon substrate holder, or the furnace environment, is still to be investigated. Figure 5.2e and Figure 5.2f show the SEM images of plasma induced surface damage caused by micro-mask. The chromium layer that supposed to be removed in that particular area was hack during the wet etching process and eventually formed a micro-mask. This micro-mask will block the glass etching process and causes pits to occur.

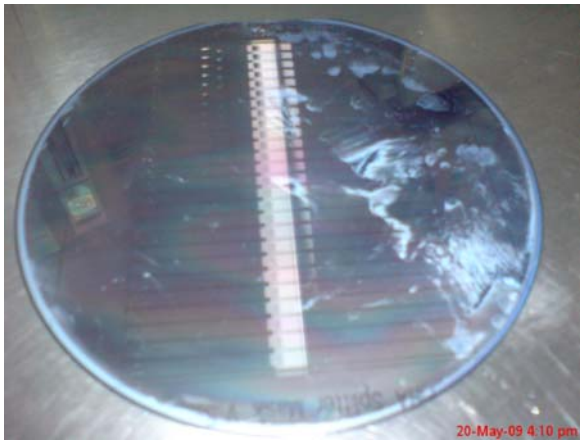

a)

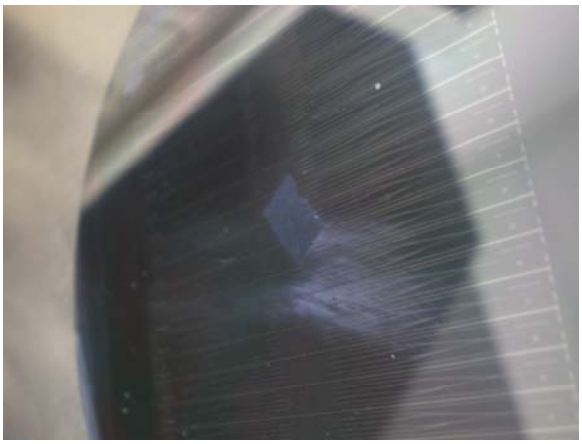

d)

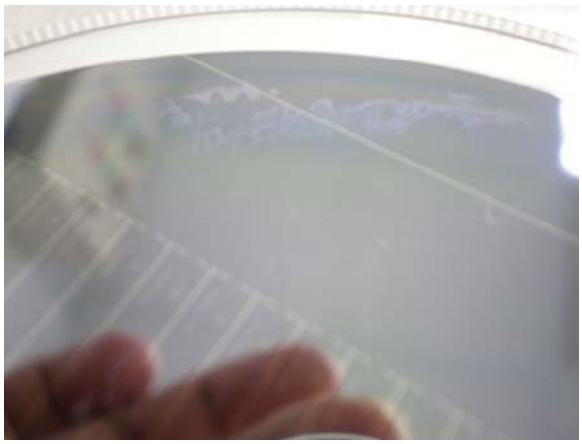

b)

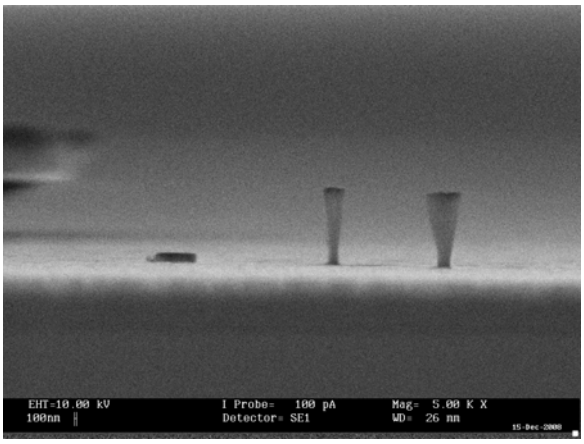

e)

c)

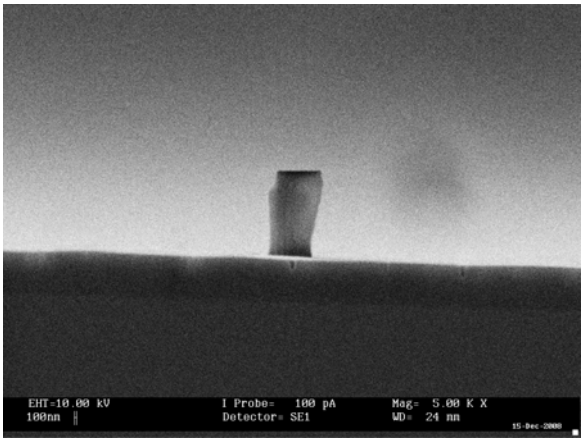

f)

Figure 5.2: Example of images showing contamination caused by external factors.

5.1.2 Contamination caused by the ICP process

Generally the sources of contamination caused by the ICP process are due to non-optimized chamber pressure and flow rate or either ICP power or Bias power was set too high. The example of these contaminations is shown in Figure 4.14d.

5.1.3 Contamination caused by sample composition

The silica glass film used for PLC applications is co-doped with other elements such as phosphorus, germanium, and boron as well as rare earth elements. Rare earth ions like erbium and neodymium were doped into the glass layer for light amplification purposes. These dopants may not react with C_2F_6 to form volatile gas [2]. As a result, these will block the etching mechanism. It is observed that the polymerization formed under this condition is uniform because a uniform white dish layer can be observed by bare eyed on the whole wafer as shown in Figure 5.3. This effect can be reduced by increasing the reactant flow rate or by mixing a certain amount of other gases like CHF_3 into the existing reactant gas CF_4 as reported by Park[2].

Figure 5.3: Polymerization that form on Erbium doped silica glass after ICP etching.

5.1.4 Effect of polymerization on waveguide

Figure 5.4 shows polymerization effects on the sample channel after ICP glass etching process. It is clearly observed that the polymers almost cover the whole side wall of the channel. This polymer is believed to disrupt the waveguiding characteristic of the channel. This is because polymer may have a different refractive index compared to the glass cladding layer which might lead to high propagation loss. Rough surface cannot be used as a platform for hybrid integration because of difficulties in alignment and this polymer may also affect the adhesiveness of over cladding during the over cladding deposition [3].

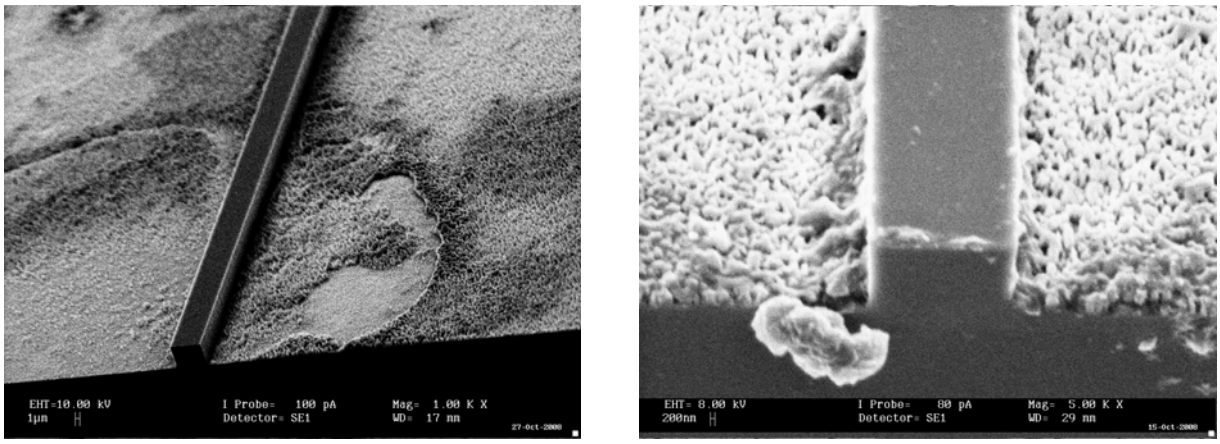

a)1000X magnification b) 5000X magnification

Figure 5.4: SEM image of polymerization on the channel.

5.2 Effect of chromium deposition on ICP etching

As mentioned in Chapter 3, chromium layer was deposited using direct current plasma grow discharge. The pressure of the chamber will have some effect on the stress of the deposited chromium. The induced stress during chromium deposition may cause variation in the hardness of the chromium layer and affect the ICP etching process especially the etching selectivity.

In general, the argon gas will be ionised by the plasma and form positive ion. This positive charge ion will then be accelerated by the electric field towards the chromium target (cathode). The bombardment between the ion and the chromium atom in the target resulted in energy transfer and the chromium atom may be sputtered out from the target. These sputtered chromium atoms are then deposited in the chamber including on our sample. When chromium was deposited at a relatively high pressure in DC sputtering, the energetic argon ions may rebound back from the target and get neutralised. The energetic neutralised argon particle will not respond to the DC electric field and may arrive on the sample. These neutral atoms arriving on the sample are more likely to be embedded in the growing film, hence it will act as contaminant in the chromium layer and reduce the density of chromium layer [4-7].

Figure 5.5 shows a constant in selectivity of ICP etching with respect to a variation of the chromium deposition pressure. Selectivity is not affected by the DC sputtering deposition pressure. The variation of the chromium density in different chromium deposition pressure

is too small in the current pressure variation range, hence did not cause any significant changes in selectivity.

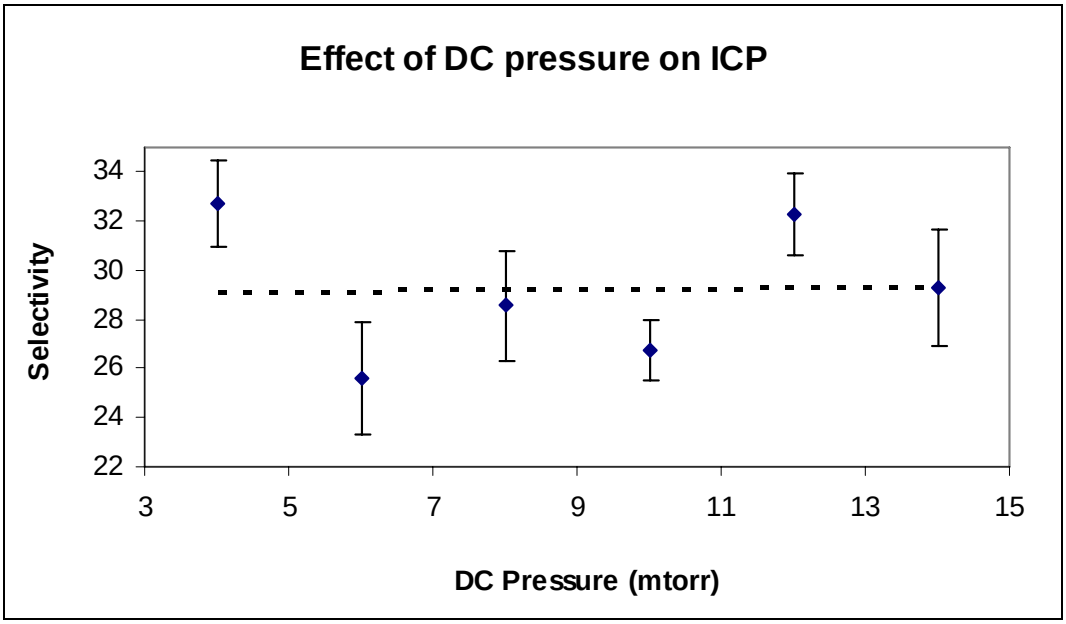

Figure 5.5: Effect of DC pressure to the selectivity of chromium to glass etching on ICP etching process. (Trend line is for indicative purpose only)

5.3 Effect of dopant in silica glass to ICP etching

The most important step in PLC fabrication is glass fabrication. In order to fabricate a glass layer with minimum propagation loss and desirable refractive index, dopants like germanium, phosphorous, and boron are usually doped into the silicon oxide glass layer. The functions of these dopants are to control the refractive index, photosensitivity, glass consolidation temperature as well as the intrinsic properties of the glass [8, 9]. Co-doping with these elements will tend to change the glass properties, and consequently affect the ICP etching. Hence it is important to study comprehensive the effect of co-doping on ICP glass etching characteristics.

5.3.1 Effect of phosphorous doping in silica glass on ICP etching

In this study, phosphorous doped silica sample (normally known as phosphosilicate glass) was prepared by FHD. Phosphorous doping is achieved by introducing $POCl_3$ precursor into the oxy-hydrogen flame during the FHD process. During the deposition process, the flow rate of $SiCl_4$ precursor, hydrogen gas and oxygen gas were fixed at 20 sccm, 5000 sccm, 5000 sccm respectively while the flow rate of $POCl_3$ gas was varied from 40 sccm to 100 sccm with intervals of 20 sccm. The soot layers formed are consolidated at 1320 ^{0}C for 1 hour. Then, DC sputtering and lithography process were carried out using the same parameters as mentioned in Chapter 3. For consistency, all four samples were etched in the same ICP etching process using default etching conditions as mentioned in Table 4.4.

Effect of $POCl_3$ flow rate on the resulting glass layer refractive index is shown in Figure 5.6 while Figure 5.7 shows the phosphorous incorporation rate in $POCl_3$ flow rate. Both Figure 5.6 and Figure 5.7 show the incorporation of phosphorous in the sample using FHD process. Phosphorous is a well known index riser hence in Figure 5.6, the refractive index increases from 1.4478 to 1.4521 as the flow rate of $POCl_3$ was increased from 40sccm to 100sccm in the FHD process [10]. This result indicates that phosphorous is being doped into the silica glass and its concentration increases as the flow rate of $POCl_3$ increases. Figure 5.7 confirms this fact where the atomic percent of phosphorous obtained from EDX increased from 0.34 atomic percent to 0.48 atomic percent where the $POCl_3$ flow rate was increased from 40 sccm to 100 sccm respectively.

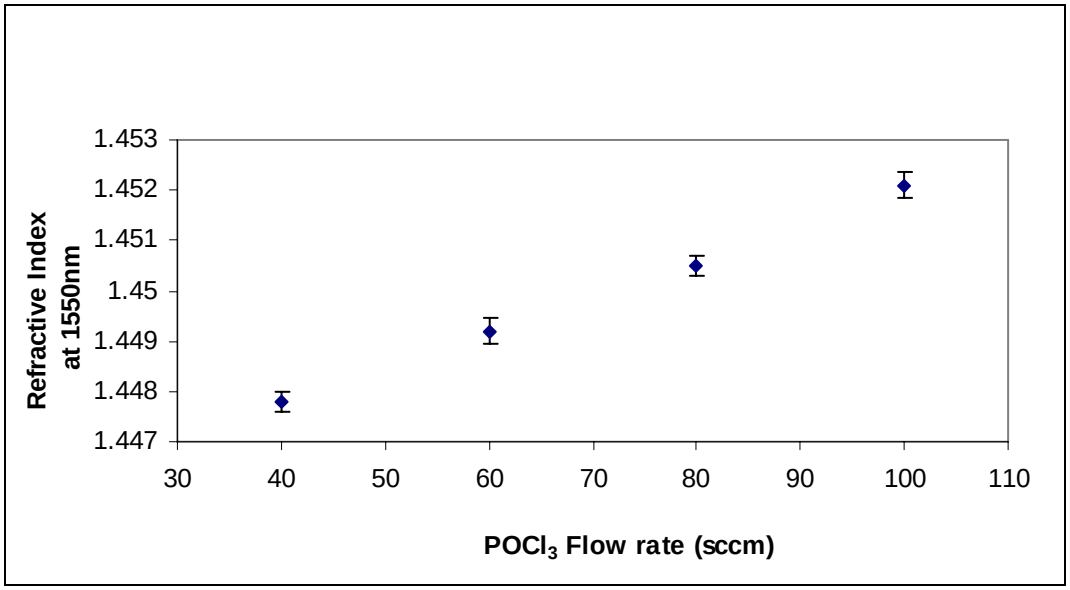

Figure 5.6: Refractive Index measured by prism coupling for different $POCl_3$ flow rates in FHD.

.

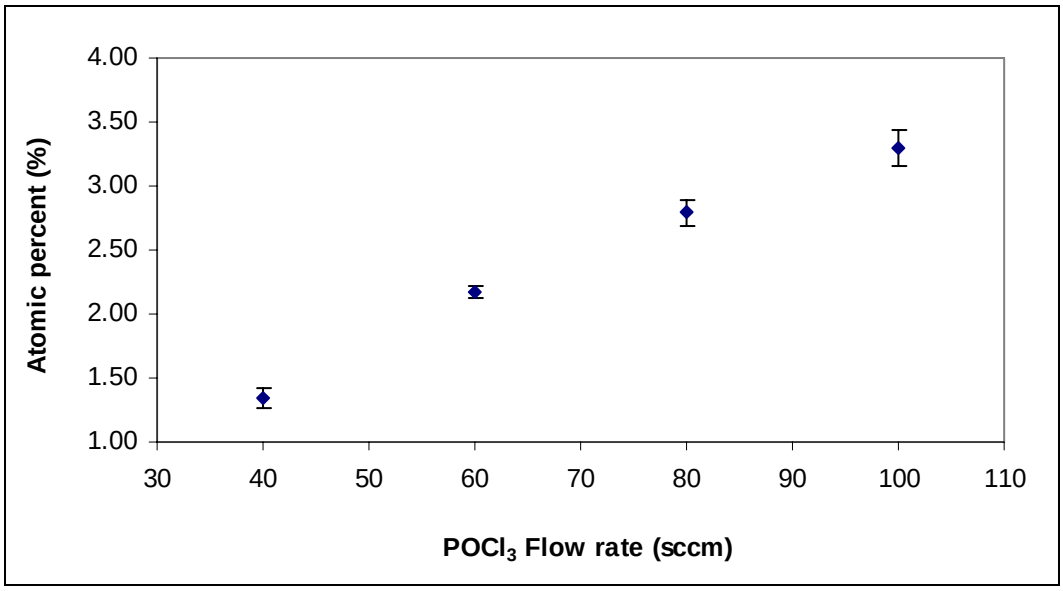

Figure 5.7: Atomic percent measured by EDX with different $POCl_3$ flow rate in FHD.

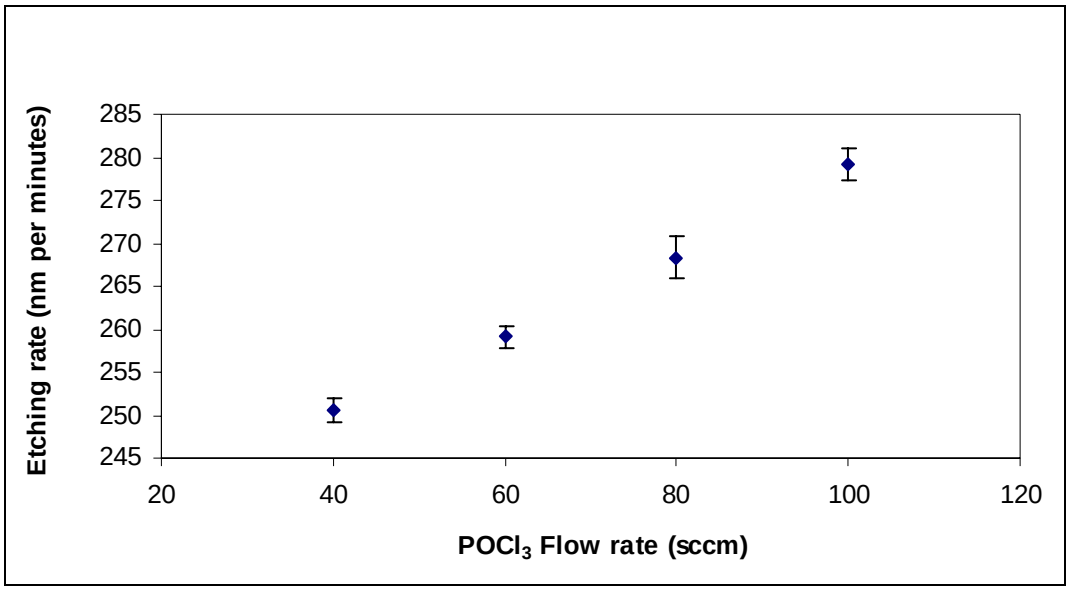

Figure 5.8: Glass etching rate against $POCl_3$ flow rate in FHD.

Figure 5.8 shows the glass etching rate dependency on the amount of $POCl_3$ flow rate applied during the FHD process. It can be seen that the etching rate increased as the concentration of phosphorous increases in the phosphosilicate glass. The doping dependency etching rate is 0.4764 nm/min/sccm. The increase in the etching rate can be explained by the change in bonding structure of the glass structure. For pure silica glass, every silicon atom is bonded to four other oxygen atoms in a tetrahedral structure. Each tetrahedron is bonded to four other tetrahedrons via silicon-oxygen bonds. However, for phosphorous atom, which is a group V element, there exist double bonds between one of the bondings with oxygen in each tetrahedron structure in phosphate glass. The atomic structure of these two glass structures are shown in Figure 5.9. In other words, each tetrahedron is bonded to only three other tetrahedron structures via the phosphorous-oxygen bond and this causes the termination of the chain structure. Termination of chain structure is not likely in non-defect silica glass. Due to this reason, the density of phosphate glass is always lower than that of silicate glass and causes the decrease in it is consolidation

temperature [10]. Therefore, as the concentration of phosphorous in phosphosilicate glass increases, the chain termination occurs more frequently. This chain termination weakens the glass molecular structure. Hence the glass matrix will require less energy to be removed in ICP etching under the same etching conditions.

Selectivity is defined as the ratio of glass layer etching rate to chromium mask layer etching rate. Hence, initially it is expected that the selectivity will increase as the concentration of phosphorous dopant increases in the sample. This is because the phosphorous dopant causes the phosphosilicate glass to be more easily etched. However, Figure 5.10 shows that the etching selectivity of phosphosilicate glass in ICP etching decreases as the concentration of phosphorous dopant increases in the phosphosilicate glass sample. This does not agree with earlier expectation.

The lower selectivity obtained in phosphosilicate glass is believed to be related to the amount of oxygen radical generated during the etching process. In pure silica glass, the atomic ratio between oxygen to silica is 2:1 (SiO_2), while in phosphate glass this ratio is 5:2 (P_2O_5). In the mechanism of Chromium Reactive Ion Etching reported by Junichi Tonotani et.al, oxygen radicals will oxidize the pure Chromium layer and form a light compounds CrO_x ($2 \leq x \leq 3$). This compound is volatile and may easily evaporates from the sample surface [11]. In phosphosilicate sample, a higher phosphorous dopant will result in more oxygen species in the etching chamber. Hence more oxygen particles will be ionised by the ICP RF power to form free radicals to react with the chromium pattern to form CrO_x

compounds. We suspect that this causes a higher etching rate of chromium and finally reduces the etching selectivity in phosphorous rich glass as shown in Figure 5.10.

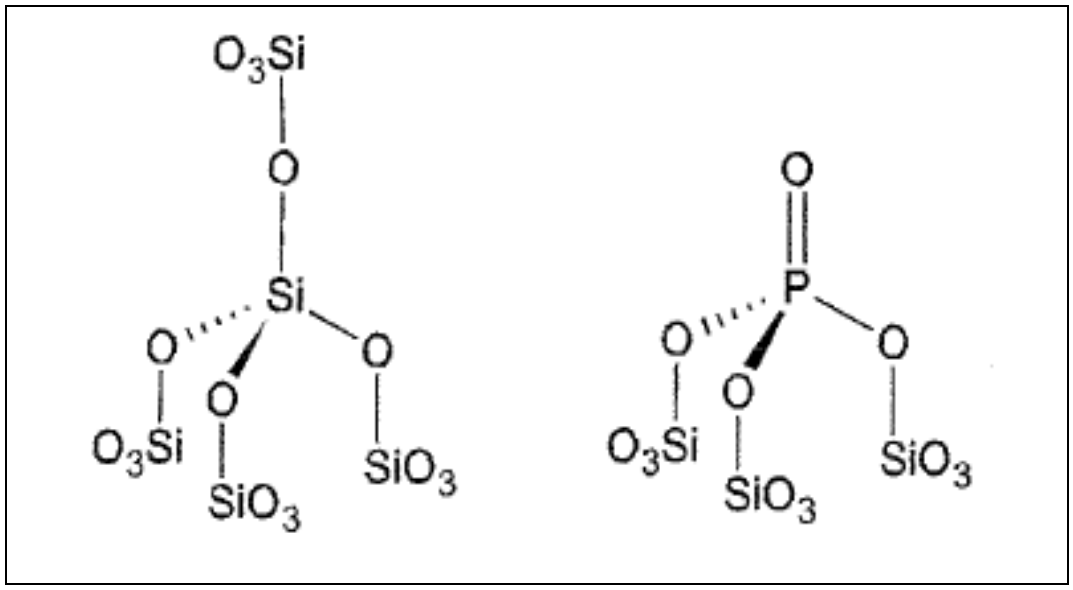

Figure 5.9: Atomic structure of silica glass and phosphosilicate glass.

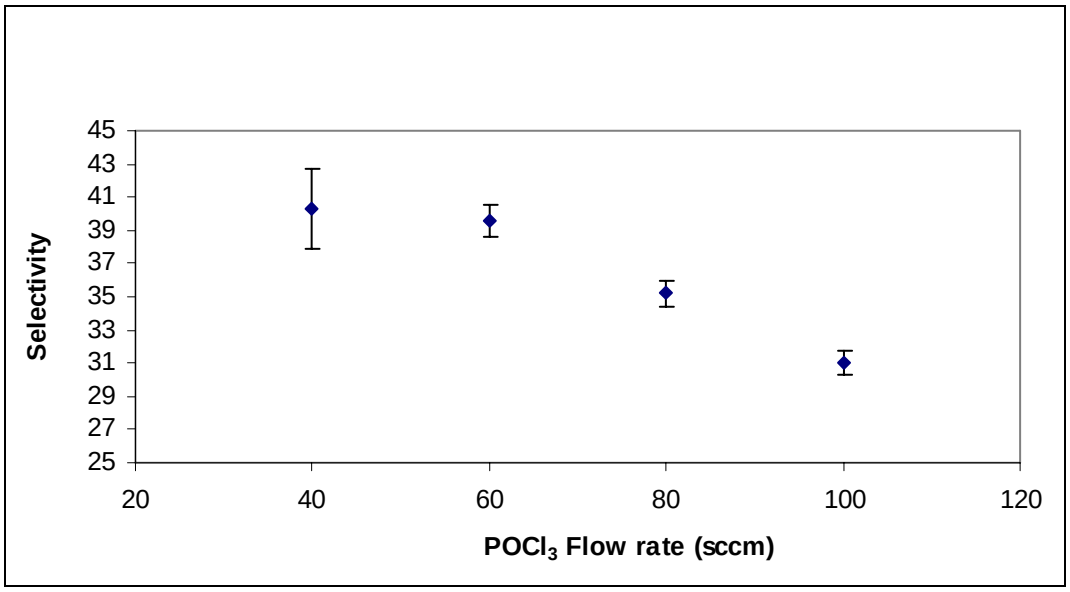

Figure 5.10: Selectivity of phosphosilicate glass to chromium in ICP etching against $POCl_3$ flow rate in FHD process.

5.3.2 Effect of Germanium doping in silica glass on ICP glass etching

Similar to Section 5.3.1, germanium doped silica sample (normally known as germanosilicate glass) was prepared using FHD by introducing $GeCl_4$ precursor into the oxy-hydrogen flame. During the deposition process, the flow rate of $SiCl_4$ precursor, hydrogen gas and oxygen gas were fixed at 20 sccm, 5000 sccm, 5000 sccm respectively while the flow rate of $POCl_3$ gas was varied from 40 sccm to 100 sccm with intervals of 20sccm. The soot layers formed are consolidated at 1320 ^{0}C for 1 hour. Then DC sputtering and lithography process were carried out using the same parameters as mentioned in chapter 3. For consistency, all four samples were etched in the same process using default etching condition as mentioned in Table 4.4.

Figure 5.11 shows the incorporation of germanium in the silica glass with respect to their precursor gas flow rate in FHD process. The germanium concentration increases from 4.63 at% to 9.75 at% when $GeCl_4$ precursor flow rate was increased from 40 sccm to 100 sccm respectively. The effect of germanium dopant to refractive index of silica glass is shown in Figure 5.12. The refractive index increases from 1.462 to 1.483 when germanium concentration increases from 4.63 at% to 9.75 at%. In other words, germanosilicate glass has a refractive index dopant dependency property of 0.0040 at%$^{-1}$. Figure 5.13 shows the etching rate for germanosilicate glass with its corresponding dopant concentration. In general, germanosilicate glass shows dopant dependent etching property. The etching rate in germanosilicate glass increases linearly from 270 nm/min for germanium concentration of 4.63 at% to 301nm/min for germanium concentration of 9.75 at%.

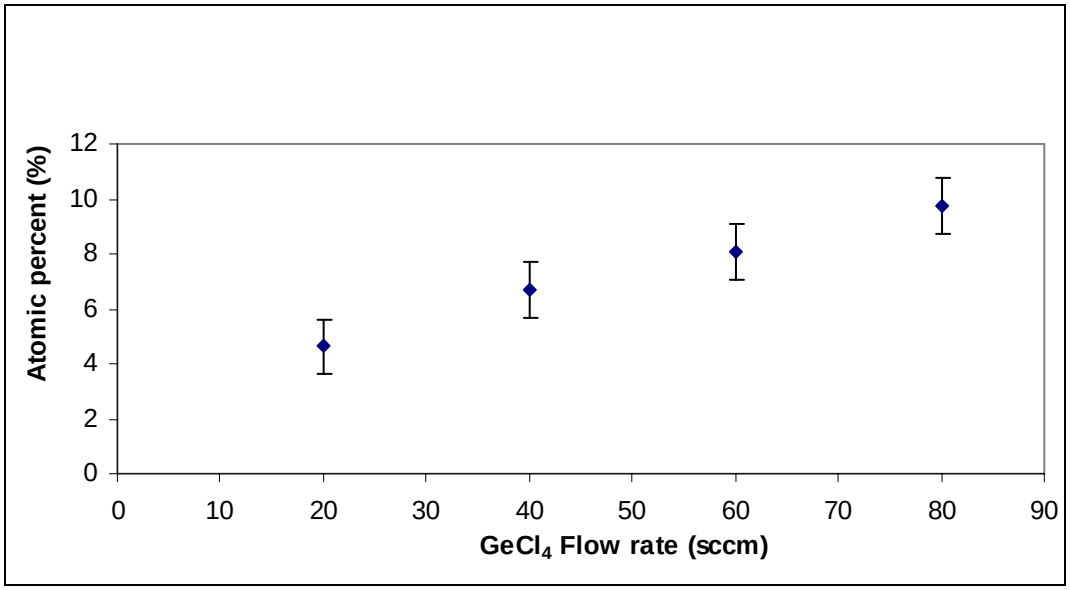

Figure 5.11: Concentration of germanium for various $GeCl_4$ flow rate in FHD (measured by EDX).

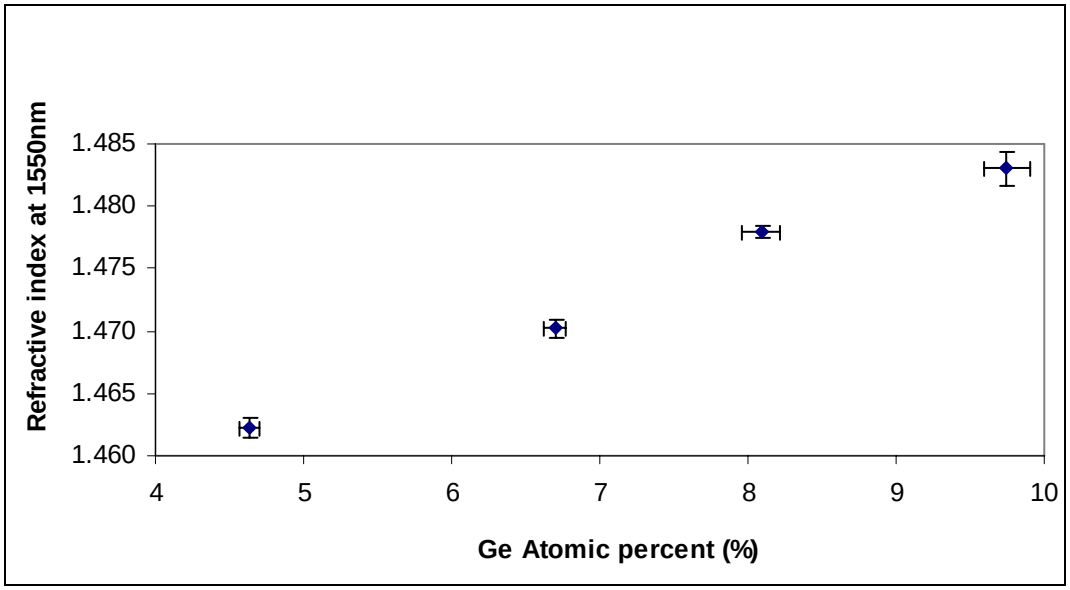

Figure 5.12: Refractive index of germanosilicate glass for various germanium concentration (measured by prism coupling method).

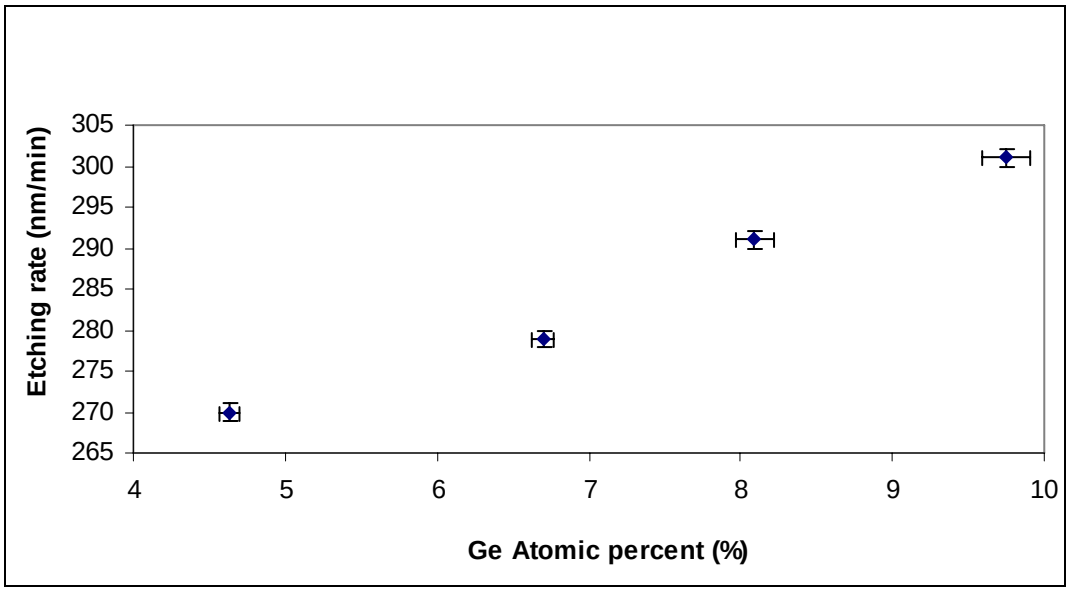

Figure 5.13: Etching rate of germanosilicate glass for various germanium concentration.

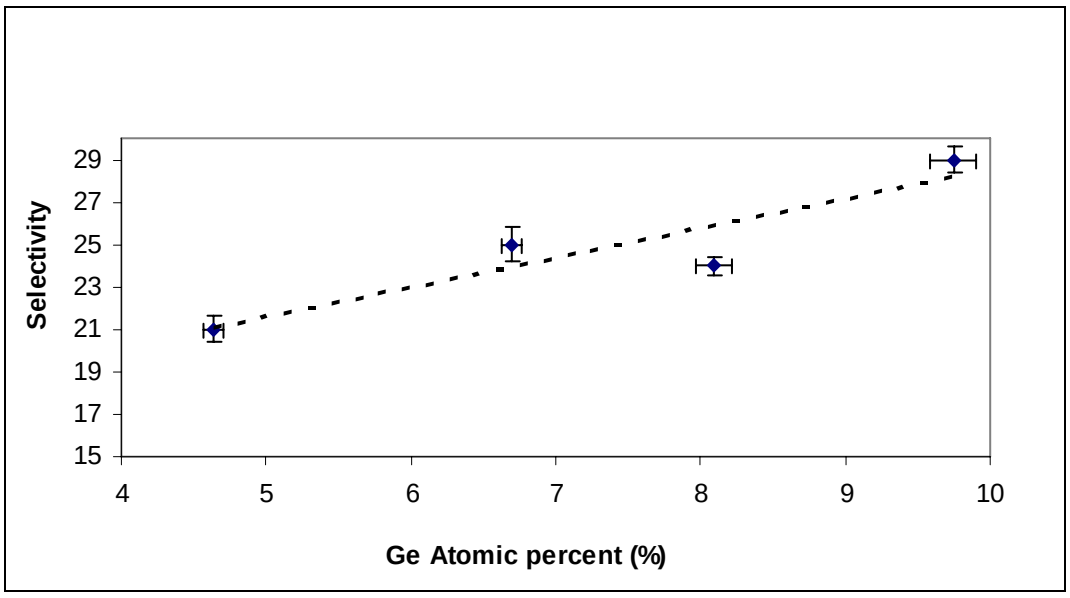

Figure 5.14: Selectivity of chromium to germanosilicate glass for various germanium concentration. (Trend line is for indicative purpose only)

Germanium is a group IV element which is the same group as silicon, hence germanium atom will just replace the silicon atom in the glass matrix. Therefore, no termination of chain structure will occur theoretically. However, because the Ge-O bond length is longer than Si-O bond by about 8% and the Ge-O-Ge bond angle is 133^{o} which is smaller than the Si-O-Si bond angle (144^{0}), mechanical stress is created on the chain structure and defects are highly possible to occur [10]. This mechanical stress increases the refractive index of the silica glass and also weakens the silica matrix and causes the etching rate to increase. Due to the property of etching rate increase in germanosilicate glass with germanium concentration in the silica glass, the selectivity of germanosilicate glass to chromium is increased too. From Figure 5.14 it can be seen that the selectivity is increased from 21 for germanium concentration of 4.63 at% to 29 for germanium concentration of 9.75 at%.

5.3.3 Comparing the dopant of Germanium and Phosphorous to ICP etching process

As discussed in Section 5.3.1 and 5.3.2, both phosphorous and germanium are good index riser for silica glass. However, the dopant dependency of etching for germanosilicate glass ($0.0040\ at\%^{-1}$) is lower than the dopant dependency in phosphosilicate glass ($0.0049\ at\%^{-1}$). The reason that causes the dopant dependent etching rate to be higher in phosphosilicate glass is because of the existence of the double bond between the phosphorous atom with one of the oxygen in the tetrahedral glass structure. Due to the existence of double bonds, defects like termination of silica glass matrix will occur for each double bonds. While in germanosilicate glass, the mechanical stress induced by bind length and bond angle mismatch only increases the probability of defects, not a definite occurrence.

In term of etching selectivity of doped silica to chromium, phosphosilicate glass has higher selectivity as compared to germanosilicate glass. However, as the concentration of phosphorous increases, selectivity of phosphosilicate glass decreases. This is due to the increase in concentration of oxygen ICP etching for phosphosilicate glass as the phosphorous incorporation increases. However, this effect was improved by adding a certain amount of hydrogen gas during the etching process as reported in Section 4.1.9.1.

As a conclusion, in terms of ICP etching point of view, phosphorous is a better candidate as dopant in silica glass to rise the refractive index since both dopant has a similar index rising strength as shown in Figure 5.15. However, the low incorporation rate of phosphorous in silica glass reduces the cost effectiveness of phosphorous doping. The low incorporation rate is due to the high volatility of phosphorous oxide which has a low sublime temperature (358 ^{o}C) and melting point (569 ^{o}C) [10]. Some of the phosphorous dopant may have evaporated during the consolidation process.

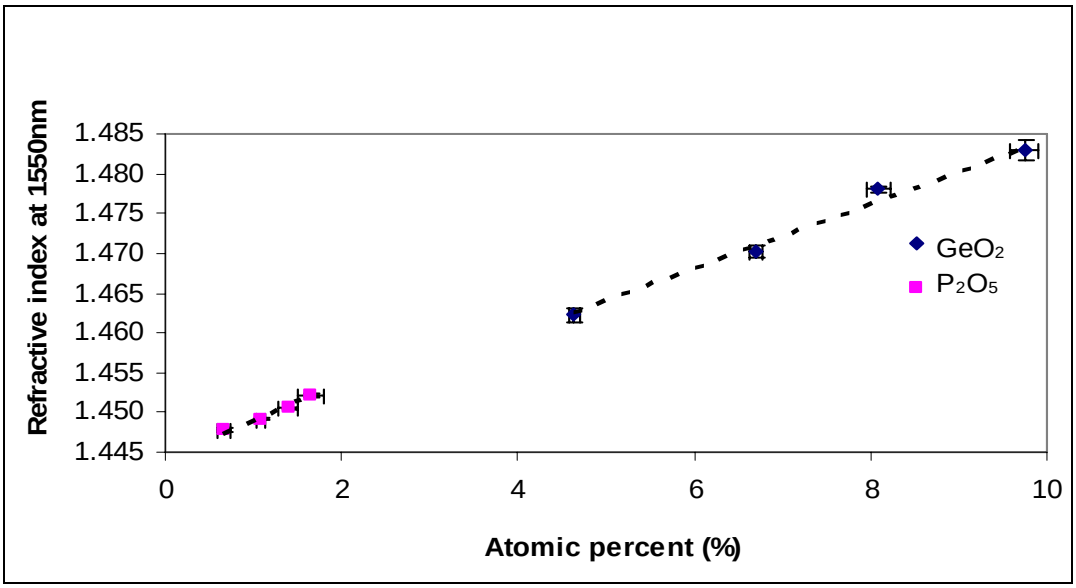

Figure 5.15:Refractive index for various dopant concentration for germanosilicate and phosphosilicate glass. (Trend line for indicative purpose only)

References

[1] D.Shin. & J.H.Eo. (2005) Plasma Etching Characteristic of Ge-B-P doped SiO_2 Film for Waveguides Fabrication. Ceramic Processing Research, 6 345-350.

[2] K.H.Park, S.Lee, K.H.Kwon and J.H.Moon. (2001). The effect of CF_4 and CHF_3 gas on the etching characteristics of Er-doped glass. Material Science Letter, 20 565-568.

[3] D.Y.Choi, J.H.Lee, D.S.Kim, & S.T.Jung. (2004). Formation of Plasma Induced Surface Darmage in Silica Glass Etching for Optical Waveguides. Journal of Applied Physics, 95 (12),8400-8407.

[4] B. Chapman. (1980). Glow Discharge Process. New York: John Wiley & Sons.

[5] K.Y.Chan & B.S. Teo. (2006). Atomic force microscopy (AFM) and X-ray diffraction (XRD) investigations of copper thin films prepared by dc magnetron sputtering technique. Microelectronics Journal, 37, 1064-1071.

[6] K.Eufinger, D.Poelman, H.Poelman, R.De Gryse and G.B.Marin. (2007). Photocatalytic activity of DC Magnetron Sputter Deposited Amorphous TiO_2 thin films. Journal of Applied Surface Science, 254, 148-152.

[7] N.N.Iosad & T.M. Klapwijk. (1999). Property of DC Magnetron Sputtered Nb and NbN films for Different Source Conditions. Journal of IEEE Transactions on Applied Superconductivity, 9 (2).

[8] X.J.Hao, E.C.Cho, G.Scardera, E.Bellet-Amalric, D.Bellet, Y.S.Shen, S.Huang, Y.D.Huang, G.Conibeer, & M.A.Green. (2009). Effect of phosphorus doping on structural and optical properties of silicon nanocrystals in SiO_2 matrix. Thin Film Solid, 517 5646-5652.

[9] P.Heimala & J.Aarnio. (1992). Refractive index behavior of phosphorus-doped planar silica waveguides. Journal of Applied Physic D, 25, 733-739.

[10] S.P.Watts. (2002). *Flame Hydrolysis Deposition of Photosensitive Silicate Layer Suitable for the Definition of Waveguiding Structures through Direct Ultraviolet Writing*. Unpublished doctoral dissertation, University of Southampton, Southampton.

[11] J.Tonotani, S.I. Ohmi, & H.Iwai. (2005). Dry Etching of Cr_2O_3/Cr Stacked Film During Resist Aashing by Oxygen Plasma. Japanese Journal of Applied Physics, 44, 114-117.

CHAPTER 6

CONCLUSIONS & FUTURE WORK

6.1 Conclusion

In this work, ICP dry etching process has been optimised for fabrication of low loss optical passive devices. The criteria used in determining the optimum parameter are based on etching rate, selectivity, side wall roughness, vertical profile and channel cleanliness. Although high etching rate with good selectivity between chromium and glass are the easiest guides to determine the optimise parameters, however in order to fabricate good low loss devices, the side wall roughness, vertical profile and cleanliness are very important too [1, 2]. Hence it is appropriate to take into all consideration before determining the optimised parameters.

Before this work has been carried out, the default ICP setting that have good vertical etching profile and clean surface only gives about 225 nm/min in etching rate with selectivity of 25. In fact, the etching rate of 225 nm/min is the highest value achieved in a previous work with the optimization of all fabrication parameters. For splitter fabrication that required 8 µm depth etching, this etching condition requires at least 36 minutes of total etching time with chromium hard mask thickness of at lease 320 nm. In terms of etching rate, this value is still acceptable but the selectivity is too low and chromium thickness of

above 300 nm is not suitable in chromium wet etching in the lithography process which will lead to jagged or rough side wall [3]. Moreover, channel tapering and large amount of pinhole are observed on the sample under SEM. This is an indication that the etching is dominantly physical etching which will usually produce low selectivity characteristic [1].

Upon optimization of ICP power, bias power, and substrate height position carried out in this work, we are able to improve the etching rate up to about 250 nm/min, but the selectivity retained at about 26 only. This result shows that by just varying the ICP power, Bias power and substrate position is not enough to improve the selectivity. This is because all three parameters are affecting more in plasma energy, plasma density plasma bombardment energy on to the sample.

The second stage of optimization involved varying the operating chamber pressure and reactant gas flow rate. The etching condition is improved to 280 nm/min in etching rate and 35 in selectivity. Both chamber pressure and reactant gas flow rate did also play an important role in plasma energy, plasma density and plasma energy as similar to the parameters that varies in the first stage of optimization. However, these parameters also play a role in controlling the freshness (or resident time) of the reactant gas by controlling the gas ejection and extraction rate for a given chamber pressure. Good control in these parameters help in the etching mechanism cycle where the time for fresh reactant gas to absorb on to the glass layer, chemical reaction between the reactant gas and glass layer, and desorption of the by product are optimised.

The selectivity is further improved to 47 (approximate to 45 in calculation) in the third stage of optimization. In this stage, small amount of hydrogen gas (about 27 %, flow rate of 9 sccm of hydrogen and 35 sccm of C_2F_6) was added in the etching process. Hydrogen radicals in the operating chamber are able to absorb the oxygen compound in the chamber to from water molecule [4]. This oxygen compound is created during the glass etching process. We believe that this oxygen compound is oxidising the chromium hard mask to form volatile particle and eventually the chromium mask etching rate increases [5]. By removing the oxygen in the chamber, the chromium mask etching rate reduces and this increases the etching selectivity. However, adding hydrogen into the chamber reduces the etching rate to about 255 nm/min. By adding other gases in to the operating chamber, the overall amount of reactant gas species that are potentially for the glass etching is reduces causes the decrease in the glass etching rate.

Using splitter fabrication as an example of comparison before and after the optimization work, the total etching time required is about 32 minutes (approximate to 35 minutes for over etching) which is only small improvement. However, the huge improvement in selectivity from 25 to 45 leads to the reduction of chromium hard mask thickness required to only about 180nm instead of 320nm (approximate to 200 nm for safety). With the thickness reduction in chromium hard mask, the defects caused by chromium wet etching is reduced and this improves the channel side wall roughness.

As a comparison to other researcher works, the optimise parameters that we obtain are comparable to their standard. For example, in Sun-Tae Jung from Samsung Electronic

Korea work, their optimise parameters gives an etching rate of 240nm/min with selectivity of about 41 (using CF_4 as reactant gas with 1100 W ICP power, 30 W bias power, 30 sccm reactant gas flow rate, and 6 mTorr operating chamber pressure).

As a summary, the optimized ICP etching parameters are shown in table 6.1.

Table 6.1: Optimized parameters for silica glass etching process.

ICP Parameter	**Set Value**
ICP Power	880 Watt
Bias Power	45 Watt
Pressure	10 mtorr
Gas	C_2F_6 and H_2
C_2F_6 gas Flow	35 sccm
H_2 gas flow	9 sccm
Working distance	5 cm

6.2 Future work

In order to further optimize the glass etching process, better understanding of the etching process from plasma generation up to by product gas extraction process are required. In order to study these effects, real time monitoring system such as Langmuir probe, XPS (X-ray Photoelectron Spectroscopy), Mass spectroscopy, or OES (Optical Emission Spectroscopy) are required.

Langmuir probe is a common technique used in plasma system to measure the ion flux, electron density, plasma temperature, and plasma floating potential. By acquiring these parameters, the density distribution and the ion energy distribution in the plasma cloud can be extrapolated. There two parameters are very important in determining the uniformity of the glass etching on the sample, and local glass etching rate. However, this technique has a disadvantage where it has the potential to contaminate the chamber. The Langmuir probe is usually made from copper and it need to probe into the chamber or required position for its sensing application. By doing so, the plasma may etch the copper probe, and resulted contamination in the chamber [4, 6].

Additionally, plasma mapping, the gas composition analysis of the plasma cloud is also important. It is advantages to know what types of gases and its concentration in the chamber during the etching process in order to identify the actual reason for polymerization and the reasons for high chromium etching rate. For example, if the etched chromium particles are known to be more dominant in their oxide form than pure atomic form, then preventing the chromium hard mask to be oxidized during the etching process might help to increase the selectivity. Real time methods that can be used to determine the gas

composition during the process are optical emission spectroscopy (OES) or mass spectroscopy. OES uses the light emission method to identify the existing of a particular gas. Each particular gas will have its unique light emission frequency hence it is possible to probe the existence of a particular gas in the plasma cloud using this principle. Moreover by measuring the intensity of each wavelength, the gas composition of the plasma cloud can be determined. While for the mass spectroscopy method, it uses the concept of different mass for different particles to identify and determine the gas composition. However, OES is preferred to use as compare to mass spectroscopy. Firstly, the OES system can be installed totally outside the chamber unlike mass spectroscopy mass need to install in side the chamber. Secondly, mass spectroscopy need extra magnetic field to attract the plasma particles during the analysis process. This extra magnetic field will disturb the plasma system and eventually affect the etching process [7, 8]

References

[1] M. L. Calvo, & V.Lakshminarayanan. (2007). Optical Waveguides:From Theory to Applied Technologies. Boca Raton:CRC Press Taylor & Francis Group.

[2] T.M.Hoa, Charles R. de Boer & Pasqualina M. Sarro. (n.d) Roughness Treatment of Silicon Surface after Deep Reactive Ion Etching. Retrived March 27, 2009, from http://www.stw.nl/NR/rdonlyres/6A9E9428-9B60-42A2-A229-C6DDD618271D/0/pham.pdf.

[3] K.H.Park, S.Lee, K.H.Kwon and J.H.Moon. (2001). The effect of CF_4 and CHF_3 gas on the etching characteristics of Er-doped glass. Material Science Letter, 20 565-568.

[4] B. Chapman. (1980). Glow Discharge Process. New York: John Wiley & Sons.

[5] J.Tonotani, S.I. Ohmi, & H.Iwai. (2005). Dry Etching of Cr_2O_3/Cr Stacked Film During Resist Aashing by Oxygen Plasma. Japanese Journal of Applied Physics, 44, 114-117.

[6] F.Chen. (1997). Introduction to Plasma Physics. New York: John Wiley & Sons.

[7] J.R.Roberts (1995). Optical Emission Spectroscopy on the Gaseous Electronic Conference RF Reference Cell. Journal of Research of the National Institute of Standards and Technology, 100, 353.

[8] T. Pettke, C.A.H., Adeline C.Ciocan & Detlef Gunther. (2000) Quadrupole Mass Spectrometry and Optical Emission Spectroscopy: Detection Capabilities and Respresentative Sampling of Short Transient Signals from Laser-ablation. Journal Anal. At. Spectrom, 15, 1149-1155.